

**The *in vitro* inhibition of adrenal
steroidogenic enzymes and modulation
of adrenal hormone production by
*Sceletium tortuosum***

by
Inge Johannes



*Thesis presented in fulfilment of the requirements for the degree
of Master of Science in the Faculty of Science at Stellenbosch*

University

UNIVERSITEIT
iYUNIVESITHI
STELLENBOSCH
UNIVERSITY

100
1918 · 2018

Supervisor: Prof. Amanda C. Swart
Co-supervisor: Prof Carine Smith

March 2018

Declaration

By submitting this thesis electronically, I declare that the entirety of the work contained therein is my own, original work, that I am the sole author thereof (save to the extent explicitly otherwise stated), that reproduction and publication thereof by Stellenbosch University will not infringe any third party rights and that I have not previously in its entirety or in part submitted it for obtaining any qualification.

March 2018

Copyright © 2018 Stellenbosch University

All rights reserved

Abstract

This study describes:

- The development and validation of an ultra-performance convergence chromatography tandem mass spectrometry (UPC²-MS/MS) analytical method for the separation, detection and quantification of 17 adrenal steroid hormones, including two C11-oxy C₂₁ steroids; and the application thereof in the kinetic characterisation of cytochrome P450 11 β -hydroxylase (CYP11B1) towards androstenedione (A4) and testosterone (T):

Kinetic characterisation showed that CYP11B1 exhibits an apparent K_m towards A4 and T of $0.21 \pm 0.07 \mu\text{M}$ and $0.34 \pm 0.13 \mu\text{M}$, respectively and V_{max} values of 315.77 ± 22.46 and $158.89 \pm 15.22 \text{ pmol/min/mg protein}$, respectively.

- The investigation into the influence of a mesembrine-enriched extract of *Sceletium tortuosum* at 0.01 and 1 mg/mL ($0.345 \mu\text{M}$ and $34.5 \mu\text{M}$) on the catalytic activity of key adrenal steroidogenic enzymes: cytochrome P450 17 β -hydroxylase/17,20-lyase (CYP17A1), 3 β -hydroxysteroid dehydrogenase (3 β HSD2), cytochrome P450 21-hydroxylase (CYP21A2), cytochrome P450 11 β -hydroxylase (CYP11B1) and aldosterone synthase (CYP11B2), expressed in HEK-293 cells:

Substrate conversion assays showed that *S. tortuosum* significantly inhibited 3 β HSD2, CYP11B1 and CYP21A2.

- The influence of *S. tortuosum* in comparison to abiraterone (Abi), 10 μM , on adrenal steroid hormone production in the H295R adrenal model endogenously expressing the full complement of steroidogenic enzymes, which catalyse the production of mineralocorticoids, glucocorticoids and adrenal androgens:

UPC²-MS/MS analyses of the basal steroid metabolites showed that while Abi resulted in a greater inhibition of the steroid shunt in the androgen pathway than in the glucocorticoid pathway due to the potent inhibition of CYP17A1, *S. tortuosum*, resulted in a greater decrease in the steroid shunt in the glucocorticoid pathway in comparison to the androgen pathway, due to the inhibition of 3 β HSD2, CYP21A2 and CYP11B1.

Opsomming

Hierdie studie beskryf:

- Die ontwikkeling en validering van 'n UPC²-MS/MS-analitiese metode vir die analise van 17 byniersteroïede, insluitend twee C11-oksi-C₂₁-steroïede; die metode is vervolgens gebruik in die kinetiese karakterisering van sitochroom P450 11β-hidroksilase (CYP11B1) met androstenedioon (A4) en testosteron (T) as substraat: Kineties karakterisering van CYP11B1 lewer 'n oënskynlike K_m van $0.21 \pm 0.07 \mu\text{M}$ en $0.34 \pm 0.13 \mu\text{M}$ vir A4 en T met V_{max} waardes van 315.77 ± 22.46 en 158.89 ± 15.22 pmol/min/mg proteïen vir A4 en T, onderskeidelik.
- Die ondersoek na die invloed van 'n mesembrien-verykte ekstrak van *S. tortuosum*, teen 0.01 en 1 mg/mL ($0.345 \mu\text{M}$ and $34.5 \mu\text{M}$), op die aktiwiteit van bynierensieme wat steroïedbiosintese kataliseer: sitochroom P450 17β- hidroksilase/17,20-liase (CYP17A1), 3β-hidroksisteroïed dehidrogenase (3βHSD2), sitochroom P450 21-hidroksilase (CYP21A2), sitochroom P450 11β-hidroksilase (CYP11B1) en aldosteroonsintase (CYP11B2), uitgedruk in HEK-293 selle; *S. tortuosum* inhibeer die omsetting van natuurlike steroïedsubstrate gekataliseer deur 3βHSD2, CYP11B1 en CYP21A2.
- Die invloed van *S. tortuosum* vergeleke met abirateron (Abi), $10 \mu\text{M}$, op steroïedhormoon produksie in H295R selle – 'n menslike bynierkarsinoomsellyn wat die volle komplement steroïed-kataliseerende ensieme bevat wat die produksie van mineralokortikoïede, glukokortikoïede en bynierandrogene kataliseer: UPC²-MS/MS analise van basale steroïedmetaboliete toon dat Abi ($10\mu\text{M}$) 'n groter inhibisie op androgeen produksie het as gevolg van die inhibisie van CYP17A1 vergelykend met die produksie van glukokortikoïede, terwyl *S. tortuosum* 'n afname in die produksie van glukokortikoïede tot gevolg het met 'n kleiner invloed op die produksie van androgene, as gevolg van die inhibisie van 3βHSD2, CYP21A2 en CYP11B1.

Dedicated to my parents, who have afforded me opportunities that are unimaginable to most

Acknowledgements

I hereby wish to express my sincere gratitude to:

Prof Amanda Swart, for being an impeccable woman in science, a role model whose guidance and unwavering support is unrivalled. Thank you for the endless help during this study and the preparation of this thesis.

Prof Carine Smith, thank you for your assistance and guidance

Prof Pieter Swart, your heart-warming smiles and jokes are really appreciated. Thank you for your advice and input when needed.

Ms Ralie Louw, thank you for always helping and ensuring that the lab is the running smoothly.

NRF, for financial support

Central Analytical Facility Stellenbosch for free use of the equipment and for assistance.

My colleagues in the lab, for always being kind and helpful with special mention to Jonathan, Liezl and Rachelle. You guys have been my sanity for the last two years. Thank you.

My parents, for your love, support, encouragement and understanding.

Rodwan, for always being my lighthouse. Thank you for your understanding, your love and your never-ending motivation.

Table of Contents

Chapter 1	1
Introduction	1
Chapter 2	4
The bioactivity of <i>Sceletium tortuosum</i>	4
2.1 Introduction	4
2.2 History and background	4
2.3 The biological properties and metabolism of <i>Sceletium tortuosum</i> compounds	5
2.4 Physiological activity of <i>Sceletium tortuosum</i>	9
2.4.1 The influence of <i>Sceletium tortuosum</i> extracts on the neurological system	9
2.4.2 Safety and tolerability of <i>Sceletium tortuosum</i>	10
Chapter 3	12
Adrenal Steroidogenesis	12
3.1 Introduction	12
3.2 Anatomy of the adrenal gland	12
3.3 Enzymes involved in adrenal steroid hormone biosynthesis	13
3.3.1 Cytochrome P450 enzymes	14
3.3.2 Hydroxysteroid dehydrogenases	17
3.4 The adrenal steroidogenic pathway	17
3.5 Diseases of adrenal steroid hormone biosynthesis	19
3.5.1 Mineralocorticoids	19
3.5.2 Glucocorticoids	20
3.5.3 Adrenal androgens	20
3.5 <i>Sceletium tortuosum</i> and the steroid pathway	21
Chapter 4	23
The development and validation of a UPC²-MS/MS method for analysis of endogenous adrenal steroids	23
4.1 Introduction	23
4.2 Methodology	24
4.2.1 Reagents	24
4.2.2 Preparation of standards and samples	24

4.2.3 Steroid extractions	25
4.2.4 Instrumentation.....	25
4.2.5 Chromatographic conditions.....	25
4.2.6 Method validation	26
4.3 Results.....	29
4.3.1 Calibration Range	29
4.3.2 Accuracy and precision	29
4.3.3 Recovery, matrix effects and process efficiency	29
4.4 Discussion	34
4.5 Implementation of the UPC²-MS/MS method: kinetic characterization of CYP11B1 towards A4 and T	35
4.5.1 Cell culture and transfection	35
4.5.2 Conversion of A4 and T by CYP11B1 in transiently transfected HEK-293 cells	36
4.5.3 The determination of kinetic parameters: K_m and V_{max} values	36
4.5.4 Results.....	37
4.5.5 Discussion.....	39
Chapter 5	41
An investigation into the influence of <i>S. tortuosum</i> on adrenal steroidogenesis.....	41
5.1 Introduction	41
5.2 Methodology	43
5.2.1 Materials.....	43
5.2.2 Purification of plasmid DNA.....	44
5.2.3 Enzyme assays in transiently transfected HEK-293 cells.....	45
5.2.4 Enzymatic assays in H295R cells.....	45
5.2.5 Cell viability	46
5.2.6 Protein determination	46
5.2.7 Steroid extraction	47
5.2.8 Separation and quantification of steroid metabolites using UPC ² -MS/MS	47
5.2.9 Statistical analysis.....	47
5.3 Results.....	48
5.3.1 The influence of <i>S. tortuosum</i> extract on cell viability.....	48
5.3.2 The influence of <i>S. tortuosum</i> extract on CYP17A1	49
5.3.3 The influence of <i>S. tortuosum</i> extract on CYP21A2	51
5.3.4 The influence of <i>S. tortuosum</i> extract on CYP11B1	53
5.3.5 The influence of <i>S. tortuosum</i> extract on CYP11B2	56

5.3.6 The influence of <i>S. tortuosum</i> extract on 3 β HSD2.....	58
5.3.7 The influence of <i>S. tortuosum</i> on adrenal steroid hormones in H295R cells.....	60
5.4 Discussion	65
Chapter 6	69
Conclusion	69
References	72

List of Figures

Figure 2.1: *S. tortuosum* – typical depiction of the skeletal venation on the dried leaves

Figure 2.2: Geographical distribution of *S. tortuosum* in South Africa

Figure 2.3: Structures of octahydroindole alkaloids found in *S. tortuosum*

Figure 2.4: Proposed biosynthesis of alkaloids in *S. tortuosum*. Arrows represent multiple reactions in the pathway

Figure 3.1: Schematic representation of the zones of the adrenal cortex

Figure 3.2: Structure of cholesterol (left) and the steroid backbone (right).

Figure 3.3: Schematic representation of electron transport systems involved in the catalytic activity of the P450 enzymes in the mitochondria (left) and microsomes (right).

Figure 3.4: Enzymatic reaction cycle of the cytochrome P450 enzymes.

Figure 3.5: Adrenal hormone biosynthesis

Figure 4.1: UPC²-MS/MS chromatographic separation of 17 steroid metabolites and three deuterated steroid standards. Structures and retention times of steroids (shaded peaks) are indicated on each chromatogram.

Figure 4.2: Analysis of progress curves for A4 (A) and T (B) determined using steroid conversion assays in HEK293 cells transiently expressing CYP11B1 and ADX. Data were fitted to the Michaelis-Menten equation, using non-linear regression. Each point represent an initial rate for a time course assay, performed in triplicate and expressed as mean \pm SD (n=3). Data was analysed using GraphPad Prism (version 6) (GraphPad Software, San Diego, California)

Figure 5.1: Toxicity of *S. tortuosum* extract on HEK293 cells. Cells were treated with *S. tortuosum*, at two concentrations, 0.01 and 1 mg/mL, for 24 hours after which the AlamarBlue® assay was conducted and the fluorescence measured. Results are expressed

as the mean relative fluorescent units (RFU) per mg total protein \pm SD (n=3, ns=not significant).

Figure 5.2: Enzymatic reactions catalysed by CYP17A1 (orange).

Figure 5.3: Analysis of substrate conversion in HEK293 cells expressing CYP17A1. Substrate remaining after the addition of 1 μ M PREG (A) and PROG (B) in the absence (control) and presence of *S. tortuosum* extract at two concentrations. The experiment was performed in triplicate and analysed by a one-way ANOVA, followed by a Dunnett's multiple comparison test. Results are expressed as the mean \pm SEM (n=3, ns = non-significant) (n=3, ns=not significant).

Figure 5.4: Enzymatic reactions catalysed by CYP21A1 (red).

Figure 5.5: Analysis of substrate conversion in HEK293 cells expressing CYP21A2. Substrate remaining after the addition of 1 μ M PROG (A) and 17OHPROG (B) in the absence (control) and presence of *S. tortuosum* extract at two concentrations. The experiment was performed in triplicate and analysed by a one-way ANOVA, followed by a Dunnett's multiple comparison test. Results are expressed as the mean \pm SEM (n=3, ns = non-significant) (n=3, ns=not significant).

Figure 5.6: The enzymatic reactions catalysed by CYP11B1 (blue).

Figure 5.7: Analysis of substrate conversion in HEK293 cells expressing CYP11B1 and ADX. Substrate remaining after the addition of 1 μ M 11-deoxycortisol (A), A4 (B) and T (C) in the absence (control) and presence of *S. tortuosum* extract at two concentrations. The experiment was performed in triplicate and analysed by a one-way ANOVA, followed by a Dunnett's multiple comparison test. Results are expressed as the mean \pm SEM (n=3, ns = not significant, * P <0.05, ** P <0.01).

Figure 5.8: Enzymatic reactions catalysed by CYP11B2 (yellow).

Figure 5.9: Analysis of substrate conversion in HEK293 cells expressing CYP11B2 and ADX. Substrate remaining after the addition of 1 μ M DOC (A), A4 (B) and T (C) in the absence (control) and presence of *S. tortuosum* extract at two concentrations. The

experiment was performed in triplicate and analysed by a one-way ANOVA, followed by a Dunnett's multiple comparison test. Results are expressed as the mean \pm SEM (n=3, ns=not significant, ** P <0.01, *** P <0.001).

Figure 5.10: Enzymatic reactions catalysed by 3 β HSD2 (green).

Figure 5.11: Analysis of substrate conversion in HEK293 cells expressing 3 β HSD2. Substrate remaining after the addition of 1 μ M PREG (A) and DHEA (C) in the absence (control) and presence of *S. tortuosum* extract at two concentrations. (B) shows product formed after the addition of 1 μ M 17OHPREG. The experiment was performed in triplicate and analysed by a one-way ANOVA, followed by a Dunnett's multiple comparison test. Results are expressed as the mean \pm SEM (n=3, ns = non-significant) (n=3, ns=not significant, * P <0.05, ** P <0.01).

Figure 5.12A: Steroid production in the glucocorticoid (green block) and mineralocorticoid pathway (red block) of adrenal steroidogenesis. Cells were exposed to *S. tortuosum* at 0.01 and 1 mg/mL and 10 μ M Abi under basal conditions. Results are represented as mean \pm SD (n=3).

Figure 5.12B: Steroid production in the androgen pathway of adrenal steroidogenesis. Cells were exposed to *S. tortuosum* at 0.01 and 1 mg/mL and 10 μ M Abi under basal conditions. Results are represented as mean \pm SD (n=3).

List of Tables

Table 4.1: UPC² solvent parameters for the chromatographic separation of the metabolites.

Table 4.2: Molecular ion species, MRM mass transitions, mass spectrometer conditions (cone voltage, collision energy) and retention time for each metabolite. Internal standard: PROG-d₉, A4-d₇, T-d₂.

Table 4.3: Method validation data: LOD (ng/mL), LOQ (ng/mL), r^2 , accuracy (%RSD, n = 4) and precision (%RSD, n = 4).

Table 4.4: Method validation data: Recovery (%; n = 3); matrix effect (%; n = 3) and process efficiency (%; n = 3).

Table 4.5: Kinetic parameters, apparent K_m and V_{max} values generated by progress curve analysis, and catalytic efficiency (V_{max}/K_m) determined for CYP11B1. * represents reported values reproduced from [1].

Table 5.1: Basal steroid metabolites produced in adrenal H295R cells in the absence and presence of *S. tortuosum* at 0.01 and 1 mg/mL in comparison to abiraterone (10 μ M) after 48 h.

Abbreviations and Symbols

11 β HSD	11 β -hydroxysteroid dehydrogenase
17 β HSD	17 β -hydroxysteroid dehydrogenase
11KDHT	11-keto-5 α -dihydrotestosterone
11KT	11-ketotestosterone
11OHA4	11 β -hydroxyandrostenedione
11OHT	11-hydroxytestosterone
11 α OHP4	11 α -hydroxyprogesterone
11 β OHP4	11 β -hydroxyprogesterone
16OHPROG	16-hydroxyprogesterone
17OHPREG	17-hydroxypregnenolone
17OHPROG	17-hydroxyprogesterone
18OHCORT	18-hydroxycorticosterone
21-OHD	21-hydroxylase deficiency
3 β HSD2	3 β -hydroxysteroid dehydrogenase type 2
5-HT	5-hydroxytryptamine
A4	Androstenedione
A4-d ₇	4-androsten-3,17-dione 2,2,4,6,6,16,16-d ₇
Abi	Abiraterone
ABPR	Automated back pressure regulator
ACTH	Adrenocorticotrophic hormone
ALDO	Aldosterone
Ang II	Angiotensin II
BCA	Bicinchoninic acid
BSA	Bovine serum albumin
cAMP	Cyclic adenosine monophosphate
CAH	Congenital adrenal hyperplasia
CDKs	Cyclin-dependent kinases
CCS	Cosmic calf serum
CO ₂	Carbon dioxide
CORT	Corticosterone
CRPC	Castration resistant prostate cancer
CYP11A1/P450scc	Cytochrome P450 cholesterol side-chain cleavage

CYP17A1	Cytochrome P450 17 α -hydroxylase/17,20-lyase
CYP11B1	Cytochrome P450 11 β -hydroxylase
CYP11B2	Cytochrome P450 aldosterone synthase
CYP21A2	Cytochrome P450 21-hydroxylase
D4A	Δ^4 -abiraterone
DHEA	Dehydroepiandrosterone
DHEA-S	Dehydroepiandrosterone sulphate
DHT	Dihydrotestosterone
DMEM	Dulbecco's modified eagle's medium
DNA	Deoxyribonucleic acid
DOC	Deoxycorticosterone
ECG	Electrocardiogram
EDTA	Ethylenediaminetetraacetic acid
ER	Endoplasmic reticulum
ESI+	Electrospray ionization in positive mode
FAD	flavinadenine dinucleotide
FBS	Fetal bovine serum
FDA	US Food and Drug Administration
FMN	Flavinmononucleotide
GABA	Gamma butyric acid
GC-MS	Gas chromatography-mass spectrometry
GR	Glucocorticoid receptor
H295R	Human adrenocortical carcinoma cell line
HEK-293	Human embryonic kidney cell line
HSDs	Hydroxysteroid dehydrogenases
IMM	inner mitochondrial membrane
LB	Lysogeny broth
LC-MS/MS	Liquid chromatography tandem mass spectrometry
LDLs	Low-density lipoproteins
LOD	Limit of detection
LOQ	Limit of quantification
K_m	Michaelis-Menten constant
MR	Mineralocorticoid receptor
MRI	Magnetic resonance imaging
MRM	Multiple reaction monitoring

MTBE	Methyl <i>tert</i> -butyl ether
MTT	3-[4, 5-dimethylthiazol-2-yl]-2, 5-diphenyl tetrazolium bromide
NF- κ B	Nuclear factor kappa B
NADPH	Nicotinamide adenine dinucleotide phosphate
NMR	Nuclear magnetic resonance spectroscopy
OMM	Outer mitochondrial membrane
P450	Cytochrome P450
PBS	Phosphate Buffer Saline
PCa	Prostate cancer
PDE	Phosphodiesterase
PDE3	Phosphodiesterase 3
PDE4	Phosphodiesterase 4
POR	P450 oxidoreductase
PREG	Pregnenelone
PROG	Progesterone
Prog- d ₉	Progesterone-2, 2, 4, 6, 6, 17 α , 21, 21, 21-d ₉
RAAS	Renin-angiotensin-aldosterone-system
RPM	Revolutions per minute
RSD	Relative standard deviation
SD	Standard deviation
SEM	Standard error of the mean
SERT	Serotonin transporter
SFC	Supercritical fluid chromatography
SRD5A	5 α -reductase
SSRIs	Selective serotonin reuptake inhibitors
StAR	Steroid acute regulatory protein
T	Testosterone
T-d ₂	Testosterone-1, 2-d ₂
ULOQ	Upper limit of quantification
UPC ² -MS/MS	UltraPerformance convergence chromatography tandem mass spectrometry
VMAT-2	Vesicular monoamine transporter
V_{max}	Maximum velocity of enzymatic reaction

Chapter 1

Introduction

Sceletium tortuosum, a succulent plant unique to the south-western region of South Africa, has anecdotally been used for the alleviation of stress and anxiety and to promote a sense of well-being and calmness. Traditionally, the Khoi people of South Africa used *S. tortuosum* during times of hunting as a supplement to combat hunger. Khoi pastoralists also utilised this plant to induce a meditative state during times of worship [2, 3]. *S. tortuosum* is rich in alkaloids and is currently used as an herbal supplement for the treatment of symptoms that are associated with stress. The effects experienced upon consumption hint to both neurological and endocrinological involvement [4]. Alkaloids have been well-documented to possess a multitude of biological effects. These include antitumor, antibacterial, antifungal, antimalarial, antiviral as well as pain-relieving properties [4, 5].

It has been reported that extracts of *S. tortuosum* affect the central nervous system via the reuptake of 5-hydroxytryptamine (5-HT), the inhibition of the expression of the serotonin transporter (SERT) and the upregulation of monoamine release and storage [6, 7]. In terms of endocrine involvement, it has been shown that the plant is able to modulate steroid production in H295R cells, an adenocarcinoma cell line. *S. tortuosum* therefore offers potential as a therapeutic agent in the treatment of hormone-related diseases [4].

Adrenal hormone biosynthesis occurs in the adrenal gland with cholesterol being the precursor of all the adrenal steroid hormones. Ultimately, adrenal steroid biosynthesis results in the formation of mineralocorticoids in the *zona glomerulosa*, glucocorticoids in the *zona fasciculata*, and adrenal androgens in the *zona reticularis*. The mineralocorticoid, aldosterone, is essential in the maintenance of blood pressure, while cortisol, a glucocorticoid, amongst other functions, modulates the stress response and plays a role in inflammation and lipid metabolism [8–12]. The adrenal androgens, dehydroepiandrosterone (DHEA) and androstenedione (A4), are weak androgen precursor hormones. The adrenal also produces high levels of 11 β -hydroxyandrostenedione (11OHA4) [13], a weak androgen that was thought to have no metabolic function up until recently, when it was shown that it is a precursor metabolite to more potent androgens, 11keto-testosterone (11KT) and 11keto-dihydrotestosterone (11KDHT) [14–16]. *S. tortuosum* has been shown to have

possible inhibitory effects on CYP17A1 and 3 β HSD2, adrenal enzymes that catalyse the biosynthesis of DHEA and A4, respectively [4]. This suggests possible modulation of androgen production in the adrenal and thereby decreasing the contribution of adrenal androgens to the androgen pool.

Since *S. tortuosum* appears to have potential as a therapeutic agent by modulating adrenal steroid hormone production, the central aim of this thesis was to determine the influence of *S. tortuosum* on adrenal steroid hormone production *in vitro*, specifically on the adrenal enzymes in isolation, without the interference of competing enzymes. In order to accurately quantify and separate all the adrenal steroid hormones, a UPC²-MS/MS method was developed, validated and implemented in adrenal steroid analyses and in the kinetic characterization of CYP11B1. This allowed for accurate concentration determinations due to increased sensitivity, while decreasing time and cost.

In Chapter 2, *S. tortuosum* is discussed in terms of its history, biological properties and metabolism. The main focus of this chapter is the physiological bioactivity of *S. tortuosum*.

Chapter 3 entails an overview of adrenal steroidogenesis, describing the enzymes that catalyse adrenal steroid hormone production as well as the physiological activity of these steroid hormones. Disease states of the adrenal are discussed as well as the influence of *S. tortuosum* on adrenal steroidogenesis.

Chapter 4 and 5 addresses the specific aims necessary to achieve the central aim of this thesis and can be summarized as follows:

- to develop and validate a UPC²-MS/MS method for the detection, separation and quantification of 17 steroid metabolites;
- to implement the UPC²-MS/MS method in the kinetic characterisation of P450 11 β -hydroxylase (CYP11B1) towards A4 and testosterone (T);
- to determine the influence of *S. tortuosum* on key adrenal steroidogenic enzymes – CYP17A1, CYP21A2, CYP11B1, CYP11B2 and 3 β HSD2;
- to determine the influence of *S. tortuosum* on basal steroid hormone production in H295R cells, and compare inhibitory profiles with the inhibitory effects of abiraterone (Abi).

Chapter 4 will focus on the methodology pertaining to the development and validation of the UPC²-MS/MS method while presenting the implementation thereof in the determination of the kinetic parameters of CYP11B1 towards A4 and T.

Chapter 5 describes the influence of *S. tortuosum* on the adrenal steroidogenic enzymes, CYP17A1, CYP21A2, 3BHSD2, CYP11B1 and CYP11B2. The influence of *S. tortuosum* on steroid hormone production in H295R cells was subsequently investigated, and assayed under basal conditions to determine the effects on adrenal steroid output.

Chapter 6 comprises a general discussion of the results obtained and focuses on the main conclusions that were drawn from these findings as well as future perspectives.

Chapter 2

The bioactivity of *Sceletium tortuosum*

2.1 Introduction

Mankind has a tradition of utilizing indigenous plants in the treatment of a plethora of ailments with an inherent tendency to look to nature for remedies and cures for ailments. For millennia, indigenous tribes have turned to nature for answers, living in a symbiosis that modern man cannot fully accept or embrace. The indigenous people of South Africa, specifically the Khoi, have used plants for medicinal purposes, one such being *Sceletium tortuosum*, a succulent plant indigenous to South Africa.

2.2 History and background

S. tortuosum belongs to the genus *Sceletium* and forms part of the Aizoaceae family. The genus *Sceletium* can be divided into two phenotypes: the tortuosum and the emarcidum [17].

The first known record of *S. tortuosum* is an illustration of the plant in the journal of Simon van der Stel, documenting his expedition to Namaqualand in 1685 [18]. The classic depiction entailed characteristic features inherent to plants of this genus. The leaf venation pattern of dried leaves resembles a skeleton, hence the name “*Sceletium*”, derived from the Latin word *Sceletus* (fig. 2.1). The species can also be recognized based on distinct characteristics regarding the flower, fruit and seeds. The flowers can be white, yellow or pale pink and the fruit capsule holds the dark-coloured kidney-shaped seeds. The succulent is indigenous to the south western region of South Africa and flourishes in arid conditions that are characteristic of this region (fig. 2.2) [3].

Sceletium was highly regarded by the Khoi. The whole plant- roots, stems and leaves, was harvested and milled with stones. The plant material was dried and stored in sheepskins and chewed to induce intoxication. Khoi hunter-gatherers consumed the plant to relieve hunger and thirst and to combat fatigue during long hunting trips so as to cope with the arid

environment. Khoi pastoralists used the plant to induce a trance to enable meditation and enhance spirituality. The plant, colloquially known as “kanna”, was traded amongst the indigenous people as well as with the Dutch. More recently, the impact of *S. tortuosum* can be seen in the commercial availability of health supplements that contain extracts of the plant. These health products claim that *S. tortuosum* is a stress-relieving, anti-anxiety, mood-elevating herbal supplement [3, 19]. Trade around the use of *Sceletium* has soared over the last decade, specifically marketed as a product named Zembrin[®], with declarations that perhaps the plant extract can rival Prozac in the treatment of mood disorders [20]



Figure 2.1: *S. tortuosum* – classical depiction of the skeletal venation on the dried leaves [3].

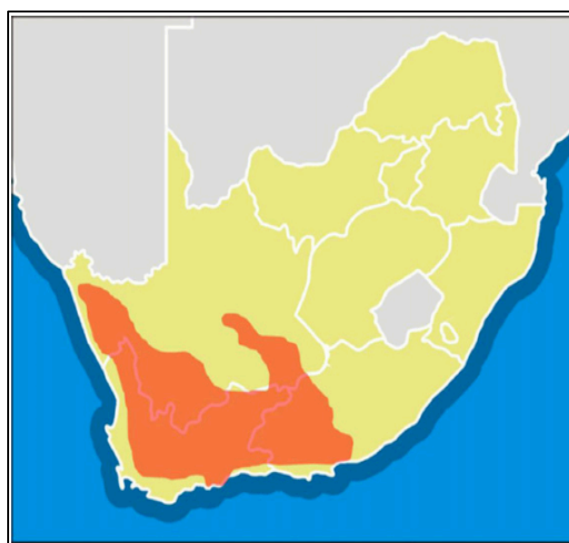


Figure 2.2: Geographical distribution of *S. tortuosum* in South Africa [3].

2.3 The biological properties and metabolism of *Sceletium tortuosum* compounds

The effects experienced upon the consumption of the plant has been attributed to a group of compounds called alkaloids. Alkaloids are secondary plant metabolites and is thought have a protective function in plants. Alkaloids have a wide range of biological activities in humans and have been shown to possess antitumor, antibacterial, antifungal, antimalarial, antiviral, pain-relieving and cholinesterase inhibitory activity [5].

The *tortuosum* types contain alkaloids whereas the *emarcidum* type does not contain alkaloids that are characteristic of the *tortuosum* types. The first instance that implied the

presence of the alkaloids in the plant was in studies done in 1896 by Meiring. He performed the first *in vivo* assay injecting frogs subcutaneously with mesembrine. A fast physiological response ensued with the only recorded responses being malaise and decreased appetite. Later, in 1914, Zwicky analysed samples from the *Scelletium* genus, reporting the occurrence of alkaloids in more than 50% of the plants. He managed to partially characterize and isolate mesembrine [17, 18, 21]. In *S.tortuosum* particularly, the most dominant alkaloid is (–)-mesembrine. Other alkaloids that are also present in the plant are mesembrenone, Δ^7 -mesembrenone, mesembranol and *epi*-mesembranol (fig. 2.3) [5, 17]. Environmental conditions such as light and temperature, plant age and the fermentation process all influence the total alkaloid content and composition in the plant. *S. tortuosum* has the highest total alkaloid content in the genus [22, 23].

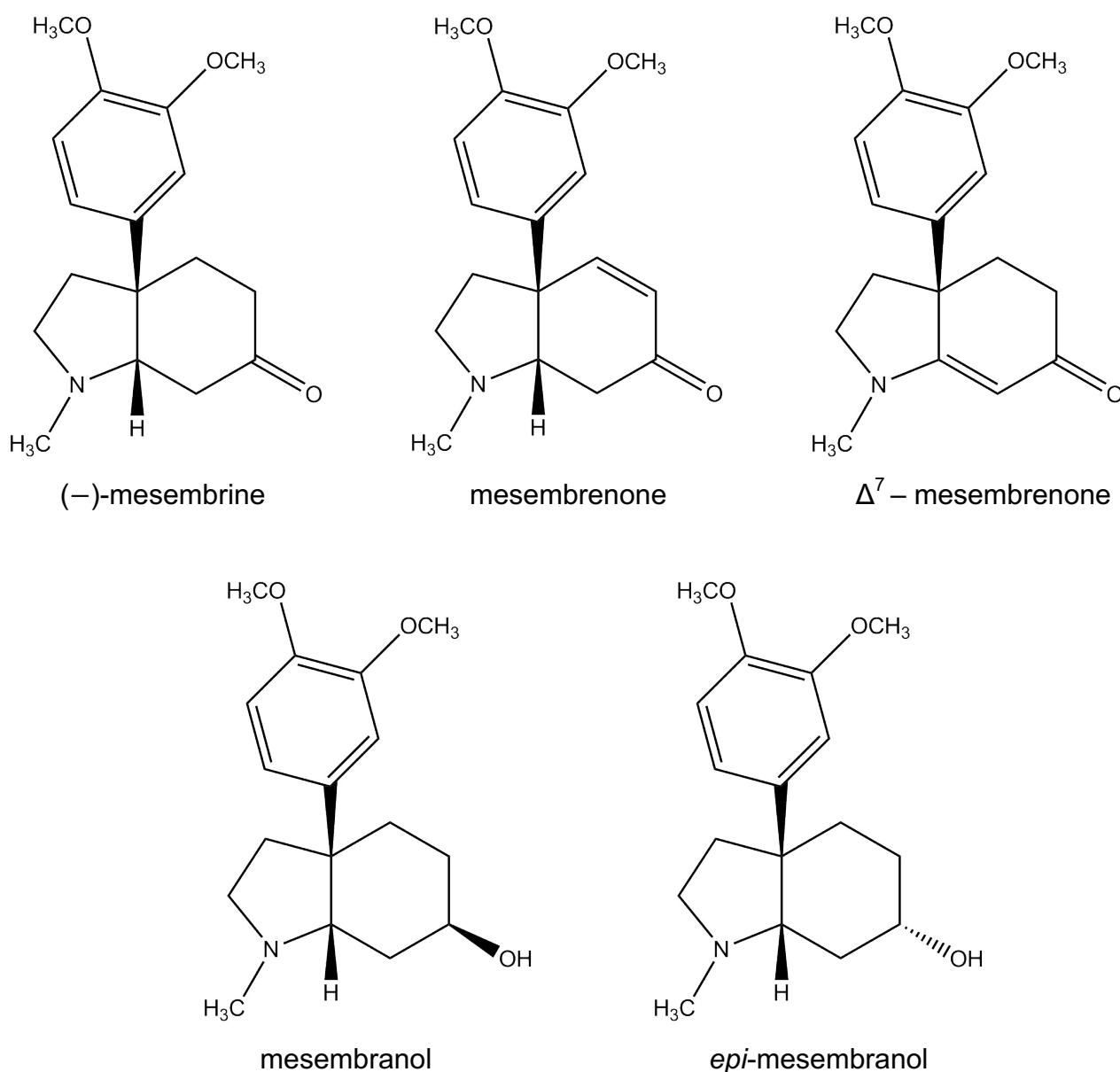


Figure 2.3: Structures of octahydroindole alkaloids found in *S. tortuosum* [5, 21, 24].

These alkaloids belong to the octahydroindole class and are biosynthesised in the plant. The proposed mechanism of biosynthesis is based on the aromatic group originating from phenylalanine and the perhydroindole ring being derived from tyrosine [21, 24]. The phenylalanine and tyrosine precursors yield two intermediates that undergo further reactions in the pathway to yield sceletenone and ultimately mesembrine (fig. 2.4) [21, 25].

Limited data is available on the exact metabolism and excretion of the mesembrine alkaloids in humans. A study by Meyer *et al* proposed pathways for the metabolism of alkaloids in the human body. Human liver preparations were incubated with 25 μM of mesembrine and mesembrenone each, the major alkaloids in *S. tortuosum*. The alkaloids were isolated from plant material by Soxhlet extraction and confirmed using nuclear magnetic resonance (NMR) spectroscopy. Their results showed that the two alkaloids can undergo either *O*-demethylation or *N*-demethylation based on the cytochrome P450 enzyme catalysing their metabolism in the liver. The enzymes that catalyse these reactions are CYP1A2, CYP2B6, CYP2C19, CYP2D6, CYP3A4, CYP3A5 and CYP2C9. Rat urinary samples were also analysed after administration of 1mg/1Kg Body Weight of *S. tortuosum*. However, these metabolites could not be identified possibly due to low formation rates of these metabolites and the concentration thereof being below the limit of detection. Ultimately, the proposed metabolic pathway pointed to various modifications that can occur that will lead to the excretion of these alkaloids. The modifications include *N*-demethylation, *O*-demethylation, hydroxylation, *N*-oxidation and reduction of the keto group. The metabolites of *O*-demethylation are excreted as glucuronides and sulfates [21, 26].

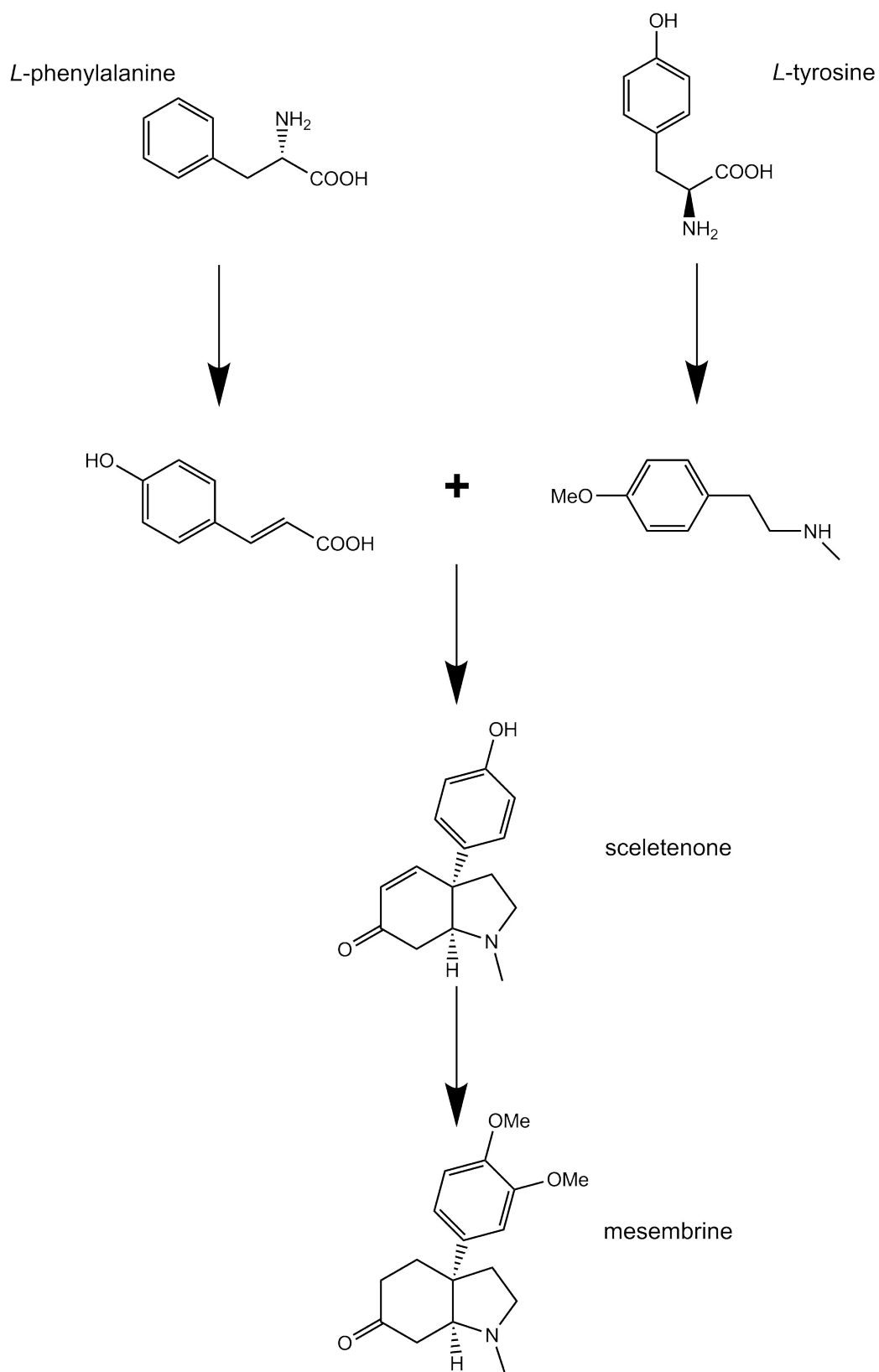


Figure 2.4: Proposed biosynthesis of alkaloids in *S. tortuosum*. Arrows represent multiple reactions in the pathway. Adapted from [21].

2.4 Physiological activity of *Sceletium tortuosum*

The bioactivity of the plant extracts has been attributed to the major alkaloids in *S. tortuosum*, which mimic the structures of well-known natural human neurotransmitters, such as serotonin. The classic indole group forms the basis of these molecules. Recently, scientific interest has developed into the potential application of these compounds in the treatment of clinical conditions such as depression, anxiety and other mood disorders. Neurologically, potential targets of alkaloids include phosphodiesterases, cholinesterases, the uptake of norepinephrine and dopamine as well as hypothalamus-amygdala coupling.

2.4.1 The influence of *Sceletium tortuosum* extracts on the neurological system

The first record of the psychotropic effects of the consumption of *S. tortuosum* was documented next to the illustration of the plant in Simon van der Stel's journal. The quote reads: "This plant is found with the Namaquaas and then only on some of their mountains... It is held by them and surrounding tribes in as great esteem as the betel or areca with the Indians. They chew its stem as well as the roots, mostly all day, and become intoxicated by it, so that on account of this effect and its fragrance and hearty taste one can expect some profit from its cultivation" [27]. These anecdotal effects have yet to be comprehensively studied.

Research into the anecdotal effects of *S. tortuosum* has yielded significant results surrounding the neurological system. A US patent in 2001 claimed that *S. tortuosum* inhibited the reuptake of 5-hydroxytryptamine (5-HT) [28]. The effects of Zembrin[®], a commercially available standardized ethanolic extract made from dried plant material, was tested on a host of receptors. Ragioligand binding assays revealed potent inhibition of the 5-HT transporter, bearing a striking resemblance to the pharmacological mechanisms of selective serotonin reuptake inhibitors (SSRIs). In this study the effect on the activity of two enzymes, specifically phosphodiesterase (PDE) and cholinesterase, was also tested. These enzymes play a role in the breakdown of cyclic adenosine monophosphate (cAMP) and acetylcholine, respectively. The results showed that Zembrin[®] fully inhibited phosphodiesterase 4 (PDE4) and inhibited phosphodiesterase 3 (PDE3) within the range of 87-89%. On the other hand, cholinesterase activity was only inhibited by 5-10% at high doses of the extract. The extract also showed slight inhibition of other phosphodiesterases. These results point to a possible mechanism of action by which *S. tortuosum* exhibits its anxiolytic and antidepressant effects [22]. At increased concentrations, the extract has

binding activity to gamma butyric acid (GABA), μ -opioid, δ 2-opioid, cholecystokinin-1, EP4 prostaglandin and melatonin-1 receptors [3, 22].

A subsequent study points to a different mechanism of action for the possible effects induced by *S. tortuosum* in which Trimesemine™, a commercially available extract, was tested. The hypothesis was that perhaps monoamine release could play a role in the effects observed when administering the extract. The data suggested that high doses of the extract inhibited the expression of the serotonin transporter (SERT) and upregulated the expression of vesicular monoamine transporter (VMAT-2), a transporter that plays a role in both monoamine release and storage [6].

Studies in humans have shown that a single dose of *S. tortuosum* reduces the connectivity between the amygdala and hypothalamus. This was assessed using magnetic resonance imaging (MRI) during a facial recognition task in response to fearful facial expressions. This data further corroborates the dual 5-HT reuptake inhibition and PDE4 inhibition reported by Harvey *et al*, suggesting that the anxiolytic potential of this extract could be due to the mitigation of the responsivity of the subcortical threat circuit [7].

While most of the data available hints at neurological involvement, a study by Swart and Smith showed that Trimesemine™, a mesembrine-rich extract, was able to modulate the production of mineralocorticoids, glucocorticoids and adrenal androgens in the adrenal [4].

2.4.2 Safety and tolerability of *Sceletium tortuosum*

A study conducted by the Tiervlei Trial Centre in South Africa evaluated the safety and tolerability of two doses of Zembrin® [29]. The two doses were 8 mg and 25 mg and the randomized, double-blind, parallel-group, placebo-controlled study was carried out over a period of 3 months. Administration of the dose was once a day to a total of 37 subjects. Twelve subjects received the 8 mg dose and twelve received the 25 mg dose. Thirteen subjects received the placebo treatment containing lactose monohydrate, sodium starch glycolate and magnesium stearate. Safety assessments and screening included the testing of vital parameters, a physical examination, tests regarding hematology, serum biochemistry and urine analysis; an electrocardiogram (ECG) and possible adverse events. The most common occurrence during the trial was headache but was considered to be independent of the medication administered in the study and not an adverse effect. The other safety

assessments and screening yielded no significant results during the treatment period. The extract was well tolerated by all subjects and the usage thereof was deemed to be safe [21, 29].

Other human trials conducted by various other research groups also using Zembrin[®], showed positive results regarding safety and tolerability in healthy humans. However, these studies comprised small groups. Larger groups may possibly have supplied concrete evidence regarding the therapeutic potential of *S. tortuosum* [21, 30, 31].

Natural remedies have come to be more widely accepted as a preferred method of treatment for many ailments in society. However, natural remedies should not be exempt from extensive scientific studies in order to ascertain either desirable effects or adverse side-effects

Chapter 3

Adrenal Steroidogenesis

3.1 Introduction

Adrenal biosynthesis of steroid hormones is a cornerstone of hormonal homeostasis. Blood pressure, stress response and sexual development are all functions that are under the control of the hormones produced in the adrenal. The production of adrenal hormones occurs in the adrenal cortex from the cholesterol precursor. A series of enzymatic reactions catalyse the formation of three classes of hormones, grouped by function: the mineralocorticoids, glucocorticoids and adrenal androgen precursors. Functionally, the adrenal androgens are important in sexual development and maturation, whereas the mineralocorticoids are responsible for the maintenance of electrolytes and water homeostasis, while the glucocorticoids play a role in a number of processes. These processes include: macromolecule metabolism and the immune and stress responses. Various disease states can be attributed to altered profiles of adrenal steroid hormones. These disease states occur due to the hindrance of enzyme activity or enzyme expression levels.

3.2 Anatomy of the adrenal gland

The adrenal glands are suprarenal endocrine organs and consist of two segments based on structure and function: the inner medulla and the outer cortex. The inner medulla is made up of chromaffin cells that produce catecholamines. The formation and production of adrenal steroid hormones occur in the cortical cells in the outer cortex. Furthermore, the adrenal cortex can be histologically subdivided into three zones. These zones are the *zona glomerulosa*, the *zona fasciculata* and the *zona reticularis* (fig. 3.1). Different classes of steroid hormones are produced and secreted by each of these zones. The *zona glomerulosa* produces the mineralocorticoids whereas the *zona fasciculata* and *zona reticularis* produce the glucocorticoids and weak androgen precursors, respectively [8–11].

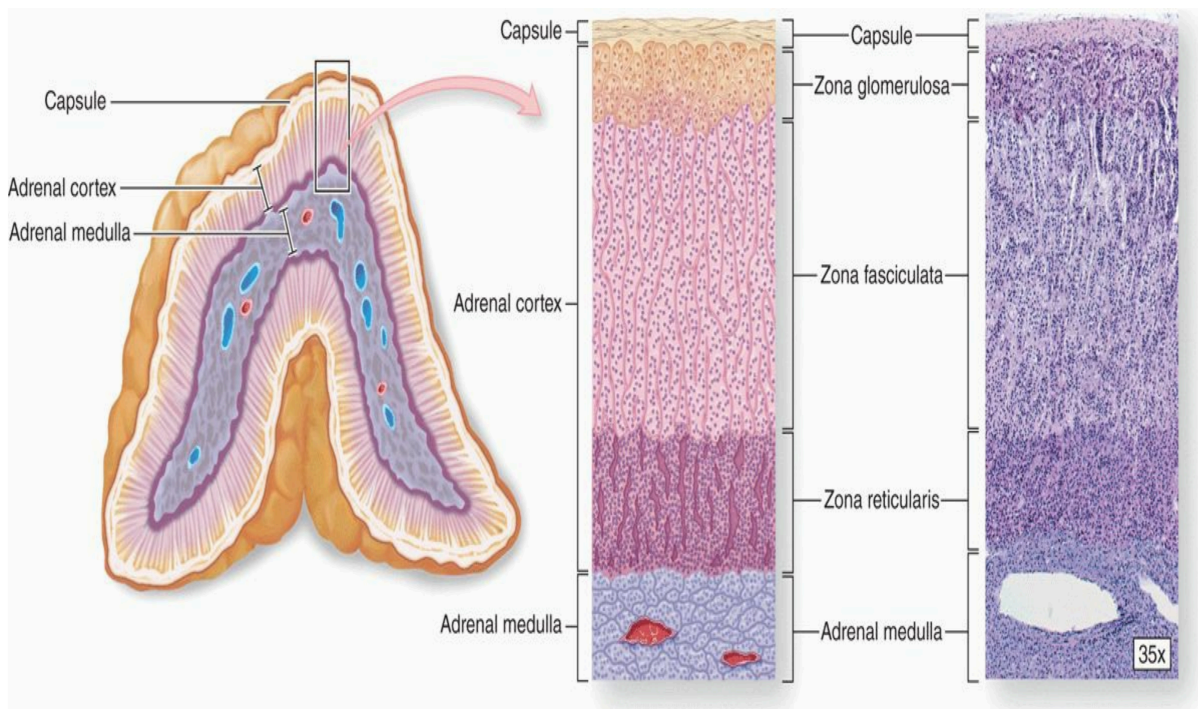


Figure 3.1 Schematic representation of the zones of the adrenal cortex [32].

3.3 Enzymes involved in adrenal steroid hormone biosynthesis

As previously mentioned, all steroid hormones are synthesised from a common precursor, cholesterol. As a result, all steroid hormones bear a close resemblance to the structure of cholesterol. The cycloperhydropentanophenanthrene ring is common to all steroids with minor variations at different carbon positions (fig. 3.2) [33].

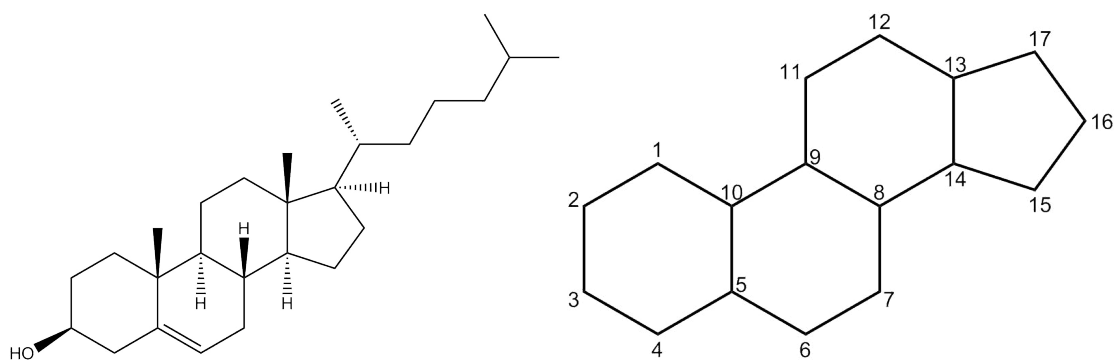
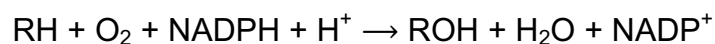


Figure 3.2: Structure of cholesterol (left) and the steroid backbone (right). Adapted from [33].

Cholesterol can be synthesised *de novo* by the human adrenal from acetate in the endoplasmic reticulum. However, the majority of the cholesterol supply is from low-density lipoproteins (LDLs) that originate from cholesterol obtained through diet [34, 35]. The initial step in adrenal steroidogenesis is the transport of cholesterol to the inner mitochondrial membrane (IMM). Steroidogenic acute regulatory protein (StAR) facilitates the transport to the IMM from the outer mitochondrial membrane (OMM) in steroidogenic cells [36, 37]. However, transport to the OMM is achieved via the binding of cholesterol to proteins that contain StAR-related lipid transfer domains [38]. The influx of free cholesterol determines the flux in the steroidogenic pathway. The transport of free cholesterol from the OMM to the IMM is therefore the rate-limiting step as the flux is completely dependent on the influx of free cholesterol. Upon entering the IMM, cholesterol is converted to the first steroid hormone in the pathway, pregnenolone (PREG) catalysed by cytochrome P450 side chain cleavage (CYP11A1 or P450scc). Subsequent enzyme-catalysed reactions occur as PREG is transported to the endoplasmic reticulum (ER) where it acts as a precursor metabolite for the production and biosynthesis of downstream adrenal steroid hormones. The enzymes that catalyse these conversions are the cytochrome P450 enzymes and the hydroxysteroid dehydrogenases (HSDs). The P450 enzymes present in the adrenal are CYP11A1 (P450scc), P450 17 α -hydroxylase/17,20 lyase (CYP17A1), P450 21-hydroxylase (CYP21A2), P450 11 β -hydroxylase (CYP11B1) and aldosterone synthase (CYP11B2), whereas the hydroxysteroid dehydrogenases include 3- β -hydroxysteroid dehydrogenase (3 β HSD), as well as low levels of 17- β -hydroxysteroid dehydrogenase (17 β HSD) and 11- β -hydroxysteroid dehydrogenase (11 β HSD) [12].

3.3.1 Cytochrome P450 enzymes

P450 enzymes are a class of oxidative enzymes known as monooxygenases. The P450 refers to pigment 450 due to the distinctive spectral property of the enzymes to absorb light at 450 nm in its reduced state. However, the inactive, reduced form of the enzyme has an absorption maximum at 420 nm [12, 39]. These enzymes function mainly by catalysing oxidative reactions using their heme center to activate molecular oxygen, and follows the general chemical reaction:



Nicotinamide adenine dinucleotide (NADPH) acts as an electron donor, linking an oxygen atom into the substrate in the form of a hydroxyl group. The P450 enzymes can be categorised biochemically in terms of their redox partner and their intracellular location. Type 1 P450 enzymes are confined to the mitochondria and function by transferring electrons from NADPH via a flavoprotein, adrenodoxin reductase, and an iron-sulphur protein, adrenodoxin, to the substrate via the heme centre of the enzyme. On the other hand, type 2 P450 enzymes are localised to the ER, with electron transfer from NADPH mediated by a dual-flavin protein, P450 oxidoreductase (POR). The electrons are first transferred to a flavinadenine dinucleotide (FAD), then to flavin mononucleotide (FMN) and lastly to the substrate (fig 3.3) [12, 40, 41].

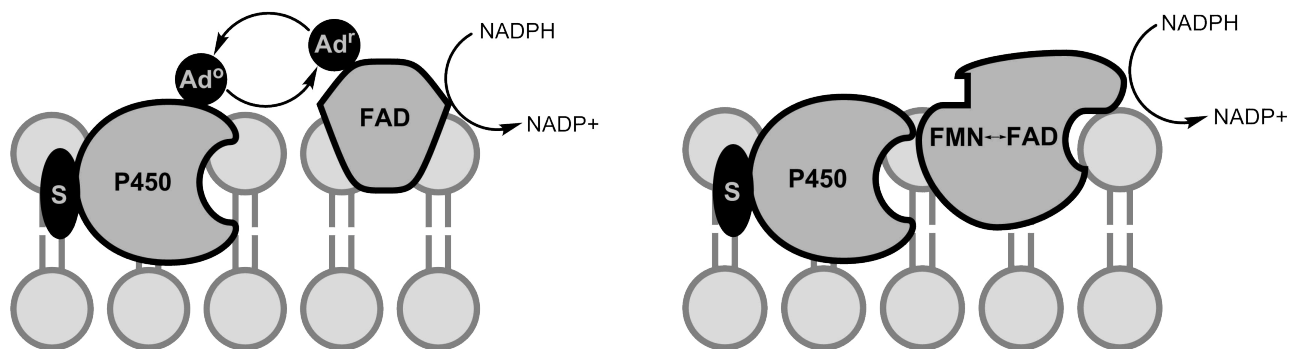


Figure 3.3 Schematic representation of electron transport systems involved in the catalytic activity of the P450 enzymes in the mitochondria (left) and microsomes (right). (Adapted from [41]).

The enzymatic reaction cycle of the P450 enzymes is a multi-step process (fig 3.4). Briefly, step 1: the enzyme exists in a resting state characterised by the low spin (LS) ferric (Fe^{III}) state, where the sixth ligand is a water molecule. Step 2: upon binding of the substrate (RH) to the enzyme, the water molecule is displaced and a high-spin enzyme-substrate complex is formed. Step 3: due to the positive reduction potential of the latter, an electron (e^-) transfer occurs and the complex is accordingly reduced to the ferrous (Fe^{II}) state. Step 4: an oxy-P450 complex is formed as a result of the binding of an oxygen molecule. Step 5a: this leads to the transfer of another electron, yielding a ferric-dioxo complex, followed

by protonation resulting in the formation of a peroxo-ferric complex (step 5b). A second protonation reaction occurs, splitting molecular oxygen. Step 6: these oxygen atoms are either bound to the ferric iron to form a reactive species, while the other is transferred to water. Step 7: the oxygen in the reactive species is transferred to the substrate, upon which the substrate is released from the active site and replaced by water, leaving the enzyme returned to the original conformation, the resting low spin state as in step 1 [42].

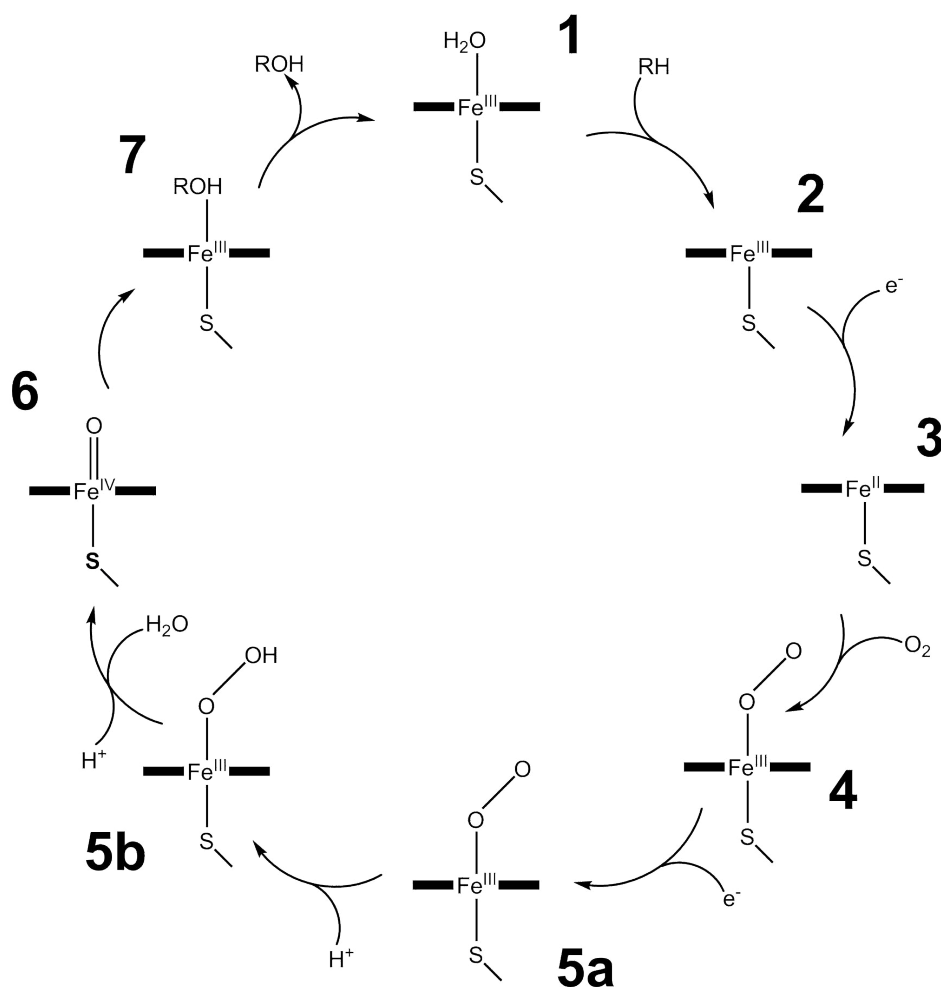


Figure 3.4: Enzymatic reaction cycle of the cytochrome P450 enzymes (Adapted from [42]).

3.3.2 Hydroxysteroid dehydrogenases

The HSDs are oxidoreductases that catalyse the conversion of hydroxyl-steroids to keto-steroids or vice versa. Based on this functionality, the HSDs can either be classified as dehydrogenases or reductases. The oxidative reaction cycle uses a cofactor, $\text{NAD}^+/\text{NADP}^+$, whereas the reductases utilize NADH/NADPH as a cofactor [12, 41, 43].

There are only three HSDs expressed in the adrenal: $3\beta\text{HSDs}$, $17\beta\text{HSDs}$ and the $11\beta\text{HSDs}$. Various types of $17\beta\text{HSDs}$ and $11\beta\text{HSDs}$ are expressed at low levels in the adrenal and mainly catalyse the conversions of steroids in peripheral tissue. However, in the adrenal, $3\beta\text{HSD2}$ is the only expressed isoform of this enzyme group. This enzyme is responsible for multiple conversions and is important for the formation of mineralocorticosteroids, glucocorticoids and androgens [41, 44, 45]. In the adrenal, $3\beta\text{HSD2}$ catalyses the formation of the Δ^4 -3-ketosteroids, progesterone (PROG), 17α -hydroxyprogesterone (17OHPROG) and androstenedione (A4), from the Δ^5 - 3β -hydroxysteroids, PREG, 17α -hydroxypregnenolone (17OHPREG) and dehydroepiandrosterone (DHEA) precursors, respectively [41].

3.4 The adrenal steroidogenic pathway

As previously stated, the initial step of steroidogenesis is the conversion of cholesterol to PREG, catalyzed by CYP11A1 in the mitochondria. After translocation to the endoplasmic reticulum PREG is subsequently directed into one of three pathways by the catalytic activity of both CYP17A1 and $3\beta\text{HSD2}$. This is a point of divergence in the steroidogenic pathway, determining whether the hormones produced are mineralocorticoids, glucocorticoids or androgen precursors. PREG is a substrate for CYP17A1, which hydroxylates the steroid to yield 17OHPREG (fig 3.5). The lyase activity, promoted by the cofactor cytochrome b5, of CYP17A1 further metabolizes 17OHPREG to yield a C19 steroid, DHEA. DHEA is an adrenal androgen precursor and the conversion thereof to A4 is catalysed by $3\beta\text{HSD2}$. CYP11B1 and $17\beta\text{HSD}$ catalyse the conversion of A4 to 11-hydroxyandrostenedione (11OHA4) and testosterone (T), respectively. This branch of the pathway is responsible for the formation of androgen precursors. The production of glucocorticoids and mineralocorticoids starts with the conversion of 17OHPREG to 17OHPROG and the conversion of PREG to PROG by $3\beta\text{HSD2}$, respectively. PROG can also be metabolized by CYP17A1 to yield 17OHPROG and 16-hydroxyprogesterone (16OHPROG), a steroid that

has not yet been elucidated in terms of function. Both 17OHPROG and PROG are further metabolized by CYP21A2 to yield 11-deoxycortisol and deoxycorticosterone (DOC). Both of these aforementioned metabolites are converted to cortisol and corticosterone (CORT) in either the glucocorticoid or mineralocorticoid pathways. CORT is subsequently converted to aldosterone (ALDO), in the mineralocorticoid branch, via the catalytic activity of CYP11B2 (fig 3.5) [12, 41, 46, 47].

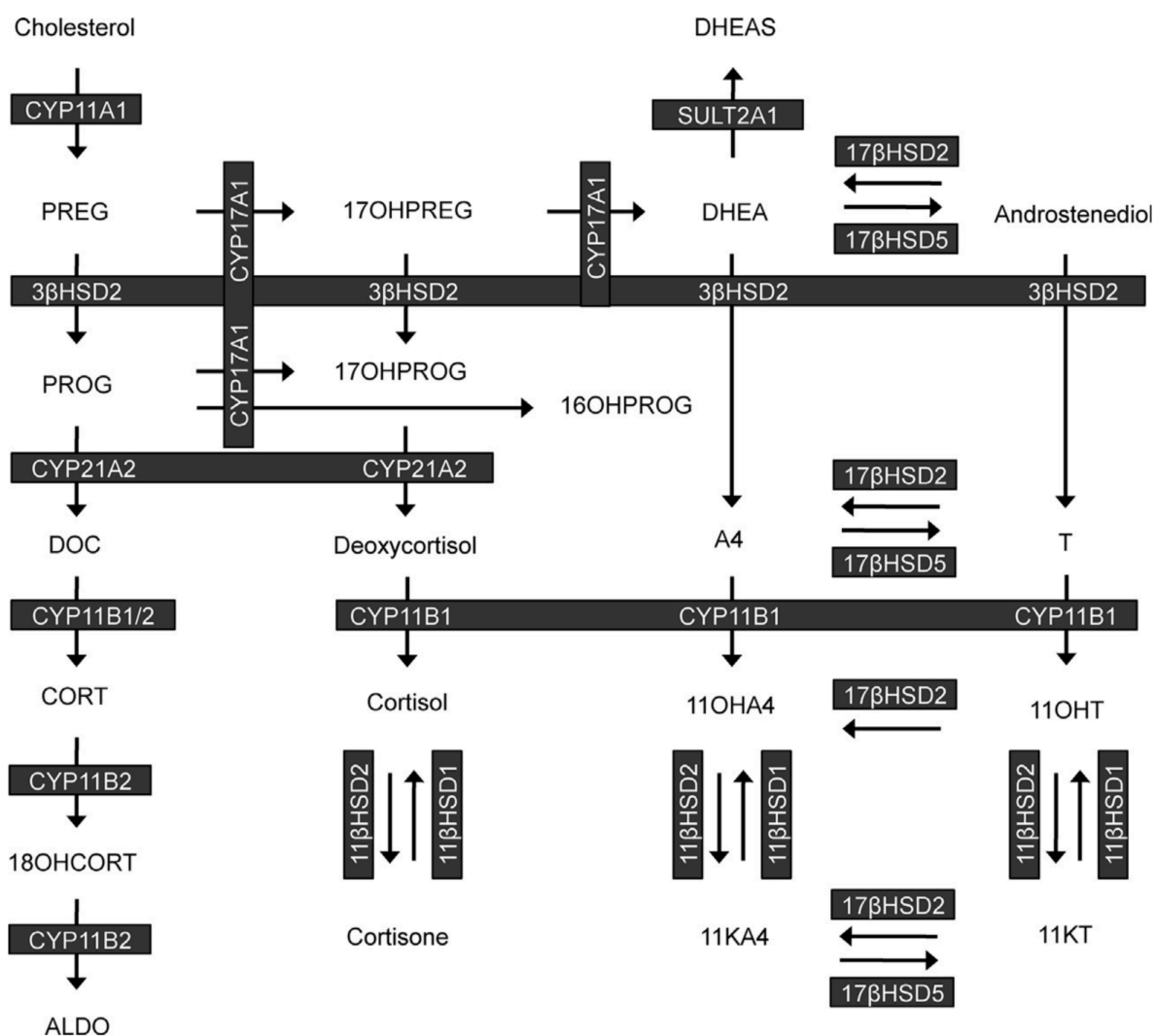


Figure 3.5: Adrenal hormone biosynthesis. Reproduced from [51].

Adrenal hormone biosynthesis is regulated and controlled by multiple systems. Adrenocorticotrophic hormone (ACTH) is one such mechanism that controls the output of adrenal hormones. It is secreted by the anterior pituitary and promotes the delivery of cholesterol to the adrenocortical cells as well as the transport thereof into the inner

mitochondrial membrane, where CYP11A1 is located [48, 49]. CYP11A1 quantitatively regulates the production of steroids whereas the expression of downstream enzymes, CYP17A1 and 3 β HSD2, being the branch-point of adrenal steroidogenesis, determines the steroid profile [12]. As the availability of cholesterol is upregulated, ACTH stimulates the formation of steroid hormones in the glucocorticoid and androgen pathways by increasing the expression of CYP11A1, CYP17A1, CYP21A2 and CYP11B1. However, the expression of CYP11B2 is regulated by the renin-angiotensin-aldosterone-system (RAAS) [41]. The mechanisms that govern the regulation and production of adrenal androgens is still unknown but there is speculation regarding the involvement of specific transcription factors controlling the expression of enzymes in the different zones of the adrenal cortex [50].

3.5 Diseases of adrenal steroid hormone biosynthesis

Due to the involvement of endocrine signalling in a myriad of physiological functions, a perturbation in the expression or activity of enzymes in the pathways that affect steroid hormones levels would impact homeostasis and lead to various clinical conditions. Several endocrine-linked diseases are characterised by abnormal steroid hormone production either due to altered enzyme expressions, or loss of stimulation from or regulation of other systems, or due to a disorder in the functioning of one or more enzymes. The role of the three steroid groups, the mineralocorticoids, the glucocorticoids, and the adrenal androgens and dysregulation of their production have various implications in disease states as based on their physiological functions.

3.5.1 Mineralocorticoids

The biologically active mineralocorticoid that is secreted by the adrenal cortex is aldosterone. Aldosterone plays an essential role in the regulation of water and electrolyte balance as well as blood pressure via its interaction with the mineralocorticoid receptor (MR). Abnormalities in the biosynthesis and metabolism of aldosterone will therefore lead to perturbations of the concentrations of electrolytes such as potassium, sodium and hydrogen, ultimately affecting an individual's ability to maintain normal blood pressure. Adrenal disorders which affect mineralocorticoid production will trigger compensatory pathways leading to abnormal stimulation, resulting in increased upstream steroid biosynthesis and attenuated hormonal effects in target tissues.

Disorders of the mineralocorticoid pathway include 11 β -hydroxylase deficiency (CYP11B), 17 α -hydroxylase (CYP17A1) deficiency and adrenal hyperplasia or adenoma; and could lead to disease states such as acquired primary adrenal failure, secondary aldosterone deficiency and primary aldosterone excess. As an example, 17 α -hydroxylase deficiency leads to a disease state characterized by lowered cortisol production, an increase in the production of ACTH and in turn the overstimulation of adrenal steroidogenesis. The overproduction of DOC is also prominent in this state, which leads to sodium retention resulting in hypertension and hypokalemia [12, 52]

3.5.2 Glucocorticoids

The biosynthesis of glucocorticoids is controlled by ACTH and the amount of cortisol secreted by the adrenal is directly proportional to ACTH stimulation. Glucocorticoid disorders can be divided into two categories, hypocortisolism and hypercortisolism. The latter is characterized by an excess production of cortisol and is due to lack of responsiveness to ACTH, an external source of stimulation other than ACTH, or an overproduction of ACTH in the pituitary gland. Hypocortisolism can be due to the lack of ACTH production or failure of the adrenal gland to synthesize cortisol in response to ACTH [53]. The primary function of cortisol is the regulation of carbohydrate, lipid and protein metabolism [35]. Glucocorticoids also play a vital role in the stress and immune response. Cortisol release is associated with immune suppression and the prevention of the onset of autoimmune diseases. Binding of cortisol to the glucocorticoid receptor (GR) results in the inhibition of transcription factors such as nuclear factor kappa B (NF- κ B) and attenuates the expression of genes encoding inflammatory regulators [54]. An example of a disease of glucocorticoid biosynthesis is Cushing's syndrome. It is as a result of chronic hypercortisolism that is caused by defects in the secretion of ACTH from the pituitary gland. Patients present with obesity, due to impeded lipid metabolism, hypertension, insulin resistance and hirsutism [55].

3.5.3 Adrenal androgens

Adrenal androgens are important precursor metabolites in the biosynthesis of more potent androgens. These potent androgens are essential for sexual development and maturation. However, the excessive or diminished production of adrenal androgens is characteristic of disease states such as congenital adrenal hyperplasia (CAH). The most common type of

CAH is caused by a disorder known as 21-hydroxylase deficiency (21-OHD). Due to the absence of catalytically active or presence of a partially active CYP21A2 to catalyse its reactions, the levels of PROG, 17OHPROG and DHEA is increased. This is a characteristic clinical manifestation and the levels of 17OHP4 is often used as a diagnostic tool. Classically, patients present with hirsutism, disturbance in the menstrual cycles and acne and alopecia [12, 56].

3.5 *Sceletium tortuosum* and the steroid pathway

The *S. tortuosum* alkaloids are well studied in the neurological system. However, the anecdotal effects of *S. tortuosum* cannot only be attributed to neurological signalling and it has been shown that endocrine signalling plays a role as well.

S. tortuosum was used in a rat study by Smith *et al*, which focused on the behaviour and changes in the levels of hormones and cytokines in the blood. Administration of the *S. tortuosum* extract for 17 days decreased the basal levels of CORT as well as the serum CORT response that was induced by stress by ~20%. This resulted in a calming effect shown by the ~30% decrease in self-soothing behaviour [57]

These studies demonstrate the *in vivo* effects of *S. tortuosum* but do not clarify the manner in which *S. tortuosum* acts to exhibits these effects. A study in an adrenal cancer cell model, H295R cells, by Swart and Smith showed that the inhibitory effects on adrenal steroidogenic enzymes detected were not only due to central nervous system perturbations, but also due to the modulation of adrenal hormone biosynthesis. This study showed the inhibitory effects of *S. tortuosum* on the production of steroids that impact the endocrine system in a cell model, that expresses all the enzymes that catalyse adrenal steroidogenesis and has the full complement of adrenal steroid hormones. This allows for a better understanding of steroid hormone biosynthesis without the interference of exogenous compounds and endogenous feedback systems [4, 58]. The study revealed that *S. tortuosum* does indeed play an inhibitory role on the adrenal steroidogenesis pathways. An extract of *S. tortuosum*, containing high mesembrine levels, inhibited CYP17A1 marked by decreased levels of 16OHPROG and increased levels of PREG. This study also suggested that at increased concentrations of *S. tortuosum*, 3 β HSD2 activity was also inhibited [4]. However, a whole cell model does not fully clarify the specific inhibitory actions on individual enzymes. It has therefore become necessary to determine the inhibitory effects of *S. tortuosum* on the

steroidogenesis pathway by assessing its influence on the individual enzymes in the pathways. This would allow for the characterization of *S. tortuosum* as a possible treatment for disease states in which pathways and enzymatic activities are affected, such as in states of chronic or acute stress and inflammation, since the influence of *S. tortuosum* on the individual enzymes have not been fully investigated.

Chapter 4

The development and validation of a UPC²-MS/MS method for analysis of endogenous adrenal steroids

4.1 Introduction

Supercritical fluid chromatography (SFC) merges the benefits of both gas chromatography-mass spectrometry (GC-MS) and liquid chromatography tandem mass spectrometry (LC-MS/MS). GC-MS offers good resolution and sensitivity but sample preparation does not allow for high-throughput analysis. Although LC-MS/MS does not require the sample preparation required for GC-MS, it does not, however, achieve the resolution of GC-MS. UPC², an SFC system, when coupled to highly sensitive tandem mass spectrometry, is a robust tool for separating and quantifying trace amounts of compounds such as complex steroid hormones that do not differ significantly in terms of structure [59–61].

The objective of this investigation was to study the effect of *S. tortuosum* on adrenal steroidogenesis in H295R cells. These cells are routinely used to study the effects of exogenous compounds on steroid hormone production *in vitro*. Using various stimulatory techniques, the production of steroids can be modified to achieve a desired output and to elucidate effects of exogenous compounds on regulatory mechanisms. The US EPA has designated H295R cells to be used in the testing of endocrine disruptors such as pesticides and other toxic substances. However, the only interest of the US EPA is the influence of these compounds on PROG, T and estrogen.

Accurate analysis of adrenal steroid hormones is critical in the assessment of natural products on adrenal steroidogenesis. Establishing steroid profiles that are as a result of perturbations to the cell system, can shed much light on steroidogenic pathways in the adrenal and the influence of the natural products on the system.

The aim of this study was to develop and validate a method using UPC²-MS/MS to separate and quantify adrenal steroid hormones to investigate the effects of *S. tortuosum* on adrenal

steroidogenesis. In addition, the method was applied in the determination of the K_m and V_{max} values of CYP11B1 for A4 and T in the biosynthesis of 11OHA4 and 11OHT.

4.2 Methodology

4.2.1 Reagents

4.2.1.1 Steroid standards

Pregnenolone, (PREG), progesterone (PROG), 17α -hydroxyprogesterone (17OHPROG), dehydroepiandrosterone (DHEA), androstenedione (A4), testosterone (T), deoxycorticosterone (DOC), corticosterone (CORT), aldosterone (ALDO), 16-hydroxyprogesterone (16OHP4), 18-hydroxycorticosterone (18OHCORT), cortisol and 11-deoxycortisol were purchased from Sigma-Aldrich (St. Louis, MO, USA). 11α -hydroxyandrostenedione (11OHA4), 11α -hydroxytestosterone (11OHT), 11α -hydroxyprogesterone (11α OHP4) and 11β -hydroxyprogesterone (11β OHP4) were purchased from Steraloids (Newport, RI, USA).

4.2.1.2 Internal standards

Progesterone-2, 2, 4, 6, 6, 17α , 21, 21, 21- d_9 (Prog- d_9), 4-androsten-3,17-dione 2,2,4,6,6,16,16- d_7 (A4- d_7) and testosterone-1, 2- d_2 (T- d_2) were purchased from Cambridge Isotopes (Tewksbury, MA, USA).

4.2.1.3 Solvents

Formic acid and methyl *tert*-butyl ether (MTBE) were purchased from Sigma-Aldrich (St. Louis, MO, USA). UHPLC-grade methanol was purchased from Merck (Darmstadt, Germany). FOODFRESH CO₂ was purchased from Afrox (Cape Town, South Africa).

4.2.2 Preparation of standards and samples

Steroids stocks of all the reference standards were prepared in absolute ethanol, each at a concentration of 1 mg/mL and stored at -20 °C until needed. Two standard master mixes,

1000 ng/mL and 1 ng/mL, were prepared in methanol from the individual stock solutions and contained all the reference steroids. Methanol was used as the solvent because it has no matrix effect. The master mixes were subsequently used to prepare the calibration standards, which ranged from 0.01 to 250 ng/mL, by adding the required volume of master mix to deionized water (no matrix) as well as to DMEM samples containing 1% penicillin-streptomycin and 10% fetal bovine serum (matrix).

4.2.3 Steroid extractions

An internal standard master mix, 100 μ L, containing 1.5 ng Prog- d₉, 1.5 ng A4-d₇ and 1.5 ng T-d₂ was prepared in deionized water and added to the standards prepared in deionized water and to the standards prepared in DMEM prior to steroid extraction. Extraction was carried out using a 1:3 ratio of sample to MTBE (vol/vol) and shaking the samples at 800 rpm for 5 minutes prior to incubation at -80 °C for an hour. This step allows the aqueous phase to freeze. The MTBE layer, containing the extracted steroids, was transferred to glass test tubes after which the MTBE was evaporated at 55 °C under a stream of nitrogen gas. The dried residues were resuspended in 150 μ L 50% methanol and stored at -20 °C pending analysis. Steroid standards were also prepared in 50% methanol, not subject to extraction, to which the deuterated internal steroid master mix was added, dried and resuspended, termed as pure reference steroids.

4.2.4 Instrumentation

The analytes were separated using an Acquity UPC² BEH C₁₈ column (2.1 mm \times 100 mm, 1.7 μ m particle size) with an Acquity UPC² system (Waters Corporation, Milford, USA). Quantitative mass spectrometric detection was carried out using a Xevo TQ-S triple quadrupole mass spectrometer (Waters, Milford, USA).

4.2.5 Chromatographic conditions

The mobile phase consisted of liquid CO₂ modified with methanol. The elution gradient used is shown in Table 4.1.

The injection volume was 2.0 μL and a continuous flow rate of 2.0 mL min^{-1} was maintained. The column temperature and automated back pressure regulator (ABPR) were set to 60 $^{\circ}\text{C}$ and 2000 psi, respectively. All steroids were scanned in multiple reaction monitoring (MRM) mode (table 4.2) using an electrospray probe in the positive ionization mode (ESI+). The instrumental settings were: capillary voltage of 3.7 kV, source temperature 150 $^{\circ}\text{C}$, desolvation temperature 350 $^{\circ}\text{C}$, desolvation gas flow 900 L/h and cone gas flow 150 L/h. Data assembly and analysis were performed using MassLynx 4.1 (Waters Corporation).

The UPC² eluent, methanol containing 1% formic acid, was mixed with the makeup fluid to ensure the ionization of the steroids by the electrospray probe. As was reported by Quanson *et al*, the eluent was shown to provide good ionization efficiency for all the analytes at the ideal flow rate of 0.2 mL/min [59].

Table 4.1: UPC² solvent parameters for the chromatographic separation of the analytes.

Time (min)	Flow rate (mL/min)	%A (CO ₂)	%B (Methanol)	Curve Gradient
Initial	2	96	4	0
1.5	2	92	8	6
1.6	2	75	25	6
1.8	2	75	25	6
2.5	2	96	4	6

4.2.6 Method validation

The standards prepared in either matrix (DMEM containing 5% pen-strep and 10% FBS) or deionized water were used to generate standard curves for each steroid metabolite. The standard range consisted of the following concentrations: 0, 0.01, 0.05, 0.1, 0.25, 0.5, 1.0, 5.0, 10, 25, 50, 100 and 250 ng mL^{-1} . The lowest concentration of the quantifier ion with a signal-to-noise (S/N) ratio greater than 3 was used to establish the limit of detection (LOD) for each analyte. The limit of quantification (LOQ) was based on both the quantifier and qualifier ion. The lowest concentration for each steroid at which a S/N ratio greater than 10 was measured for the quantifier ion, and a S/N ratio greater than 3 measured for the qualifier ion determined the LOQ. Accuracy and precision were determined for the following

concentrations: 5, 50 and 100 ng mL⁻¹. Precision was defined as the %RSD of the average response following the repeated injection (n = 4) of the same sample. Accuracy was defined as the %RSD of the average response from the analysis of independent replicate samples (n = 4). Recovery, matrix effect and process efficiency were determined at three concentrations (5, 50 and 100 ng mL⁻¹, n = 3) for each metabolite using the process described by Taylor et al [62]. Briefly, matrix effects were determined by comparing the response of standards prepared in media (DMEM containing 5% pen-strep and 10% FBS) and extracted as described above to that of standards prepared in deionized water and extracted and was calculated as follows: the difference in response between the samples prepared in deionized water and the DMEM standards representative of matrix effects were divided by the response of the DMEM standards. Recovery was determined by comparing the steroid standards which had been prepared in deionized water and extracted to the equivalent pure reference steroids. The process efficiency, which is the collection of recovery and matrix effects, was calculated by comparing the response of DMEM standards to that of the response of the pure reference steroids.

Table 4.2: Molecular ion species (analyte and abbreviation), MRM mass transitions (quantifier and qualifier), mass spectrometer conditions (cone voltage, collision energy) and retention time for each analyte. Internal standard: PROG-d₉, A4-d₇, T-d₂.

Analyte	Abbreviat ion	Mass Transitions		Cone Voltage		Collision Energy		Retention Time
		Quantifier	Qualifier					
Pregnenolone	PREG	317.24 > 281.24	317.24 > 159.07	16	16	12	18	1.17
Progesterone	PROG	315.2 > 97	315.2 > 109	28	28	20	26	0.74
17-hydroxyprogesterone	17OHPROG	331.1 > 97	331.1 > 109	26	26	22	28	1.39
Dehydroepiandrosterone	DHEA	271.2 > 253.2	271.2 > 243	30	30	15	15	1.21
Androstenedione	A4	287.2 > 96.9	287.2 > 108.8	30	30	15	15	0.82
11-deoxycorticosterone	DOC	331.18 > 96.98	331.18 > 108.97	28	28	22	26	1.15
11-deoxycortisol	S	347.3 > 109.1	347.3 > 97.1	30	30	30	26	2.05
Testosterone	T	289.2 > 97.2	289.2 > 109	30	30	22	22	1.56
Corticosterone	CORT	347.2 > 121.1	347.2 > 97.1	26	26	20	20	2.13
Cortisol	F	363.3 > 121.1	363.3 > 97.1	26	26	23	30	2.24
Aldosterone	ALDO	361 > 343	361 > 315	30	30	18	20	2.20
11 α -hydroxyandrostenedione	11OHA4	303.2 > 267.2	303.2 > 121	30	30	15	30	1.70
11-hydroxytestosterone	11OHT	305.3 > 269	305.3 > 121	35	35	15	20	2.23
11 α -hydroxyprogesterone	11 α OHP4	331.2 > 295.2	331.2 > 121	30	30	15	30	2.09
11 β -hydroxyprogesterone	11 β OHP4	331.2 > 121	331.2 > 295	30	30	20	20	1.86
16-hydroxyprogesterone	16OHP4	331.2 > 108.9	331.2 > 97	30	30	15	15	2.06
18-hydroxycorticosterone	18OHCORT	363.2 > 269.2	363.2 > 147	30	30	15	22	2.35
Progesterone-2, 2, 4, 6, 6, 17 α , 21, 21, 21-d ₉	PROG-d ₉	324.2 > 100	324.2 > 113	30	30	20	25	0.73
4-androsten-3,17-dione 2,2,4,6,6,16,16-d ₇	A4-d ₇	294.3 > 100	294.3 > 113	25	25	25	25	0.82
Testosterone-1, 2-d ₂	T-d ₂	291 > 111.2	291 > 99.1	30	30	30	20	1.56

4.3 Results

A UPC²-MS/MS was developed that can be used to identify and quantify 17 adrenal steroids, including all of the adrenal steroid pathway metabolites, with the exception of 17OHPREG in 2.5 minutes using a 1.7 μm particle size, BEH C₁₈ column. The chromatograms for each metabolite are depicted in figure 1.

4.3.1 Calibration Range

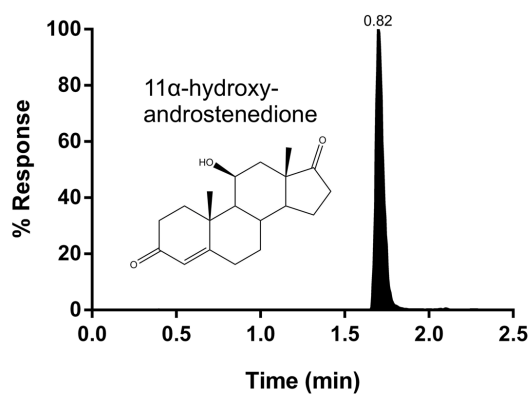
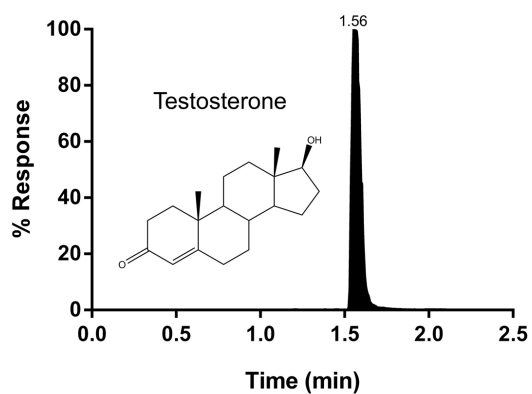
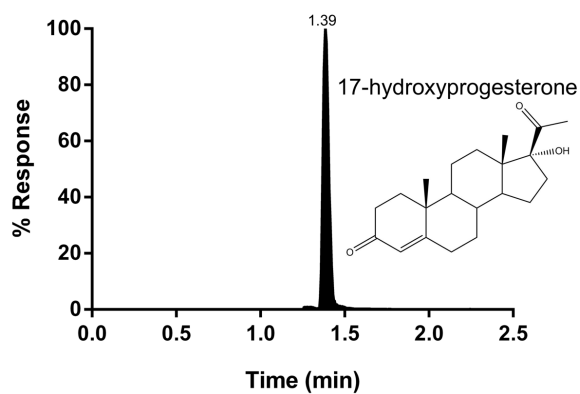
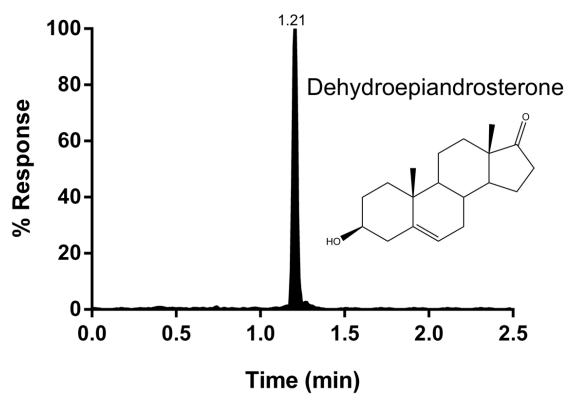
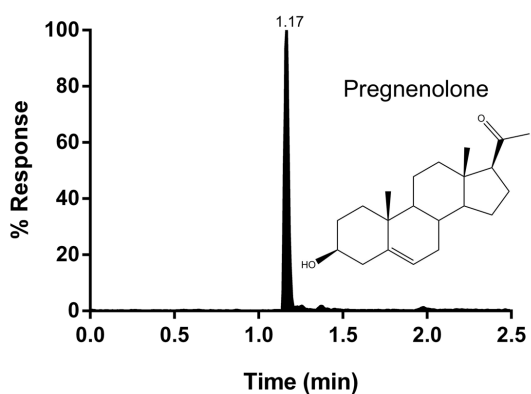
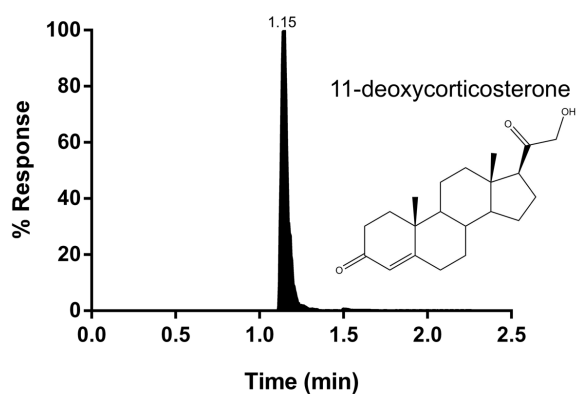
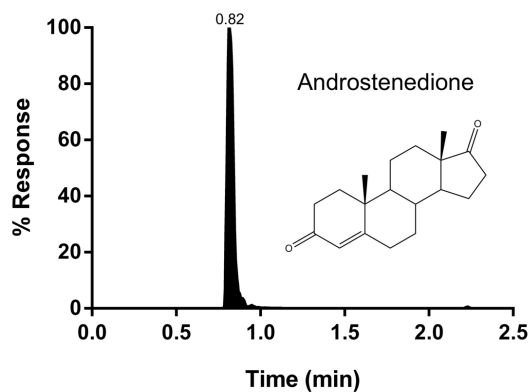
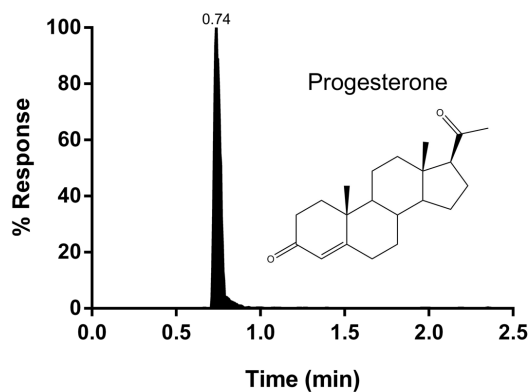
Method validation was performed for all the metabolites. LOQs ranged from 0.01 to 25 ng/mL. Quadratic fits with acceptable r^2 -values were obtained for standard curves, which included a 250 ng/mL standard but due to saturation of the detector, linearity of the standard curves was compromised at this concentration. This standard was therefore excluded and the upper limit of quantification (ULOQ) was determined to be 100 ng/mL.

4.3.2 Accuracy and precision

Accuracy and precision were determined at three concentrations within the calibration range for each steroid (table 4.3). Acceptable %RSDs were acquired for the three concentrations for both accuracy and precision. Both accuracy and precision were less than 20% at all three concentrations.

4.3.3 Recovery, matrix effects and process efficiency

Recovery, matrix effect and process efficiency are shown in Table 4.4. Recovery ranged from 28.8 to 189.0 % for all concentrations (5, 50 and 100 ng/mL). Matrix effects ranged from 52.5% ion suppression for 18OHCORT to 73.1% ion enhancement for 11OHT. The process efficiency ranged from 39.8 to 139.2% at a concentration of 5 ng/mL. At higher concentrations (50 and 100 ng/mL), the process efficiency ranged from 49.0% to 135.4%.



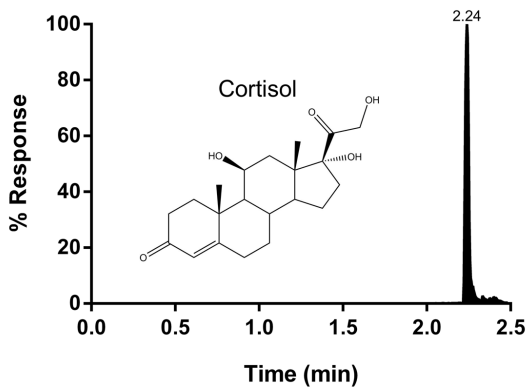
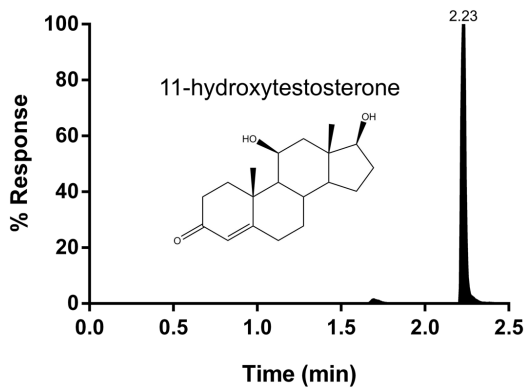
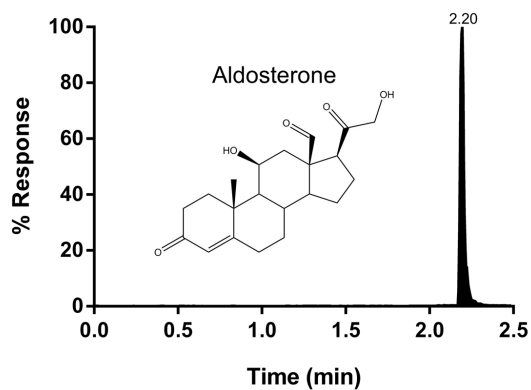
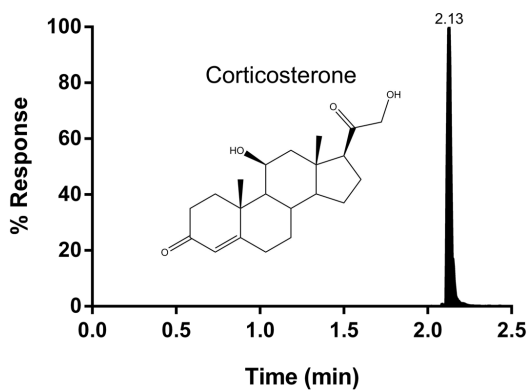
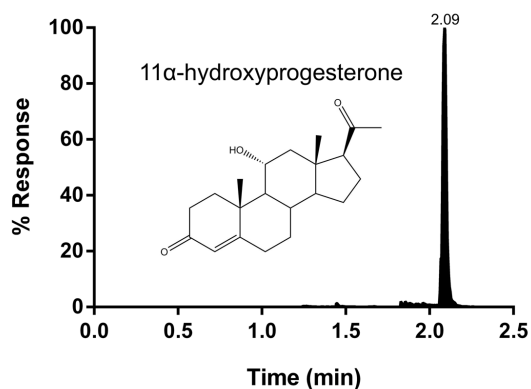
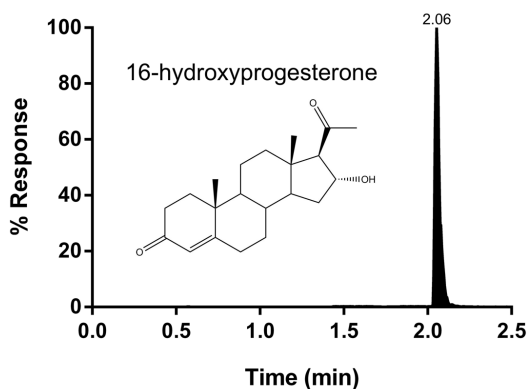
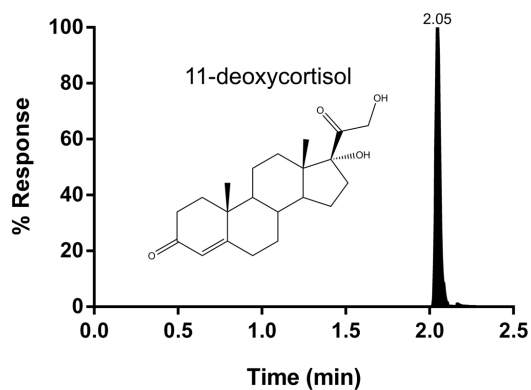
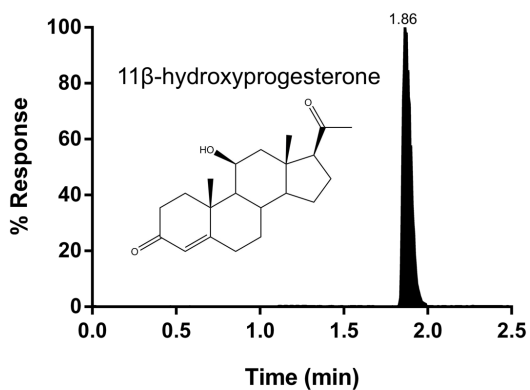


Table 4.3: Method validation data: LOD (ng/mL), LOQ (ng/mL), r^2 , accuracy (%RSD, n = 4) and precision (%RSD, n = 4).

Analyte	LOD (ng/mL)	LOQ (ng/mL)	r^2	Accuracy %RSD			Precision %RSD		
				Response Area			Response Area		
				5 ng/mL	50 ng/mL	100 ng/mL	5 ng/mL	50 ng/mL	100 ng/mL
PREG	0.5	1	0.9797	2.7	3.9	5.5	4.2	12.6	2.7
PROG	0.05	0.1	0.9946	13.3	10.0	4.6	6.5	16.4	11.8
17OHPROG	0.05	0.1	0.9792	3.8	6.9	2.7	8.6	18.6	4.2
DHEA	5	25	0.9692	<LOQ	5.9	3.6	<LOQ	14.2	3.0
A4	0.01	0.01	0.9892	3.9	9.9	1.6	16.4	16.4	13.8
DOC	0.01	0.05	0.9972	8.5	2.6	0.6	10.1	6.7	5.1
S	0.25	0.25	0.9991	2.7	4.6	7.2	11.0	14.0	4.9
T	0.01	0.01	0.9933	5.2	0.7	3.4	5.7	9.8	1.4
CORT	0.1	0.25	0.9917	7.1	13.2	10.0	8.8	12.4	5.1
F	0.01	0.01	0.9959	4.8	0.9	2.3	4.5	4.7	0.6
ALDO	5	5	0.9876	2.0	0.8	7.8	3.7	7.9	13.4
11OHA4	0.01	0.01	0.9909	4.8	3.9	1.9	8.9	10.8	3.0
11OHT	0.25	0.5	0.9993	4.2	2.6	1.7	6.8	3.4	5.7
11 α OHP4	0.05	0.1	0.9700	5.3	16.7	3.8	11.7	13.1	19.4
11 β OHP4	0.05	0.25	0.9895	1.4	1.3	1.2	8.6	0.7	4.2
16OHP4	0.05	0.1	0.9982	5.4	4.8	6.0	5.1	9.8	18.9
18OHCORT	0.25	0.5	0.9966	5.4	10.7	6.3	17.0	14.2	11.2

Table 4.4: Method validation data: Recovery (%; n = 3); Matrix Effect (%; n = 3) and Process Efficiency (%; n = 3).

Analyte	Recovery (%)			Matrix Effect (%)			Process Efficiency (%)		
	5 ng/mL	50 ng/mL	100 ng/mL	5 ng/mL	50 ng/mL	100 ng/mL	5 ng/mL	50 ng/mL	100 ng/mL
PREG	28.8	54.7	81.2	38.2	-10.5	4.2	39.8	49.0	84.6
PROG	90.0	53.8	133.9	-9.8	2.0	-29.6	81.2	54.8	94.2
17OHPROG	104.5	64.6	99.3	-15.7	-7.3	-17.2	88.1	59.9	82.2
DHEA	<LOQ	64.8	84.0	<LOQ	-7.0	-10.3	<LOQ	60.3	75.3
A4	95.1	76.3	121.9	-14.3	-14.6	-28.7	81.6	65.2	86.9
DOC	84.4	69.4	85.0	11.9	28.9	-21.0	94.5	89.5	67.2
S	143.7	71.3	116.2	-30.0	20.9	-24.5	100.6	86.2	87.7
T	56.9	56.8	94.9	3.2	20.4	-2.1	58.7	68.4	93.0
CORT	124.9	63.9	115.6	11.4	20.3	-25.2	139.2	77.0	86.4
F	102.6	49.9	61.2	1.6	34.1	-19.9	104.2	67.0	49.0
ALDO	<LOQ	67.2	81.1	<LOQ	56.3	-39.1	<LOQ	105.0	49.3
11OHA4	93.3	60.7	102.7	-17.7	-9.3	-19.9	76.8	55.0	82.3
11OHT	36.9	41.7	78.5	73.1	46.9	-16.2	63.9	61.2	65.8
11 α OHP4	54.4	95.9	104.5	37.1	3.3	29.5	74.6	99.0	135.4
11 β OHP4	61.4	85.9	83.8	17.8	1.4	4.2	72.4	87.1	87.3
16OHP4	147.6	177.8	90.3	-17.9	-24.7	33.7	121.1	133.9	120.7
18OHCORT	189.0	65.1	83.7	-52.5	20.8	7.2	89.8	78.6	89.8

4.4 Discussion

The UPC²-MS/MS method which was developed and validated enables the separation and quantification of seventeen steroids characteristic of the adrenal output. This method can be used to study steroid metabolism in whole cell models, specifically H295R cells, which will be undertaken in the next chapter. H295R cells are an immortalised adrenal cancer cell model that expresses the full complement of steroidogenic enzymes that catalyse the biosynthesis of adrenal hormones [58]. These cells can be stimulated to mimic physiological conditions and modulate steroid production. In addition, these cells are an ideal system to study the effects of medicinal plants on the hormones produced by the adrenal gland.

In an investigation into the influence of Rooibos on the endocrine system, Schloms *et al* previously described a UHPLC-MS/MS method separating and quantifying 21 adrenal steroid hormones [47]. However, the lowest and highest standard was 0.2 ng/μL and 4000 ng/μL, respectively. The total run time was 13 minutes with LOQs ranging from 0.2 to 500 ng/mL. Comparatively, the UPC²-MS/MS method offers a shorter run time of 2.5 minutes and LOQs ranging from 0.1 – 25 ng/mL. This is an improvement to the UHPLC method as high-throughput analysis can be obtained due to a shorter run time, saving both time and cost. The LOQs demonstrate the sensitivity of the UPC²-MS/MS system and allows for more accurate quantification of steroid metabolites, especially in whole cell systems where only trace amounts may be present. The UPC²-MS/MS method also takes into consideration the effects of the matrix thereby accounting for the enhancement and suppression of ions, that could potentially result in inaccurate quantification. This can be overcome if both the samples and standards are prepared in the same matrix and extracted under the same conditions. Low recovery and process efficiency can be compensated for by the pre-extraction addition of internal standards with subsequent normalisation accommodating steroid loss during the sample preparation process.

The method described in this aim will be used to analyse the effects of *S. tortuosum* on steroid hormone levels in assays performed in H295R cells and on specific steroidogenic enzymes in substrate conversion assays. Another advantage of using this method, is that samples consisting of substrate and product collected in conversion assays can be pooled and multiplexed. This involves the cost effective analysis of multiple samples in a single chromatographic run. The application of this will be described later. Ultimately, this method

can be extended to quantify physiological levels of steroid hormones in complex biological media.

4.5 Implementation of the UPC²-MS/MS method: kinetic characterization of CYP11B1 towards A4 and T

The adrenal produces 11OHA4, which is quantitatively, the largest contributor in terms of adrenal androgen output, with the exception of DHEA and DHEA-S [13]. It was assumed for many decades that 11OHA4 was a dead-end adrenal product with no particular function. Our laboratory recently reported that CYP11B1 and CYP11B2 is capable of hydroxylating A4 and T to form 11OHA4 and 11OHT, however the conversion by CYP11B2 was negligible and possibly not physiologically relevant [14]. First labeled as a weak androgen precursor, the metabolic fate of 11OHA4 has since been determined. It has been shown to be metabolized in peripheral steroidogenic tissue to the more potent androgens, 11KT and 11KDHT, the latter being a keto-derivative of DHT. The novelty of this discovery has led to renewed interest in 11OHA4. In prostate cells, it has been shown to be the initial steroid substrate in a new pathway, the 11OHA4 pathway, where a number of catalytic steps, through the action of 5 α -reductase (SRD5A), 11 β HSD and 17 β HSD, ultimately yield 11KDHT [63]. Prostate cancer (PCa) tissue and plasma analyses has shown that the levels of 11OHA4, 11KT and 11KDHT are significantly higher than A4, T and DHT [15]. Due to the output of the adrenal resulting in high levels of 11OHA4, it is therefore essential to characterize the kinetic parameters of the novel CYP11B1 substrates, A4 and T. As kinetic determination experiments are laborious and sample numbers are substantial, requiring efficient sample collecting and analysis. The UPC²-MS/MS method described above permits multiplex analysis, resulting in a 50% decrease in samples and cost, due to the efficient application of the method in the kinetic characterization of CYP11B1 towards A4 and T.

4.5.1 Cell culture and transfection

Human embryonic kidney 293 (HEK-293) cells were purchased from American Type Culture Collection (Manassas, USA). Plasmid constructs pCMV-hCYP11B1 was a kind gift from Prof Walter Miller (University of California, San Francisco) and the ADX (adrenal ferredoxin) vector construct was donated by Prof RC Tuckey (The University of Western Australia, Crawley). The pCI-neo plasmid construct, used as a negative control alongside transient transfections, was purchased from Promega (Madison, USA). HEK-293 cells were cultured

in DMEM supplemented with 1.5 g NaHCO₃, 10% FBS and 1% penicillin-streptomycin. The culture environment was 37°C, 5% CO₂ and a relative humidity of 90%. Confluent cells were seeded into Corning® CellBIND® surface 100mm culture dishes at a density of 2 x 10⁵ cells/mL and incubated for 24 hours. After 24 hours, HEK-293 cells were transiently co-transfected with 5 µg pCMV-hCYP11B1/dish and 5 µg pCIneo-hADX/dish using XtremeGene DNA transfection reagent, according to manufacturer's instructions.

4.5.2 Conversion of A4 and T by CYP11B1 in transiently transfected HEK-293 cells

Transiently transfected HEK-293 cells were incubated for 48 hours. Culture medium was replaced with fresh media containing the relevant steroids at the desired concentrations. The kinetics parameters of CYP11B1 was ascertained towards A4 and T by assaying the conversion of A4 and T, independently, spanning a range of concentrations (0.2, 0.4, 0.8, 1.0, 3.5 and 5 µM), at specific time intervals. These time course assays were completed within 24 hours and aliquots were collected at specific time intervals for each of the concentrations for each steroid. The samples for A4 and T, at the same concentration and time interval, were pooled upon collection, allowing for multiplex analysis. Prior to steroid extraction, PROG-d₉, A4-d₇, T-d₂ were added as internal standards, the steroids extracted and resuspended, followed by subsequent analysis by UPC²-MS/MS as previously described. The cells, for all time intervals, were collected for protein determination using the Pierce™ BCA Assay Kit according to the manufacturer's instructions. Briefly, the cells were rinsed with sterile phosphate-buffered saline (PBS, pH 7.4) and collected in Eppendorf® microfuge tubes. Cells were pelleted using a benchtop centrifuge (Heraeus™ Biofuge™, Thermo Fisher Scientific, Waltham, USA) at 12 500 RPM for 5 min. The PBS was aspirated and the pellet was resuspended in 80µL passive lysis buffer. The samples were sonicated and stored at -20°C until use. Bovine serum albumin (BSA) was used to generate a standard curve. Protein concentrations ranged from 0.2 mg – 0.6 mg/mL and were used in the normalisation of data collected in the determination of the V_{max} values.

4.5.3 The determination of kinetic parameters: K_m and V_{max} values

The data was plotted (substrate concentration (µM) vs time (min)) to yield progress curves and were analysed using linear regression analysis to determine the linear ranges. The linear ranges are representative of the initial velocities for each substrate concentration The

initial velocity was plotted against the substrate concentration and fitted to a non-linear regression curve using the Michaelis-Menten equation:

$$Y = V_{\max} * X / (K_m + X)$$

where X = initial substrate concentration,
and Y = initial velocity

4.5.4 Results

Initial reaction rates were determined for A4 and T as substrates at concentrations ranging from 0.2 μM to 5 μM in HEK-293 cells transiently transfected with CYP11B1 and ADX. Data was used to generate progress curves and fitted to the Michaelis-Menten equation (fig. 4.2) and the kinetic parameters, the apparent K_m and the V_{\max} , were determined.

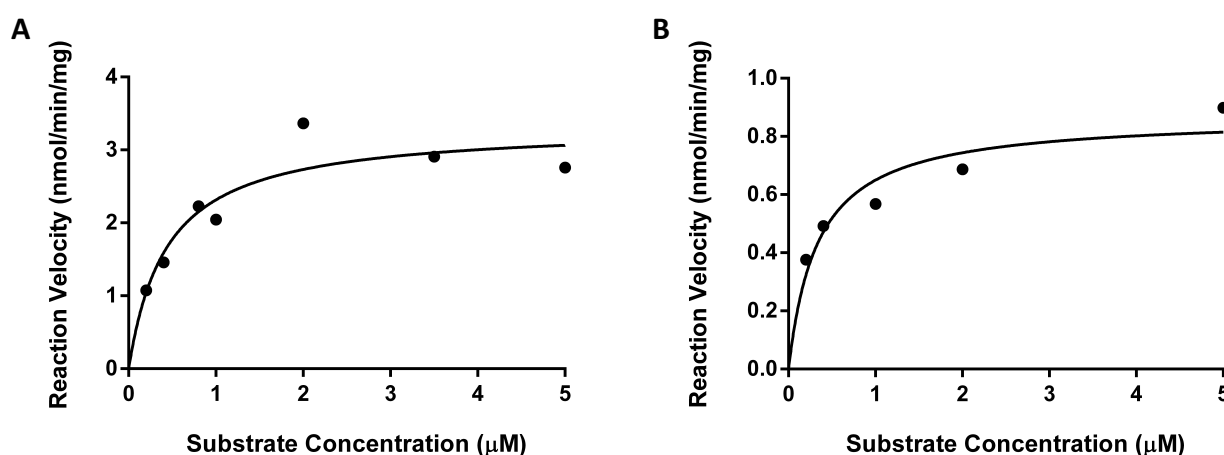


Figure 4.2: Analysis of progress curves for A4 (A) and T (B) determined using steroid conversion assays in HEK-293 cells transiently expressing CYP11B1 and ADX. Data were fitted to the Michaelis-Menten equation, using non-linear regression. Each point represents an initial rate for a time course assay, performed in triplicate and expressed as mean \pm SD (n=3). Data was analysed using GraphPad Prism (version 6) (GraphPad Software, San Diego, California).

The kinetic parameters for CYP11B1 determined in this study are shown in Table 4.5. The K_m and V_{max} values, as reported by Polar *et al*, for the natural ligands, 11-deoxycortisol and DOC are also depicted [1]. The apparent K_m is defined as the affinity of an enzyme for a substrate and is the concentration required to reach half the maximal velocity V_{max} defined as the maximum rate of a reaction, depicting the manner in which an enzyme behaves at high substrate concentrations. A lower K_m indicates a higher affinity of the enzyme towards the substrate and contrariwise [64]. A4 has the lowest K_m , 0.21 μM , when compared to the other substrates, T, 11-deoxycortisol and DOC. The V_{max} for the conversion of A4 to 11OHA4 (315.77 pmol/min/mg) is significantly higher than the other substrates. This could be due to the substrate binding more readily as indicated by the apparent K_m , resulting in the high turnover of substrate. Limitations in this study could not allow for the determination of the catalytic constant (k_{cat}) as this is based on purified enzyme at a known concentration. Therefore, V_{max}/K_m functions as an indication of catalytic efficiency with a higher ratio signifying a greater reaction efficiency. The catalytic efficiency of the reaction of A4 is 3.2-fold, 8.5-fold and 9-fold higher than the conversion of T, 11-deoxycortisol and DOC, respectively. Comparatively, it can be seen that the conversion of A4 to 11OHA4 by CYP11B1 is the most efficient, based on the high catalytic efficiency.

Table 4.5: Kinetic parameters, apparent K_m and V_{max} values generated by progress curve analysis, and catalytic efficiency (V_{max}/K_m) determined for CYP11B1. * represents reported values reproduced from [1].

Substrate	K_m (μM)	V_{max} (pmol/min/mg)	V_{max}/K_m
Androstenedione	0.21 \pm 0.07	315.77 \pm 22.46	1504
Testosterone	0.34 \pm 0.13	158.89 \pm 15.22	467
11-deoxycortisol*	0.6 \pm 0.1	106 \pm 6	176
11-deoxycorticosterone*	1.2 \pm 0.8	200 \pm 12	167

4.5.5 Discussion

The adrenal has been shown to secrete high levels of 11OHA4 [13]. Although it was assumed for some time that the CYP11B isoforms may catalyse the hydroxylation of A and T at C11, these *in vitro* reactions were only carried out in our laboratory recently, showing that formation of 11OHA4 in the adrenal is the result of the hydroxylation of A4 catalysed by CYP11B1. The metabolic fate of the weak androgen, 11OHA4 was unknown, as previously mentioned. However, it was shown to be a significant contributor to the pool of active androgens, especially in prostate cells and PCa cells, resulting in the formation of potent androgens, 11KT and 11KDHT [13–15]. Due to the novelty in this finding, this study aimed to elucidate the kinetic parameters exhibited by CYP11B1 towards A4 and T.

The data from the current study suggest that conversion of A4 to 11OHA4 by CYP11B1 is the most catalytically efficient when compared to T, 11-deoxycortisol and DOC. A4 has the lowest K_m and highest V_{max} , indicating that even though the enzyme has a high affinity for A4, tight binding does not hamper substrate turnover, with relatively efficient substrate turnover even at high substrate concentrations. V_{max} is reached at ~0.4 μ M indicating that at a low substrate concentration CYP11B1 is saturated with A4, while catalysing substrate conversion at a high turnover rate. In the adrenal, CYP11B1 catalyses the conversion of 11-deoxycortisol, DOC, T and A4. This results in competition between substrates for the enzyme. However, based on data from this study, A4 theoretically out-competes the other substrates. The resultant outcome is the formation of increased amounts of 11OHA4. Increased amounts of 11OHA4 and 11OHT, in adrenal vein samples, has been reported in literature. Women were treated with ACTH, a hormone that upregulates CYP11B1, resulting in 5.2 and 5.5-fold increases in 11OHA4 and 11OHT levels [13].

Even though the *in vitro* conversion of A4 and T by CYP11B1 is catalytically efficient, more so than DOC and 11-deoxycortisol, adrenal cortisol output far exceeds that of 11OHA4 and 11OHT, with the former also being 100 times higher than 11OHT in the adrenal. It should be noted that the kinetic parameters for A4 and T were determined under the same experimental conditions and may as such differ from those conditions in which DOC and 11-deoxycortisol were determined. Furthermore, it is possible that *in vivo* competition at cellular level for the same enzyme may influence substrate turnover and product formation catalysed by the same enzyme. In addition, levels of upstream precursor steroids and substrates would influence steroid production *in vivo*, together with the levels and zonal expression of steroidogenic enzymes.

Taken together, the kinetic parameters indicate that CYP11B1 exhibits a higher catalytic efficiency towards A4 than it does towards T. This provides evidence for the high concentrations of 11OHA4 detected in adrenal vein samples when compared to 11OHT in that A4 is converted to 11OHA4 more efficiently than the C11-hydroxylation of T. Furthermore, these androgens could perhaps modulate cortisol production in the adrenal due to potential competition between the substrates.

Chapter 5

An investigation into the influence of *S. tortuosum* on adrenal steroidogenesis

5.1 Introduction

S. tortuosum is held in high regard by the indigenous tribes of South Africa due to its properties as a medicinal herb in the alleviation of hunger and fatigue. Various studies have been carried out to assess the influence of *S. tortuosum* on the central nervous system, stemming from the plant's potential in the induction of a trance-like state during times of worship. These studies have elucidated possible mechanisms to which these effects of *S. tortuosum* may be attributed. For example, it was recently shown that a single dose of the plant extract modulated the connectivity between that amygdala and hypothalamus [7]. However, this study was limited as it did not include neurological parameters surrounding the population tested, such as anxiety and depression [4]. Furthermore, research has shown that the possible mechanism of action by which *S. tortuosum* elicits these effects is via the stimulation of the reuptake of 5-HT, inhibition of the expression of SERT and the upregulation of monoamine release and storage [3, 6, 22]. The anecdotal claims surrounding the desirable effects of *S. tortuosum*, like inducing states of calmness and tranquility, alleviating stress and symptoms related to stress, however, hints at the possible involvement of both the neurological and endocrine systems as both of these systems are implicated in the stress response [3, 4, 27, 65].

The influence of *S. tortuosum* on endocrine signaling has not been as extensively investigated. However, a recent study by Swart and Smith did examine the effects of an *S. tortuosum* extract, rich in mesembrine, on adrenal steroid hormone biosynthesis. Adrenal steroidogenesis is important for homeostasis as the hormones produced play vital roles in blood pressure control, regulation of stress and inflammation and the production of potent androgens. H295R cells are commonly used to investigate adrenal steroid hormone biosynthesis as these cells express the full complement of adrenal steroidogenic enzymes and are capable of producing all the steroid hormones. This cell model is therefore an appropriate cell line to investigate the influence of biological compounds on adrenal hormone biosynthesis. The aforementioned study showed that *S. tortuosum* is capable of modulating glucocorticoid, mineralocorticoid and androgen production in H295R cells [4].

They reported on the effects of *S. tortuosum* over a range of concentrations and, considering a mid-concentration, their data suggested the inhibition of CYP17A1. Basal PREG and PROG levels were increased significantly together with a 2.5-fold decrease in 16OHPROG, a dead-end product. In addition, adrenal androgen production decreased and while DHEA, A4 and 11OHA4 decreased 2-fold there was a 4-fold decrease in testosterone levels. Taken together, these data suggest the possible inhibition by *S. tortuosum* of CYP17A1, 3 β HSD2 and 17 β HSD5 [4]. These enzymes play an important role in the formation of weak adrenal precursor androgens and the inhibition thereof could be beneficial in disease states that are androgen-dependent, such as PCa. Basal levels of cortisol were also significantly decreased over the entire concentration range and analysis of the mineralocorticoids under forskolin-stimulated conditions revealed a decrease in the formation of ALDO at the highest dose (1 mg/mL).

Due to the evidence suggesting that *S. tortuosum* might have potential as a CYP17A1 inhibitor, abiraterone (Abi) was included as a means of comparison in the present study for comparative purposes. Abi is a CYP17A1 inhibitor thereby blocking endogenous biosynthesis of androgens in steroidogenic tissue as well as the formation adrenal androgens. It is administered as abiraterone acetate to promote bioavailability and is normally used alongside prednisone, a synthetic glucocorticoid, in the treatment of castration-resistant prostate cancer (CRPC). In H295R cells, Abi increases PREG and PROG but decreases all the other downstream metabolites. Abi is metabolised and converted to a more potent metabolite, Δ^4 -abiraterone (D4A), by 3 β HSD2. D4A inhibits CYP17A1, 3 β HSD2 and SRD5A, providing further evidence for the anti-tumour activity as tumour progression is dependent on the synthesis of DHT by these enzymes [66–69].

It is possible that the effects of *S. tortuosum* on adrenal hormone production may be attributed to mesembrine, the major alkaloid in *S. tortuosum*, since the study by Swart and Smith was conducted using a mesembrine-rich preparation, in which the compound contributed more than 80% of the total alkaloids present. The alkaloids in *S. tortuosum* may act in the same manner as Abi by inhibiting CYP17A1, and thereby modulating steroid hormone production or may exhibit effects similar to other alkaloids reported to possess anticancer properties, providing a comprehensive therapeutic agent in the treatment of hormone-dependent cancers, such as PCa. Alkaloids have been well documented to have antitumor, antibacterial, antifungal, antimalarial, antiviral, pain-relieving and cholinesterase inhibitory activity [5]. Some alkaloids have been developed successfully as

chemotherapeutic agents. Other alkaloids, such as berberine, evodiamine, matrine and piperine also exhibit anticancer properties and act via numerous mechanisms. Berberine has been shown to inhibit the proliferation of multiple cancer cell lines and induced apoptosis whereas avodiamine inhibited angiogenesis, tumour invasion and metastasis [70]. *S. tortuosum* is rich in alkaloids with mesembrine being the most abundant alkaloid present [17, 18, 21]. Most notably, a chemotherapeutic alkaloid that is similar in structure to mesembrine, is rohitukine. Rohitukine was first isolated from *Amoora rohikuta* and exhibited various biological effects ranging from immunomodulatory and anti-inflammatory effects to anti-fertility activity. Due to the framework the chemical structure rohitukine possesses, it provides a basis for the derivatization and synthesis of new molecules which may possess desirable effects while improving ADME properties. Flavopiridol, a derivative of rohitukine, for example, acts via interfering with the phosphorylation of cyclin-dependent kinases (CDKs) thereby hindering activation as well as blocking the progression of the cell cycle at G1 and G2, in human tumour cells and is currently being tested in phase II clinical trials [71–73].

The current study therefore aims to clarify the inhibitory effects of *S. tortuosum* on adrenal steroidogenic enzymes. To do so, the effects of a lyophilised extract of *S. tortuosum*, Trimesemine, on steroidogenesis will be compared to those of Abi used in the treatment of PCa, in H295R cells. Abi is a known CYP17A1 inhibitor used clinically to inhibit androgen production, specifically that of testosterone. The influence of *S. tortuosum* on adrenal steroidogenic enzymes will be determined in HEK-293 cells heterologously expressing CYP17A1, CYP21A2, CYP11B1, CYP11B2 and 3 β HSD2. These assays eliminate the competition of steroidogenic enzymes for the same substrates, which is characteristic of steroid metabolism assayed in the adrenal H295R whole cell system. These studies will shed light on the effects of *S. tortuosum* on specific adrenal steroidogenic enzymes and clarify the modulatory effects on adrenal hormone production.

5.2 Methodology

5.2.1 Materials

An extract of *S. tortuosum*, marketed as Trimesemine™, was obtained from Botanical Resource Holdings Pty (Ltd) an affiliate of Verve Dynamics (Somerset West, South Africa). Steroids were purchased from Steraloids (Newport, USA) and Sigma-Aldrich (St. Louis, MO, USA). Deuterated steroids (internal standards) was purchased from Cambridge isotopes (Andover, MA, USA). Methyl tertiary-butyl ether (MTBE) and Dulbecc's modified Eagle's

Medium (DMEM) was bought from Sigma-Aldrich (St. Louis, MO, USA). DMEM/F12 and gentamicin were purchased from Invitrogen/Gibco (Grand Island, New York, USA). Wizard® Plus Midipreps DNA purification system was supplied by Promega Biotech (Madison, WI, USA). XtremeGene HP® DNA transfection reagent was purchased from Roche Diagnostics (Mannheim, Germany). Penicillin, streptomycin, FBS and trypsin-EDTA were supplied by Gibco BRL (Gaithersburg, MD, USA). Cosmic calf serum was supplied by HyClone®, Thermo Scientific (Waltham, MA, USA). Tissue culture plates and dishes were purchased from Corning® (New York, USA). Trypan blue stain (0.4%) as well as the cell count plates were acquired from Invitrogen (Eugene, USA). Forskolin was purchased from Sigma-Aldrich (St. Louis, MA, USA). Abiraterone (Abi) was purchased from Selleckchem (Houston, TX, USA). The Acquity UPC² BEH C₁₈ column (2.1 mm × 100 mm, 1.7 μm particle size) was obtained from Waters (Milford, USA). All other chemical reagents were of premium quality and procured from reliable scientific distributors.

5.2.1.1 Cell models and vectors

HEK-293 cells were purchased from American Type Culture Collection (Manassas, VA, USA). H295R cells were a kind gift from Prof William Rainey (University of Michigan, Ann Arbor). CYP17A1 was a kind gift from Professor Christa Flück (University Children's Hospital BernBern). The CYP11B1 and CYP11B2 vector constructs were kind gifts from Prof Walter Miller (University of California, San Francisco) and the ADX (adrenal ferredoxin) vector construct was donated by Prof RC Tuckey (The University of Western Australia, Crawley). The constructs for 3βHSD2, CYP21A2 and pCI-neo were purchased from Promega (Madison, USA).

5.2.2 Purification of plasmid DNA

Mammalian expression vectors, pcDNA3-CYP17, pcDNA6-hCYP21A2, pCDNA6-3βHSD2 and pCMV4-hCYP11B1, pCMV-hCYP11B2, pCIneo-ADX and the control plasmid pCIneo, were prepared by streaking out frozen *E.coli* stocks (JM109 strain) on ampicillin (100 μg/mL) lysogeny broth (LB)-agar plates and incubated overnight at 37 °C. Selective pressure allowed for single colonies to be selected and inoculated in 5 mL LB, containing 5 μL ampicillin (100 mg/mL). The 5 mL cultures were incubated at 37 °C for 8 hours. After the first incubation, a second larger inoculate was prepared by the addition of 150 μL of the starter culture and 150 μL Ampicillin (100 mg/mL) to 150 mL LB. Cultures were incubated for another ±16 hours at 37 °C on a Innova shaking-incubator (New Brunswick, Canada) at 225 rpm. Bacterial cells were collected by centrifugation, lysed and plasmids

purified with a DNA extraction column using the Wizard® Plus Midipreps DNA Purification System, according to manufacturer's instructions. DNA plasmid purity and concentration were determined using UV spectrophotometry at 260nm and 280nm on the Cary60 UV-Vis (Agilent technologies; Santa Clara, CA, USA). Purified DNA was stored at -20°C until use. The integrity and purity of the DNA were further analysed using agarose gel electrophoresis. DNA yields ranged between 0.1 and 0.5 µg/µL.

5.2.3 Enzyme assays in transiently transfected HEK-293 cells

Cells were maintained in DMEM culture media supplemented with 10% FBS and 1% penicillin-streptomycin. The atmosphere was kept stable at 37 °C, 5% CO₂ and 90% relative humidity. Cells were counted using the Countess® automated cell counter (Invitrogen, Eugene, USA) and upon experimentation, seeded in 24 well Corning® CellBIND® surface plates at a seeding density of 2x10⁵ cells/mL. After 24 hours, cells were transiently transfected with 0.5 µg plasmid DNA (human CYP17A1, human CYP21A2, human 3βHSD2, human CYP11B1 and ADX; human CYP11B2 and ADX) per well using XtremeGene DNA transfection reagent according to manufacturer's instructions. A plasmid containing no DNA insert, pCI-neo, was used as a negative control. Cells were incubated for 48 hours before the media was aspirated and replaced with fresh media containing 1 µM of the appropriate steroid substrate, with and without the appropriate concentration of *S. tortuosum* (0.01 or 1 mg/mL). Steroids were dissolved in absolute ethanol (1 mg/mL) and diluted in the culture medium to obtain the desired concentration. Substrate conversion in the presence of *S. tortuosum* was assayed by the addition of 20 µL extract alongside the appropriate steroid, resulting in a final concentration of 0.01 mg/mL and 1.00 mg/mL. Prior to addition, the extract was dissolved in culture medium to a final concentration of 0.25 mg/mL and 25 mg/mL. After 8 hours, media aliquots were collected, placed in screw cap tubes and stored at -20 °C until steroid extraction. Samples from multiple conversion assays in which substrates and products differed, were pooled prior to extraction. Multiplex analysis was carried out in which samples were analysed in a single chromatographic run allowing effective separation of the different metabolites.

5.2.4 Enzymatic assays in H295R cells

The influence of an *S. tortuosum* extract on steroid hormone production in H295R cells was assayed under basal conditions. H295R cells were cultured at 37 °C, 5% CO₂ and 90% relative humidity in culture medium, DMEM/F12 media supplemented with 1.5 g/L NaHCO₃,

1% penicillin streptomycin, 0.01% gentamicin and 10% cosmic calf serum (CCS). Confluent cells were plated into 24 well plates at a density of 2×10^5 cells/mL. Cells were incubated for 48 h. After 48 hours, the medium was replaced with experimental medium (growth medium containing 0.1% cosmic calf serum) to which the appropriate treatments were added. Steroid metabolism was assayed in the presence of *S. tortuosum* extract by the addition of extract (20 μ L per well) to a final concentration of 0.01 and 1.0 mg extract/mL as well as Abi at a concentration of 10 μ M. After 48 h, media aliquots were removed and stored in glass tubes at -20 °C until extraction.

5.2.5 Cell viability

The alamarBlue® assay was used in this study to assess the influence of *S. tortuosum* on cell viability in HEK-293 cells. Plant extracts have been shown to interfere with 3- [4,5-dimethylthiazol-2-yl]-2,5-diphenyl tetrazolium bromide in the MTT cell viability assay which is commonly used to assay cell viability [74]. In order to exclude the possible interference by the plant extract, the alamarBlue® assay was therefore used. This assay allows the analysis of viable cells based on the ability of cells to maintain a reducing environment within the cytosol. The active ingredient in the alamarBlue® reagent, resazurin, can permeate the cell wall and is non-fluorescent. Upon entering the cells, the resazurin is constantly converted by live cells to resofurin, a fluorescent compound. The overall fluorescence is thereby amplified and subsequently detected.

HEK-293 cells were plated in a 24 well plate at a density of 2×10^5 cells/mL. After 24 hours, the cells were treated with *S. tortuosum*, at two concentrations, 0.01 mg/mL and 1 mg/mL. Cells were incubated for 24 hours before the addition of 10X alamarBlue® reagent. The alamarBlue® reagent (10X), 50 μ L, was added to each well and incubated for 4 hours in an incubator, protected from direct light. Thereafter the fluorescence was read using an excitation wavelength of 540-570 nm and emission wavelength of 580-610 nm. The media was aspirated and cells were washed once with PBS and collected into individual micro-centrifuge tubes and centrifuged at 13,000 x g for 10 min using a bench-top centrifuge (Heraeus™ Biofuge™, Thermo Scientific, USA). The pellet was redissolved in 50 μ L passive lysis buffer and stored at -20 °C until determination of protein concentration.

5.2.6 Protein determination

Protein concentration determination was performed on the lysates from the alamarBlue® assay. This is to act as a normalization control for the alamarBlue® assay. The lysates were

thawed and sonicated for 10 minutes. Bovine serum albumin (BSA) protein standards were prepared in passive lysis buffer with a calibration range of 0 – 2000 $\mu\text{g/mL}$. Samples were analysed using the standard BSA curve generated using the Pierce BCA Protein Assay Kit, in accordance with the manufacturer's instructions. Only 10 μL of both sample and standard were used as passive lysis buffer interferes with the Pierce BCA Protein Assay Kit.

5.2.7 Steroid extraction

Samples were allowed to reach room temperature prior to extraction. Steroid reference standards were prepared in media for analyses, at a range of 0 ng/mL to 250 ng/mL, and also subjected to extraction procedures. Steroids were extracted by liquid/liquid extraction using MTBE at 1:3 volume of media to MTBE after the addition of 100 μL internal standard mix consisting of PROG-d₉, A4-d₇, T-d₂ (1.5 ng each) prior to extraction. Samples and standards were vortexed at 800 RPM for 5 minutes and placed at -80 °C for an hour. The liquid organic phase was transferred to test tubes and dried under nitrogen at 55 °C. The dried residue (samples and standards) were resuspended in 150 μL 50% methanol and stored at -20 °C until analysis.

5.2.8 Separation and quantification of steroid metabolites using UPC²-MS/MS

The steroids of interest were analysed by UPC²-MS/MS using the method described in chapter 4. The separation was achieved in a single chromatographic step which ensured efficient separation followed by the quantification of steroids.

5.2.9 Statistical analysis

All experiments were performed in triplicate and the subsequent results are given as means \pm SEM. However, results for the H295R assay are given as means \pm SD. Statistics for the single conversion assays were calculated by a one-way ANOVA, followed by a Dunnett's multiple comparison test. Statistics for the H295R assays were calculated by a two-way ANOVA, followed by a Dunnett's multiple comparison test. All statistics were calculated using GraphPad Prism (version 6) software (GraphPad Software, San Diego, California). Differences were considered statistically significant at $P < 0.05$.

5.3 Results

5.3.1 The influence of *S. tortuosum* extract on cell viability

Cell viability was determined using the alamarBlue® assay that is based on the reduction potential of the cellular environment of live cells. The influence of *S. tortuosum* at two concentrations, 0.01 mg/mL and 1 mg/mL, was assayed after 24 hours (fig 5.1). The fluorescence was normalised to total protein concentration. The addition of *S. tortuosum* did not result in a significant decrease in cell viability, with viability at both concentrations remaining at $\pm 10\%$ of the control.

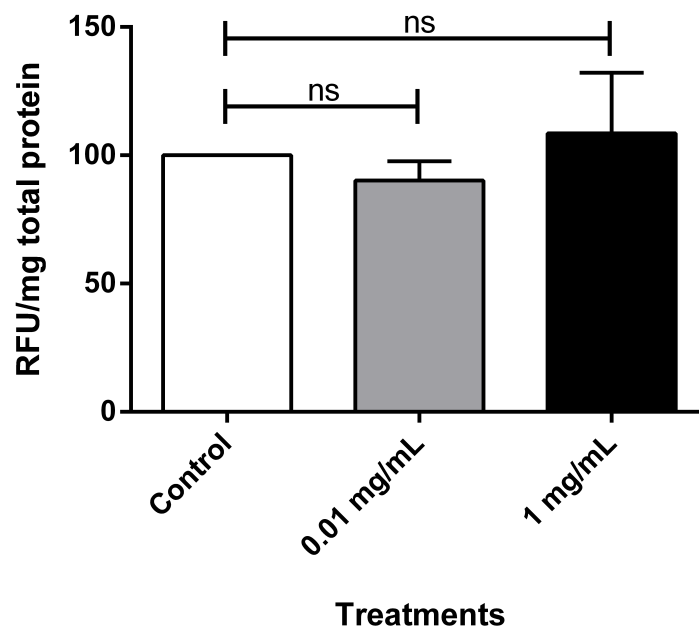


Figure 5.1: Toxicity of *S. tortuosum* extract on HEK-293 cells. Cells were treated with *S. tortuosum*, at two concentrations 0.01 and 1 mg/mL, for 24 hours after which the AlamarBlue® assay was conducted and the fluorescence measured. Results are expressed as the mean relative fluorescent units (RFU) per mg total protein \pm SD (n=3, ns=not significant).

5.3.2 The influence of *S. tortuosum* extract on CYP17A1

CYP17A1 catalyses the conversion of PREG to 17OHPREG and DHEA while PROG is converted 17OHPROG in humans (fig 5.2). This is the first step of adrenal steroidogenesis after the side chain cleavage of cholesterol by CYP11A1.

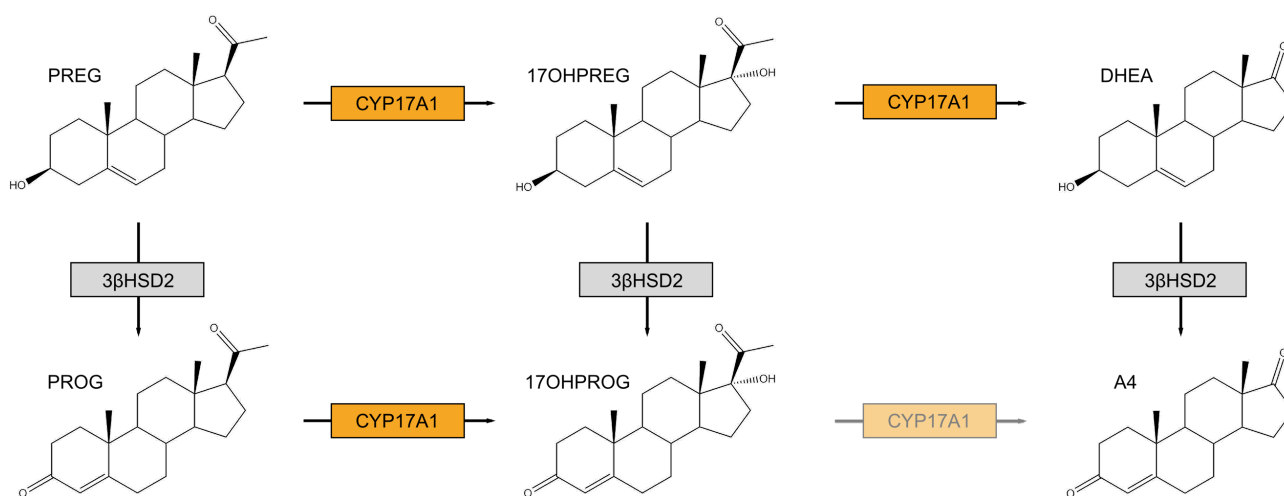


Figure 5.2: Enzymatic reactions catalysed by CYP17A1 (orange).

The influence of *S. tortuosum* on the conversion of PREG to 17OHPREG and PROG to 17OHPROG was investigated in HEK-293 cells transiently transfected with CYP17A1 at two concentrations of *S. tortuosum* extract, 0.01 mg/mL and 1 mg/mL. Substrate was added together with *S. tortuosum* and incubated for 8 hours to determine any inhibitory effects (fig 5.3)

The *S. tortuosum* extract did not show any significant effects on the conversion of PREG to 17OHPREG after 8 hours. Approximately, 0.6 μ M PREG was converted under control conditions with the experimental conditions being comparable to the control (fig 5.3A).

However, 0.3 μ M of PROG was converted after 8 hours under control conditions with the

conversion being comparable to the control in the presence of both 0.01 mg/mL and 1 mg/mL *S.tortuosum* (fig 5.3B).

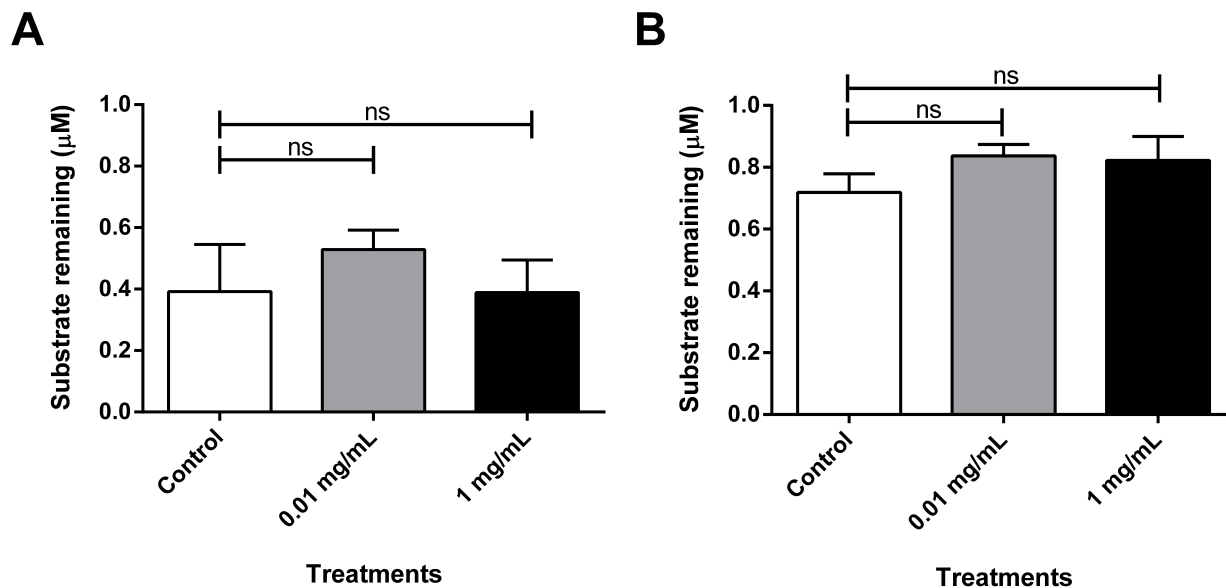


Figure 5.3: Analysis of substrate conversion in HEK-293 cells expressing CYP17A1. Substrate remaining after the addition of 1 μM PREG (A) and PROG (B) in the absence (control) and presence of *S. tortuosum* extract at two concentrations. The experiment was performed in triplicate and analysed by a one-way ANOVA, followed by a Dunnett's multiple comparison test. Results are expressed as the mean \pm SEM (n=3, ns=nonsignificant)

5.3.3 The influence of *S. tortuosum* extract on CYP21A2

CYP21A2 catalyses the conversion of PROG to DOC and 17OHPROG to 11-deoxycortisol (fig 5.4). These metabolites subsequently feed into the mineralocorticoid and glucocorticoid branches of adrenal steroidogenesis, ultimately yielding aldosterone and cortisol.

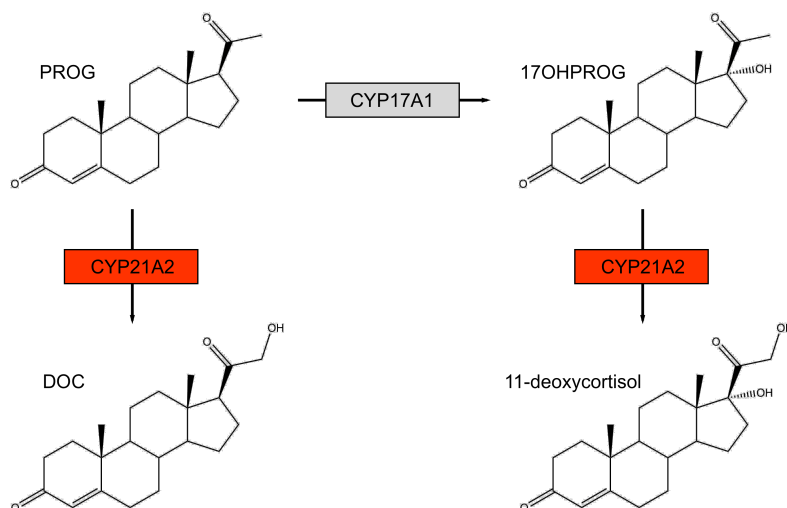


Figure 5.4: Enzymatic reactions catalysed by CYP21A1 (red).

HEK-293 cells transiently transfected with CYP21A2 were treated with *S. tortuosum* extract, 0.01 mg/mL and 1 mg/mL. The substrates, PROG and 17OHPROG, were added at 1 μ M and the effect of *S. tortuosum* was assayed after 8 hours. The substrates were added together with *S. tortuosum* extract and incubated for 8 hours to determine any effects exhibited by the extract.

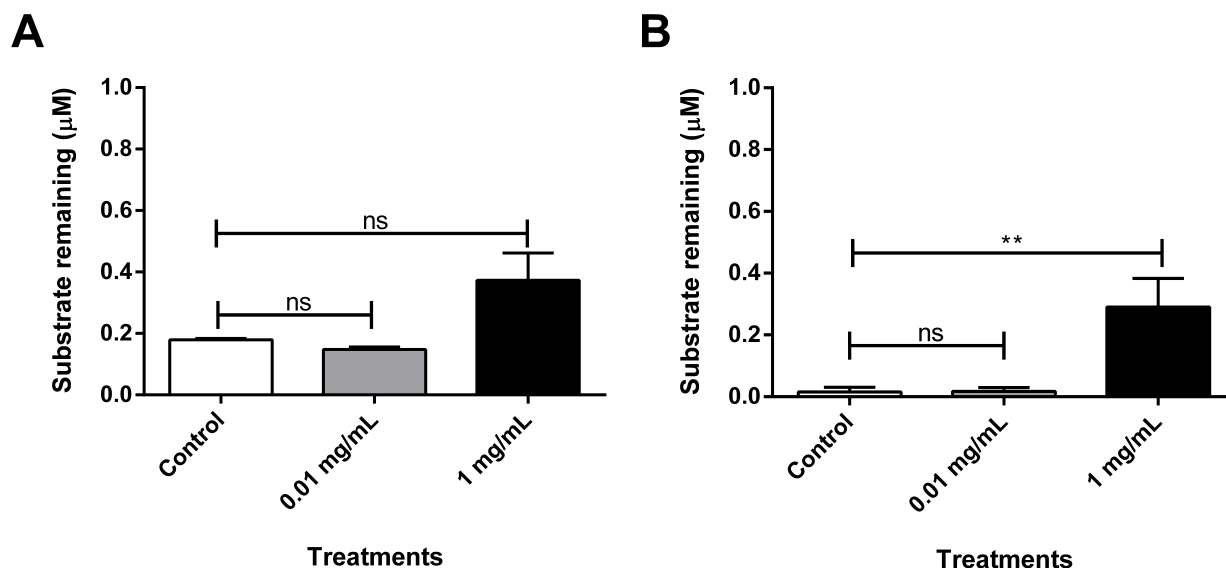


Figure 5.5: Analysis of substrate conversion in HEK-293 cells expressing CYP21A2. Substrate remaining after the addition of 1 μM PROG (A) and 17OHPROG (B) in the absence (control) and presence of *S. tortuosum* extract at two concentrations. The experiment was performed in triplicate and analysed by a one-way ANOVA, followed by a Dunnett's multiple comparison test. Results are expressed as the mean \pm SEM (n=3, ns = non-significant, ** $P < 0.01$).

Using PROG (1 μM) as substrate, a conversion to DOC was efficient (>80%). After 8 hours, neither 0.01 nor 1 mg/mL of extract caused any significant effect on the conversion of PROG to DOC with all three conditions resulting in $\pm 0.3 \mu\text{M}$ of product formed (fig 5.5A). However, with the addition of 1 μM 17OHPROG, at a higher concentration of the extract, showed a significant decrease in the product formed. Approximately 0.7 μM of 11-deoxycortisol was formed when treated with *S. tortuosum* compared to $\sim 100\%$ substrate conversion in the control assay. At a lower concentration, the addition of *S. tortuosum* resulted in no significant effect on the conversion of 17OHPROG to 11-deoxycortisol (fig 5.5B).

5.3.4 The influence of *S. tortuosum* extract on CYP11B1

In the adrenal cortex, CYP11B1 catalyses the conversion of 11-deoxycortisol to cortisol, A4 to 11OHA4 and T to 11OHT (fig 5.6).

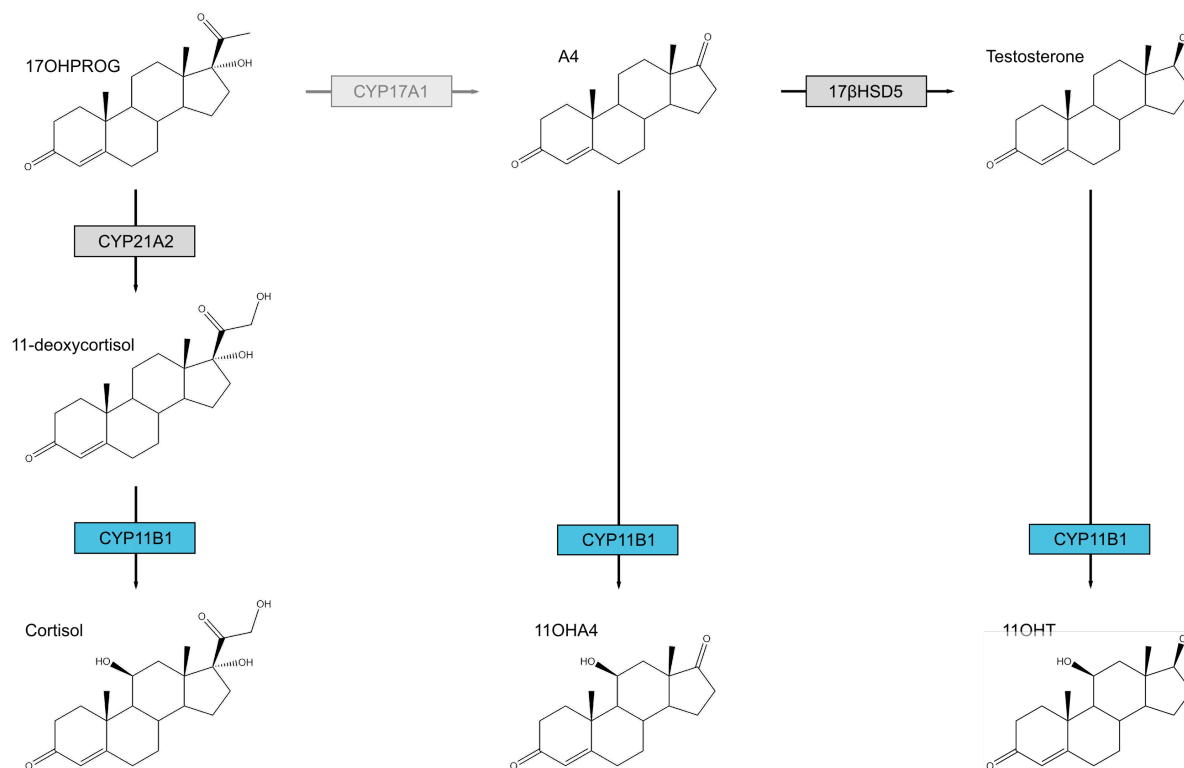


Figure 5.6: Enzymatic reactions catalysed by CYP11B1 (blue).

HEK-293 cells were transiently co-transfected with CYP11B1 and ADX. ADX supports the redox activity of the enzyme as the cell model does not sustain this function optimally. Steroid conversion of three substrates, 11-deoxycortisol, A4 and T were assayed in the presence of the *S. tortuosum* extract, for 8 hours.

The presence of *S. tortuosum* extract resulted in significant inhibition of CYP11B1 in the conversion of all three the substrates. 11-Deoxycortisol, at 1 μ M, in the absence of the extract, was fully converted to cortisol (\sim 0.95 μ M), with negligible substrate remaining. In the presence of 0.01 mg/mL extract, \sim 0.6 μ M cortisol was formed compared to \sim 0.3 μ M cortisol formed in the presence of 1 mg/mL extract (fig 5.7A). In the control conversion assay by CYP11B1 with A4 \sim 0.6 μ M of substrate was converted. Although the addition of 0.01 mg/mL *S. tortuosum* resulted in less product being formed it was not significantly lower than that which formed in the control reaction. However, the addition of 1 mg/mL

extract inhibited the conversion of A4 to 11OHA4 significantly (fig 5.7B) with negligible product being detected. T, which is not as readily converted by CYP11B1 as the other substrates, showed only a 50% conversion to 11OHT in the absence of *S. tortuosum*. In the presence of 0.01 mg/mL extract, the conversion was comparable to that of the control. However, at the higher concentration *S. tortuosum* inhibited the formation of 11OHT significantly with ~0.75 μ M substrate remaining after the assay period (fig 5.7C).

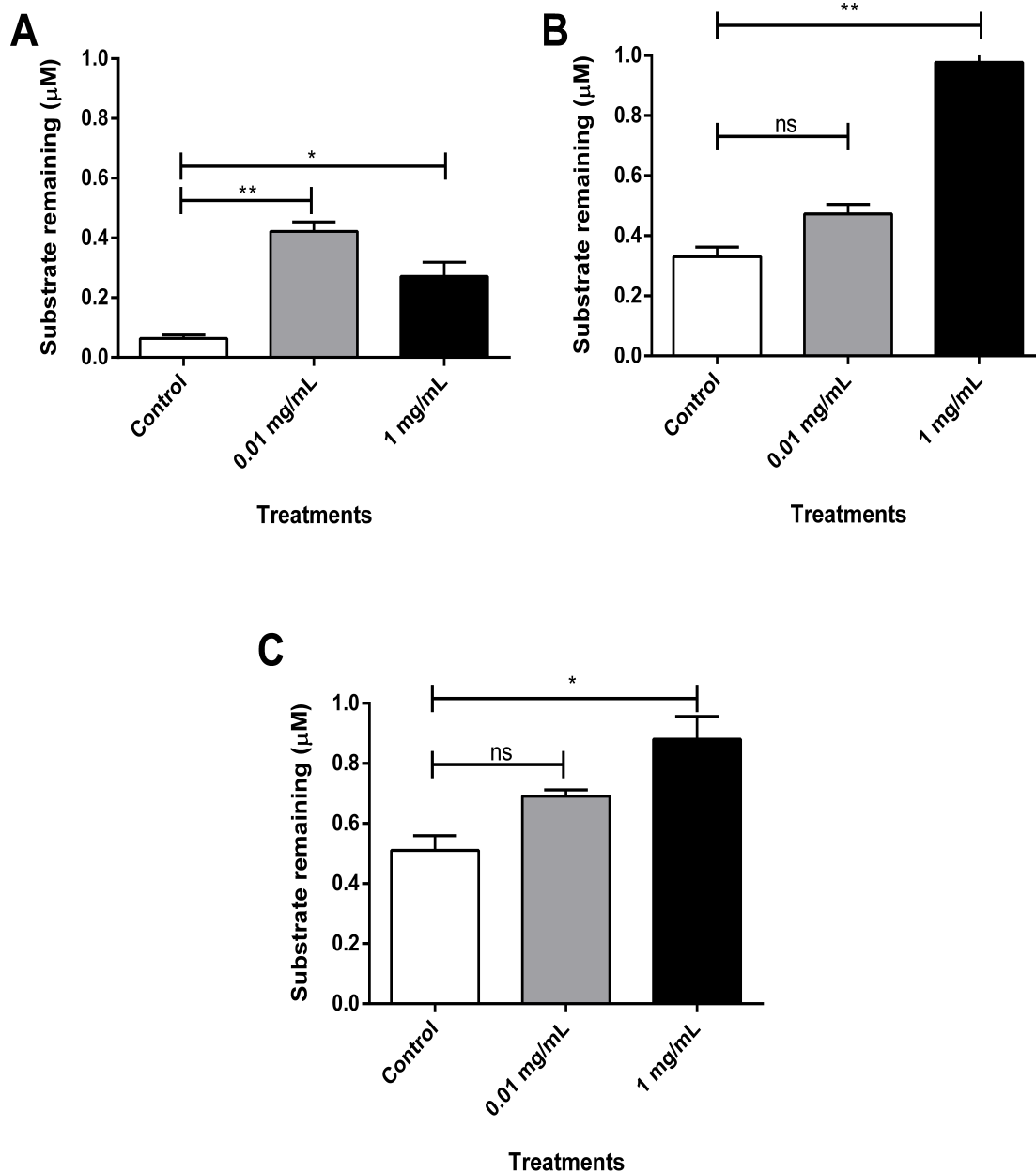


Figure 5.7: Analysis of substrate conversion in HEK-293 cells expressing CYP11B1 and ADX. Substrate remaining after the addition of 1 μM 11-deoxycortisol (A), A4 (B) and T (C) in the absence (control) and presence of *S. tortuosum* extract at two concentrations. The experiment was performed in triplicate and analysed by a one-way ANOVA, followed by a Dunnett's multiple comparison test. Results are expressed as the mean \pm SEM ($n=3$, ns = not significant, * $P < 0.05$, ** $P < 0.01$).

5.3.5 The influence of *S. tortuosum* extract on CYP11B2

In the mineralocorticoid branch of adrenal steroidogenesis, a three-step reaction is required to form aldosterone. The enzyme that catalyses these reactions is CYP11B2 which catalyses the 11 β -hydroxylation of DOC to form CORT, the first intermediate which is subsequently converted by the 18-hydroxylase activity of CYP11B2 to 18OHCORT, the second intermediate. The final step, catalysed by the 18-methyl oxidase activity of CYP11B2, converts 18OHCORT to aldosterone (fig 5.8).

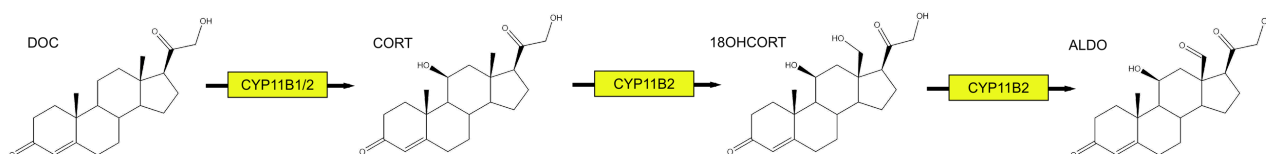


Figure 5.8: Enzymatic reactions catalysed by CYP11B2 (yellow).

In this study, HEK-293 cells were transiently co-transfected with CYP11B2 and ADX, as in the case of CYP11B1. *S. tortuosum* extract was assayed at 0.01 mg/mL and 1 mg/mL to determine the effect on the conversion of 1 μ M of three potential substrates, DOC, A4 and T. DOC is the natural ligand for CYP11B2. However, A4 and T can also be hydroxylated by CYP11B2 *in vitro*, in the production of 11OHA4 and 11OHT, respectively [14].

CYP11B2 catalysed the conversion of DOC with \sim 0.6 μ M remaining after 8 hrs. The addition of *S. tortuosum* at both concentrations had no significant inhibitory effect (fig 5.9A) as was also observed in the case of the conversion of T to 11OHT (fig 5.9C). However, when A4 was assayed, *S. tortuosum* significantly inhibited the conversion at both 0.01 mg/mL and 1 mg/mL. Although the addition of 1 mg/mL showed a greater inhibition of the enzyme, negligible substrate was converted after the assay period at both concentrations (fig 5.9B).

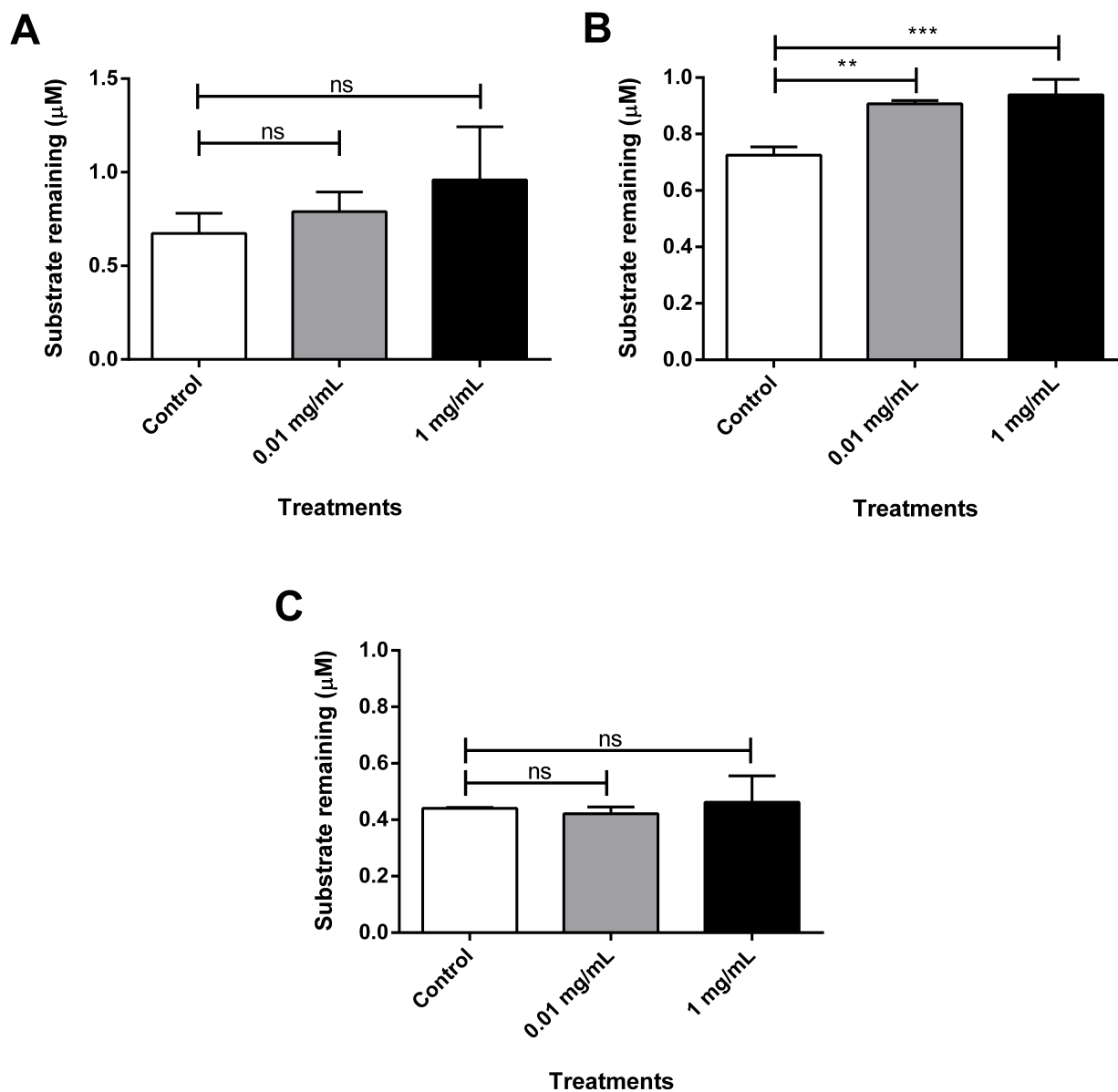


Figure 5.9: Analysis of substrate conversion in HEK-293 cells expressing CYP11B2 and ADX. Substrate remaining after the addition of 1 μM DOC (A), A4 (B) and T (C) in the absence (control) and presence of *S. tortuosum* extract at two concentrations. The experiment was performed in triplicate and analysed by a one-way ANOVA, followed by a Dunnett's multiple comparison test. Results are expressed as the mean \pm SEM ($n=3$, ns=not significant, ** $P < 0.01$, *** $P < 0.001$).

5.3.6 The influence of *S. tortuosum* extract on 3 β HSD2

3 β HSD2 is an hydroxysteroid dehydrogenase that catalyses the conversion of PREG, 17OHPREG and DHEA to PROG, 17OHPROG and A4, respectively (fig 5.10). These conversions are at a key branch point in the pathway as the conversions yield metabolites that ultimately form the mineralocorticoid, aldosterone, the glucocorticoid, cortisol, and the adrenal androgens.

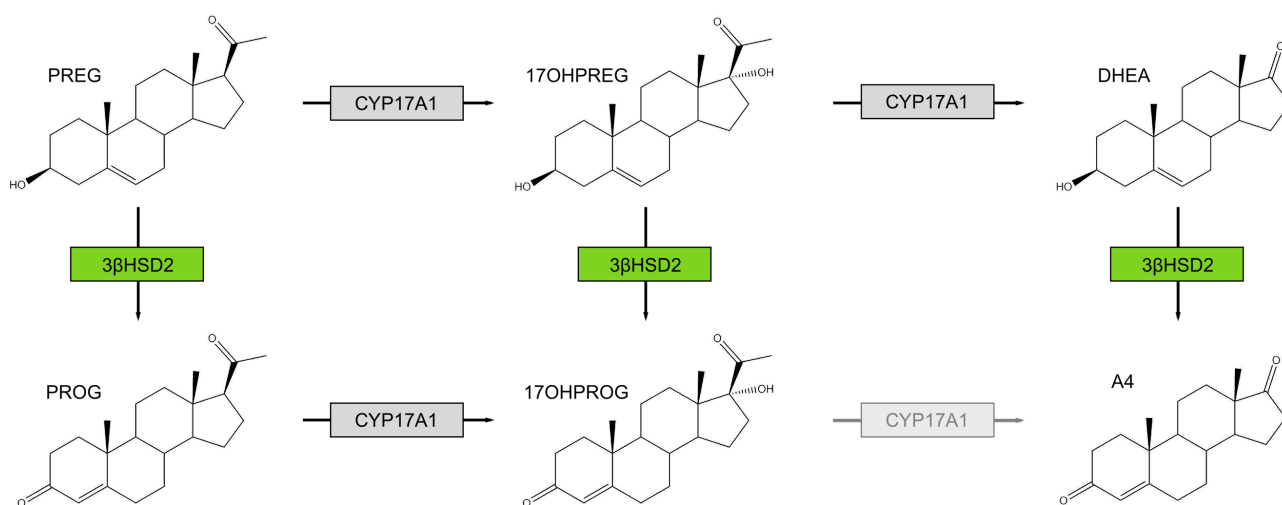


Figure 5.10: Enzymatic reactions catalysed by 3 β HSD2 (green).

The influence of *S. tortuosum* on the conversion of PREG to PROG, 17OHPREG to 17OHPROG and DHEA to A4 was investigated in HEK-293 cells transiently transfected with 3 β HSD2 with *S. tortuosum* extract added at 0.01 mg/mL and 1 mg/mL. Steroid substrate and product were analysed after the 8 hour incubation period.

The lower concentration of *S. tortuosum* had no significant effect on the conversions of 3 β HSD2 with PREG, 17OHPREG or DHEA as substrate. However, the addition of 1vmg/mL *S. tortuosum* extract significantly influenced the conversion of all three substrates when compared to the control assays without extract, showing ~40% inhibition of substrate conversion when compared to the control assay (fig 5.11). The data showing the conversion of 17OHPREG to 17OHPROG is expressed as product formation (fig 5.11B) due to the difficulty of detecting and quantifying 17OHPREG accurately with set

UPC²-MS/MS parameters as described in chapter 4. Data shows >20% substrate conversion with only 0.14 μM 11OHPROG product forming.

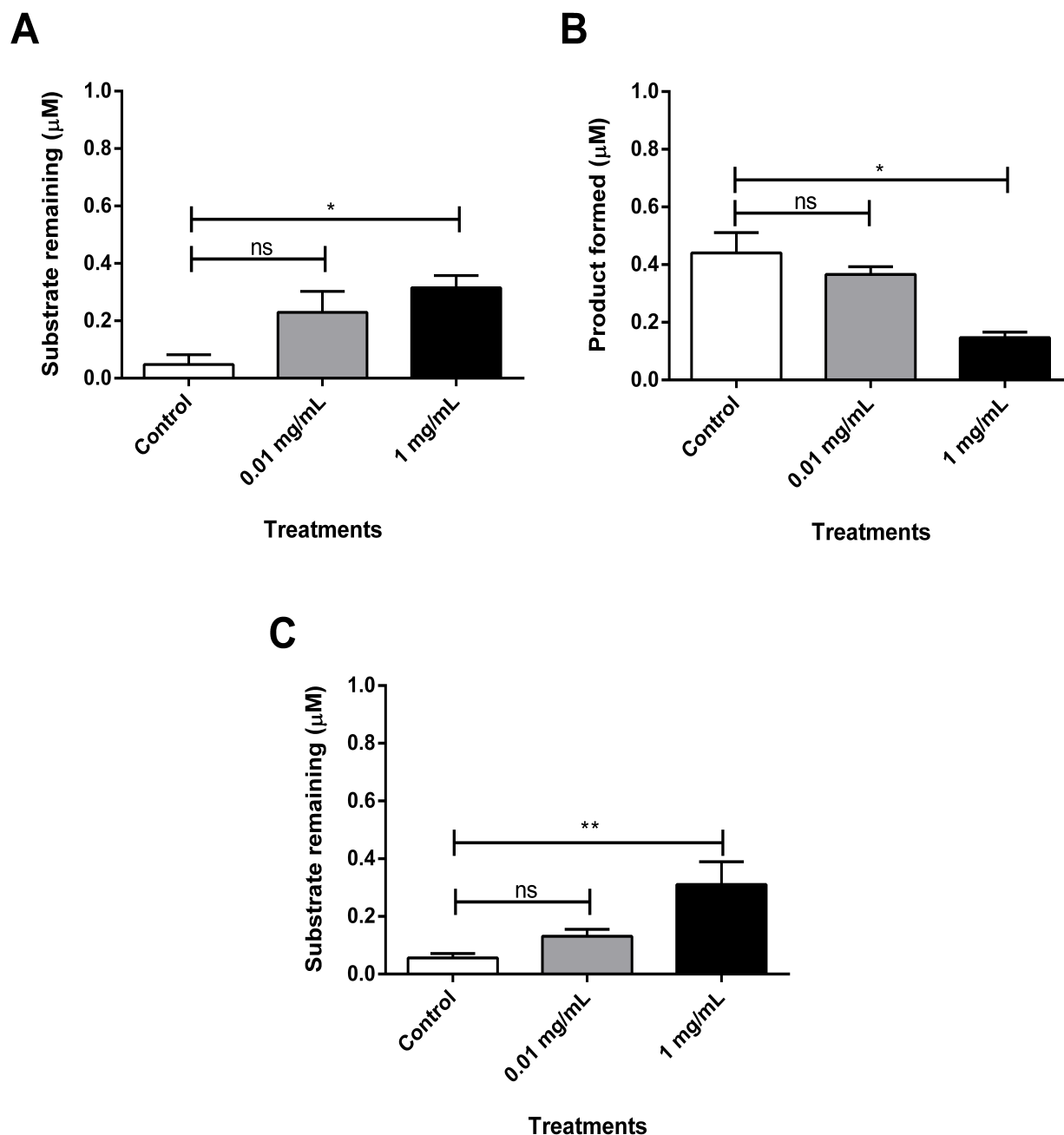


Figure 5.11: Analysis of substrate conversion in HEK-293 cells expressing 3 β HSD2. Substrate remaining after the addition of 1 μM PREG (A) and DHEA (C) in the absence (control) and presence of *S. tortuosum* extract at two concentrations. (B) shows product formed after the addition of 1 μM 17OHPREG. The experiment was performed in triplicate and analysed by a one-way ANOVA, followed by a Dunnett's multiple comparison test. Results are expressed as the mean \pm SEM ($n=3$, ns = non-significant) ($n=3$, ns=not significant, * $P<0.05$, ** $P<0.01$).

5.3.7 The influence of *S. tortuosum* on adrenal steroid hormones in H295R cells

Once the investigation into the effects of *S. tortuosum* on the individual adrenal steroidogenic enzymes had been completed, a study was carried out to determine the influence of *S. tortuosum* on global adrenal steroidogenesis, specifically on steroid hormone production. The study was conducted in H295R cells, an adrenal carcinoma cell line that is commonly used in investigations pertaining to adrenal steroid hormone biosynthesis, specifically to ascertain the influence of biological compounds on all the adrenal steroid hormones and steroidogenic enzymes.

Previous research showed that *S. tortuosum* may exhibit its effects by the inhibition of CYP17A1 due to the detection of increased PREG [2]. The current study thus focused on basal hormone production the H295R cell model to elucidate effects of *S. tortuosum* on steroidogenesis, in comparison to a well-known CYP17A1 inhibitor, Abi. It was shown in an earlier study by Rijk *et al*, that the inhibition of CYP17A1, by Abi, resulted in increased PREG and PROG levels [58].

In the present study the cell density was adjusted from 4×10^5 , used in previous studies, to 2×10^5 cells/mL in order to decrease the steroid levels in the pathways to facilitate the analyses of the effects of *S. tortuosum* on the enzymes catalysing hormone production. In addition, *S. tortuosum* was assayed at two concentrations, 0.01 mg/mL (0.345 μ M) and 1 mg/mL (34.5 μ M) and Abi at 10 μ M. *S. tortuosum* is currently marketed in capsule form containing 25mg Trimesemine/capsule with a recommended dosage of one per day, while 1000 mg Abi is administered per day (250 mg abiraterone acetate, 4x daily).

The data shows that the total steroid output is lower (6- to 8-fold) when compared to previous studies [63] (table 5.1). However, the trends observed in the individual steroid conversion assays tend to agree with the results obtained the H295R whole cell model assay. Lower steroid metabolite concentrations also ensured that the enzymes catalysing specific steps in the three pathways were not saturated with levels being below the K_m values of the enzymes for their natural substrates.

Table 5.1: Basal steroid metabolites produced in adrenal H295R cells in the absence and presence of *S. tortuosum* at 0.01 and 1 mg/mL in comparison to abiraterone (10 μ M) after 48 h.

Steroid Metabolites	Basal	<i>S. tortuosum</i> (0.01 mg/mL, 0.345 μ M)	<i>S. tortuosum</i> (1 mg/mL, 34.5 μ M)	Abiraterone (10 μ M)
	Total \pm SD (nM)	Fold change	Fold change	Fold change
PREG	4.2 \pm 0.1		\uparrow 2.3	\uparrow 6.3 *
PROG	0.2 \pm 0.01	\downarrow 1.6		\uparrow 13.6 ***
17OHPROG	17.1 \pm 0.7			\downarrow 1.8 **
DHEA	134.2 \pm 17.9		\downarrow 2.3	\downarrow 14.9 ****
A4	101.2 \pm 4.6	\downarrow 1.6	\downarrow 101.2 ****	\downarrow 101.2 ****
DOC	22.7 \pm 4.5	\downarrow 1.3	\downarrow 8.3 *	\downarrow 6.6 *
11-deoxycortisol	184.9 \pm 36.1	\downarrow 1.6 *	\downarrow 15.2 **	\downarrow 16.2 **
Testosterone	15.2 \pm 3.2	\uparrow 1.7	\downarrow 4.2	\downarrow 20.1
CORT	11.7 \pm 2.1		\downarrow 1.2	\downarrow 1.2
Cortisol	18.5 \pm 1.0	\downarrow 2.0 **	\downarrow 2.3 *	\downarrow 2.3 *
ALDO	6.0 \pm 0.7			
11OHA4	12.4 \pm 0.5		\downarrow 1.3 **	\downarrow 1.3 **
11OHT	3.3 \pm 0.4			
16OHP4	4.6 \pm 0.9		\downarrow 1.7 **	\downarrow 1.7 **
18OHCORT	9.4 \pm 0.1			
Total Steroid (nM)	533.3	\downarrow 1.2 **	\downarrow 3.8 ****	\downarrow 5.1 ****

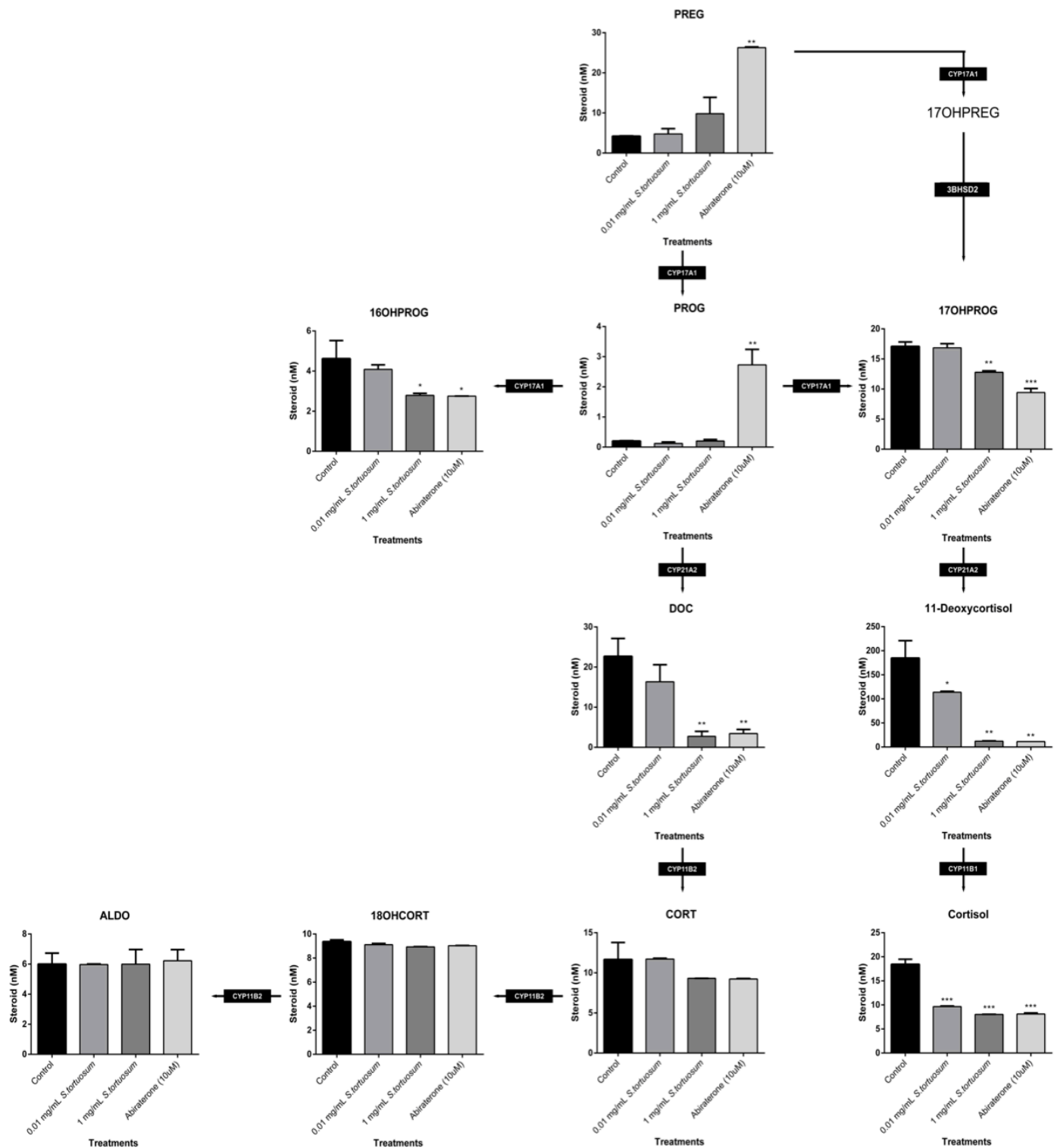


Figure 5.12A: Steroid production in the glucocorticoid (green block) and mineralocorticoid pathway (red block) of adrenal steroidogenesis. Cells were exposed to *S. tortuosum* at 0.01 and 1 mg/mL and 10 µM Abi under basal conditions. Results are represented as mean ±SD (n=3).

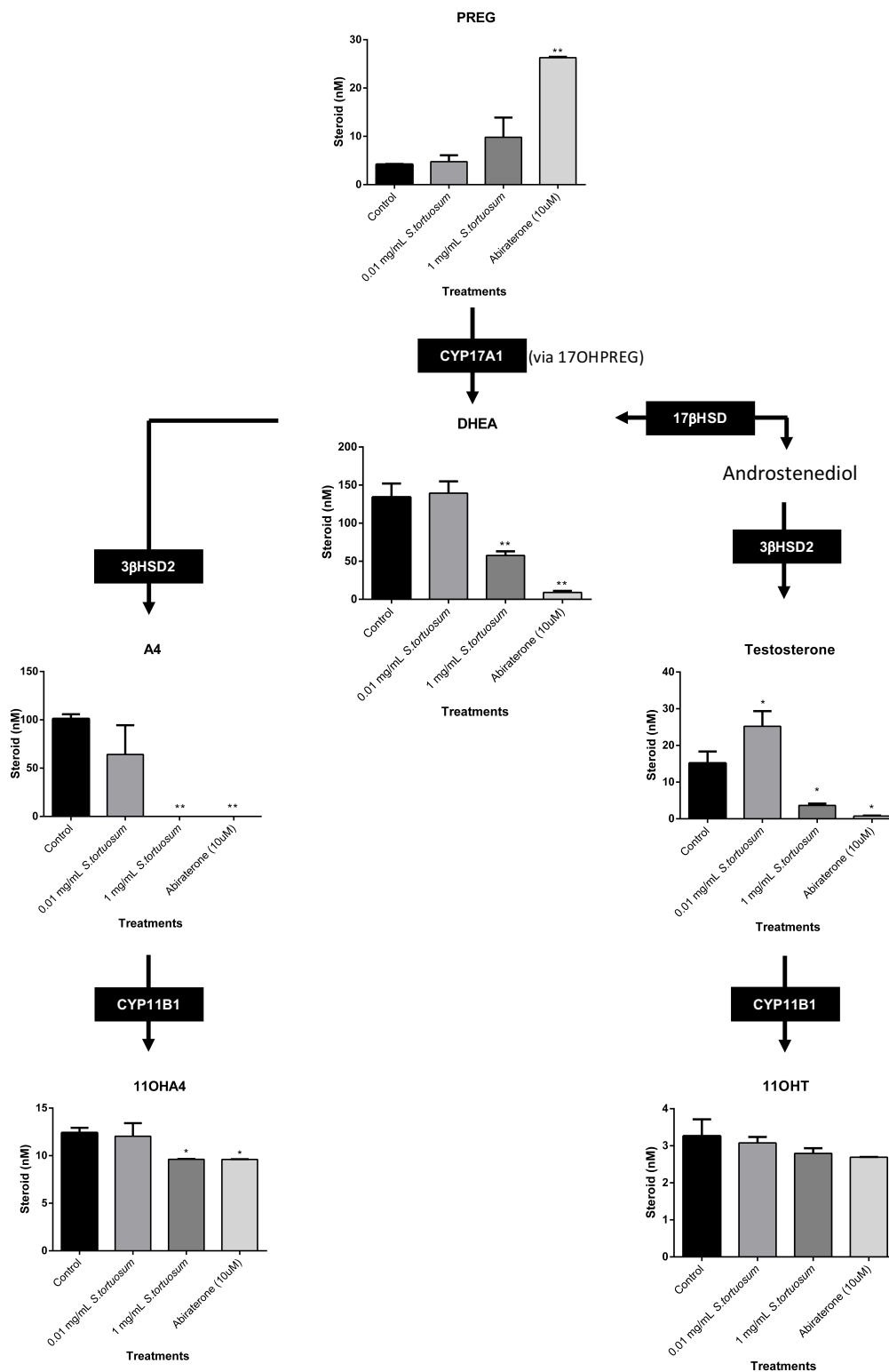


Figure 5.12B: Steroid production in the androgen pathway of adrenal steroidogenesis. Cells were exposed to *S. tortuosum* at 0.01 and 1 mg/mL and 10 μM Abi under basal conditions. Results are represented as mean ±SD (n=3).

Analyses of PREG levels (fig 5.12A) show only Abi increased PREG levels significantly (6-fold), as well as those of PROG (13.6-fold), indicative of the compound's inhibition of CYP17A1, further evident in the concomitant decrease of 16OHPROG. 16OHPROG is a dead end product as it is not metabolised further in the adrenal and thus a decrease in its levels would be a good indicator of inhibitory action. Although *S. tortuosum* increased PREG levels at the higher concentration, this was not significant, reflecting the data obtained in HEK-293 expression of CYP17A1 showing that *S. tortuosum* did not inhibit the enzyme. Interestingly the effect of *S. tortuosum* on the levels of 16OHPROG was comparable to Abi, however this could possibly be attributed to the low levels of the PROG precursor steroid as 17OHPROG production was also decreased.

Inhibition of CYP21A2 is evident in the glucocorticoid pathway in which 11-deoxycortisol levels were significantly decreased at both concentrations of *S. tortuosum extract* with 1 mg/mL having an effect comparable to that of Abi, apparent in the 15- and 16-fold decrease, respectively. Of interest, it was recently reported that Abi also inhibits CYP21A2 as well as 3β HSD2 [75, 76]. Downstream, *S. tortuosum* decreased cortisol production significantly at both concentrations, reflecting the data obtained in HEK239 cells expressing CYP11B1. Abi also inhibited cortisol production significantly suggesting possible inhibition of CYP11B1. It is however possible that the lower cortisol levels may be due to the significantly decreased precursor steroid. However, at the lower concentration of *S. tortuosum* the inhibition of cortisol was also significant even though 11-deoxycortisol levels were considerably higher than the levels detected in the presence of Abi and 1mg/mL *S. tortuosum extract*.

In the mineralocorticoid pathway, exposure to *S. tortuosum extract* at 1mg/mL significantly lowered the levels of DOC, comparable to Abi, also reflecting the inhibition of CYP21A2 in HEK-293 cells by the extract. However, neither downstream intermediates, CORT and 18OHCORT, nor ALDO were significantly influenced by *S. tortuosum* or Abi indicating that CYP11B2 was not inhibited by either and corroborating findings of conversion assay carried out in HEK-293 cells.

In the androgen pathway (fig 5.12B), DHEA levels were significantly decreased in the presence of Abi and 1 mg/mL *S. tortuosum extract*. A4 and T levels were also significantly reduced in the presence of Abi and 1 mg/mL extract, reflecting the inhibition of 3β HSD2 by *S. tortuosum* shown in HEK-293 cells and inferring inhibition of 17β HSD5. The reduction in androgens in this pathway in the presence of Abi can be ascribed to the upstream inhibition

of CYP17A1. Downstream, the production of 11OHA4 was reduced significantly by *S. tortuosum* extract at the higher concentration, while 11OHT production was not significantly affected, reflecting the inhibition observed in HEK-293 cells expressing CYP11B1.

5.4 Discussion

In this study the influence of *S. tortuosum* was investigated on individual steroidogenic enzymes catalysing the biosynthesis of adrenal steroid hormones, after which the extract was assessed in a whole cell model in order to determine the effects on steroid hormone output. Due to previous findings also suggesting that *S. tortuosum* may inhibit CYP17A1, Abi, a well-known CYP17A1 inhibitor used clinically to treat PCa, was also assayed in the H295R cells for comparative analysis with the inhibitory profile of *S. tortuosum*.

Cell viability assays in the presence of *S. tortuosum* showed that cells remained viable under the experimental conditions of the protocols which were followed in this study. The inhibitory effects observed were therefore due to interactions between the enzymes and the compounds in *S. tortuosum* as cell viability was not compromised by the experimental parameters. Previous research undertaken in our laboratory, in which the MTT assay was conducted to assess toxicity of *S. tortuosum* extracts spanning a range from 0.001 to 1 mg/mL, also showed that the extract is non-toxic to H295R cells [4].

CYP17A1 plays a pivotal role, together with 3 β HSD2, at the branch-point in adrenal hormone biosynthesis, with CYP17 channelling the steroid shunt towards the adrenal androgen pathway and 3 β HSD2 diverting metabolites into the mineralocorticoid and glucocorticoid pathways. Investigations into the influence of *S. tortuosum* extract on the catalytic activity of CYP17A1 towards PREG and PROG, conducted in HEK-293 cells transiently expressing CYP17A1, showed that *S. tortuosum* did not inhibit the enzyme. Although PREG and PROG production was not affected by *S. tortuosum*, 16OHP4 levels were significantly decreased ($P < 0.05$). This may be due to the inhibition of 3 β HSD2 modulating the shunt towards both 16- and 17OHPROG. The inhibition of the catalytic activity of CYP17A1 by Abi is apparent in the significantly increased PREG and PROG levels, corroborating previous investigations [58, 75], resulting in the decreased steroid shunt observed in the androgen pathway.

3 β HSD2, is key in the diversion of steroids into the mineralocorticoid and glucocorticoid pathways by catalysing PREG to PROG to yield mineralocorticoids and 17OHPREG to 17OHPROG to yield the glucocorticoids, while the conversion of DHEA to A4 yields the adrenal androgens. At 1 mg/mL, *S. tortuosum* extract inhibited the conversion of all three the substrates. In the adrenal cell model, inhibition of 3 β HSD2 by the extract is evident in the 17OHPROG and A4 levels being significantly decreased ($P < 0.01$), corroborating previous findings by Swart and Smith, indicating that perhaps *S. tortuosum* has the greatest inhibitory potential on the catalytic activity of 3 β HSD2 [4]. Although PROG formation was decreased from ~19nM to ~10 nM in the previous study, the low steroid concentration in the present study, ~0.2 nM does not allow for the analysis of the inhibitory potential of *S. tortuosum* in the case of PROG biosynthesis. Of interest, Abi has been shown to be a mixed competitive-noncompetitive inhibitor of 3 β HSD2 [67]. Although this study was conducted in PCa cells showing downstream implications, inhibition of the enzyme by Abi would have clinical implications affecting adrenal steroidogenesis in decreasing the production of mineralocorticoids and glucocorticoids. CYP21A2 was also recently shown to be inhibited by Abi [75], as mentioned previously and was corroborated in the present study in the decreased DOC and 11-deoxycortisol levels.

CYP21A2 catalyses the biosynthesis of PROG to DOC in the mineralocorticoid pathway and 17OHPROG to 11-deoxycortisol in the glucocorticoid pathway. The enzyme was only inhibited at the higher concentration of *S. tortuosum* extract as was shown in the HEK-293 cells expressing CYP21A2. The inhibition is reflected in the H295R cells with the production of DOC and 11-deoxycortisol being significantly decreased ($P < 0.01$), comparable to Abi. The previous study by Swart and Smith, showed that although DOC levels were reduced only in the presence of 1mg/ml, 11- deoxycortisol levels were not affected [4].

The final step in glucocorticoid production is catalysed by CYP11B1 in the conversion of 11-deoxycortisol to cortisol. Both 0.01 mg/mL and 1 mg/mL *S. tortuosum* extract inhibited the enzyme significantly with this inhibition also apparent in the H295R assays in which cortisol production was reduced significantly ($P < 0.001$) at both concentrations. Previous studies showed inhibition of cortisol production under stimulated conditions only in the presence of 1 mg/mL [4]. Basal 11-deoxycortisol levels were significantly higher (~1785 nM) [4], potentially saturating the enzyme which exhibits a K_m of 0.6 μ M towards 11-deoxycortisol. The inhibition under forskolin stimulation in which levels of cortisol were significantly higher would be possible since the enzyme is upregulated upon forskolin stimulation [77]. It should

be noted that CYP11B1 also catalyses the conversion of DOC to CORT and would therefore contribute to DOC and CORT levels in the H295R cells. Since DOC levels, which were decreased due to the upstream inhibition by CYP21A2, are below the K_m (1.2 μM) of CYP11B1 for DOC, the decreased CORT levels can be attributed to the inhibition of CYP11B1 since *S. tortuosum* did not inhibit CYP11B2. A4 and T are also substrates for CYP11B1 and although these metabolites form part of the adrenal androgen pathway, they are hydroxylated by CYP11B1 to yield 11OHA4 and 11OHT. In HEK- cells, the conversion of A4 and T were inhibited significantly ($P < 0.01$ and $P < 0.05$, respectively) in the presence of 1mg/ml *S. tortuosum* extract. However, the investigation in the H295R cells showed no effect on the production of 11OHT by CYP11B1 but did show a reduction in 11OHA4 levels. Similar findings were evident with Abi also decreasing only 11OHA4 significantly suggesting potential inhibition of CYP11B1, however, the lower downstream adrenal androgens may be due to upstream CYP17A1 inhibition.

In the mineralocorticoid pathway CYP11B2 catalyses the formation of aldosterone from DOC, via CORT and 18OHCORT. In HEK-239 cells expressing CYP11B2 *S. tortuosum* did not inhibit the conversion of DOC and even though it was a single study, the assays in H295R cells corroborate this finding. In addition, the control assays which were carried out in the absence of extract were comparable to conversion assays conducted routinely in our laboratory. The significant inhibition of A4's conversion is unlikely since *in vivo* neither A4 nor T would serve as substrates for CYP11B2 since the enzyme is expressed in the *zona glomerulosa* only, while A4 and T are produced in the *zona reticularis*. It would furthermore appear that beneficial effects of *S. tortuosum*, in terms of hypertension as was previously suggested [4], would only potentially be relevant under conditions of stress. However, since *S. tortuosum* did not significantly inhibit metabolite production downstream of DOC or ALDO levels this finding may reflect further beneficial effects as ALDO is essential in the maintenance of normal blood pressure and water and electrolyte balance.

Analyses of the steroid profiles showed that the total steroid output in the H295R cell system was lower than previous studies done in our laboratory as was mentioned previously [78, 79]. In this study UPC²-MS/MS steroid analyses allows a more sensitive approach to the detection and quantification of steroids. This enabled the use of lower cell densities to reach physiological steroid concentrations in order to assess *S. tortuosum* and enzyme interactions more accurately in the H295R system in an attempt to approximate an *in vivo*

system more closely. The steroid output detected in this study was nevertheless similar to the concentrations observed in literature [80].

Considering the mineralocorticoid branch of adrenal steroidogenesis, the combined basal steroid level which were detected was ~54.2 nM. The presence of *S. tortuosum* extract did not influence the output of mineralocorticoids in the H295R cells significantly. In the glucocorticoid pathway steroid output was ~224.8 nM (fig 5.12A – green). *S. tortuosum* extract at the lower concentration decreased the glucocorticoid output 1.6-fold while the most significant decrease is detected in the presence of 1 mg/mL and 10 μ M Abi, where the output was decreased 5.2 and 3.9-fold, respectively. Abi also influenced the glucocorticoid pathway, due to the inhibition of CYP17A1 upstream, blocking the formation of 17OHPREG and 17OHPROG and, in part, due to the probable inhibition of CYP11B1 ultimately resulting in lowered cortisol levels. For this reason, Abi is administered in conjunction with prednisone, a synthetic glucocorticoid. The androgen pathway is significantly influenced in the presence of *S. tortuosum* at 1 mg/ml as well as by Abi. Total basal steroid levels were ~287.8 nM with Abi decreasing androgen output 4.7-fold whereas *S. tortuosum* resulted in a 3-fold decrease. This suggests the *S. tortuosum* can also modulate the output of adrenal androgens, thereby decreasing the total available androgens in the androgen pool.

Taken together, it is apparent that *S. tortuosum* modulated adrenal steroid hormone biosynthesis due to the inhibition of specific adrenal steroidogenic enzymes, viz. 3 β HSD2, CYP21A2 and CYP11B1. In comparison to Abi, *S. tortuosum* did not exhibit the same inhibitory profile, suggesting that the enzymes are not affected in the same manner or to the same degree. Nevertheless, Abi showed increased PREG and PROG levels and the decrease of all the other steroid hormones, except ALDO and its immediate precursors reflecting the potent inhibition of CYP17A1 [58, 66, 68, 69, 75]. This CYP17A1 inhibition was not apparent with *S. tortuosum*. While Abi resulted in a greater inhibition of the steroid shunt in the androgen pathway than in the glucocorticoid pathway, *S. tortuosum* resulted in a greater decrease in the steroid shunt in the glucocorticoid pathway in comparison to the androgen pathway. These data suggest beneficial clinical implications for diseases that are characterised by hypercortisolism and androgen excess, without compromising the production of ALDO, exacerbating diseases characterised by abnormal blood pressure.

Chapter 6

Conclusion

The fundamental aim of this study was to investigate the influence of *S. tortuosum* on the catalytic activity of steroidogenic enzymes catalysing adrenal hormone biosynthesis. Adrenal hormone biosynthesis involves a series of enzymatic steps that ultimately result in the production of mineralocorticoids, glucocorticoids and adrenal androgens [12]. Disease states characterised by abnormal production of aldosterone, cortisol and adrenal androgens are debilitating as the adrenal steroid hormones are pivotal in the maintenance of homeostasis. Adrenal hormone biosynthesis can also be influenced in attempts to regulate the progression of hormone-dependent cancers, such as PCa. Abi, an enzyme inhibitor, is at the forefront in terms of treatment for PCa by inhibiting CYP17A1 in the adrenal and in steroidogenic tissue. As a consequence the formation of T, which gives rise to DHT, is therefore inhibited and, in the adrenal the production of androgen precursors are decreased [68, 69]. This decreases the total androgens and specifically the active androgens in the androgen pool, results in the attenuation of the progression of PCa. At present there are a number of alkaloids and alkaloid-derivatives that are being tested in clinical trials for the treatment of cancers and herbal supplements rich in alkaloids may aid therapeutic approaches. Natural plant products are still subject to scepticism due to the lack of scientific evidence supporting the use of these products. However, interest in the herbal remedies has grown and there is a growing demand for natural supplements to treat diseases. The high content of alkaloids in *S. tortuosum* has prompted a number of studies into the bioactive properties of this plant, however, few into its potential anti-cancer activity.

The current study therefore investigated the effects of *S. tortuosum* on adrenal enzymes in the pursuit of scientific evidence supporting *S. tortuosum* as a potential therapeutic agent in the treatment of hormone-dependent diseases. A comparative study was also undertaken with Abi, investigating the effect of *S. tortuosum* and Abi on adrenal hormone biosynthesis in an adrenal cell model.

This study reports on the inhibitory effect of a mesembrine enriched *S. tortuosum* preparation on the catalytic activity of CYP21A2, CYP11B1 and 3 β HSD2, heterologously

expressed in mammalian cell system. The mode of action by which *S. tortuosum* inhibited the catalytic activity of these enzymes was not the motivation of this study. However, based on the structure of the alkaloids present in the plant, *S. tortuosum* may have interplay with the active site of the enzyme. At the same time, the inhibition seen was substrate-specific, indicating that perhaps kinetic parameters of the substrates play a role in the inhibition observed.

This study also reported on the inhibitory effect of *S. tortuosum* in an adrenal carcinoma cell system, adding insight into its influence on adrenal steroidogenesis in comparison to Abi. In the analyses of basal steroid production by H295R cells, *S. tortuosum* had a marked effect on the levels of cortisol at a low and high concentration, while not influencing the production of aldosterone. However, *S. tortuosum* also had a noticeable effect on the androgen arm as it resulted in a decrease in the levels of DHEA, A4, T and 11OHA4. This suggests modulation of 3β HSD2, 17β HSD and CYP11B1. *S. tortuosum* modulated androgen production, decreasing the output of adrenal androgens and may, as such, act as a therapeutic agent in supplementing the treatment of androgen-dependent diseases, such as PCa. Abi increased PREG and PROG levels in the current study with the increase attributed to the known inhibition of the activity of CYP17A1. However, a recent study reported that Abi also inhibits the catalytic activity of CYP21A2 [75, 76]. This dual inhibition of CYP17A1 and CYP21A2 is observed in the marked decrease of cortisol and 16OHPROG with the simultaneous increase in PROG and PREG levels in the current study. Due to Abi noticeably influencing the activity of two key adrenal enzymes, it may require further investigation into potential adverse effects.

This study also described a UPC²-MS/MS method to detect, separate and quantify 17 steroid hormones. The implementation of this method allowed for a time-efficient, cost-effective analysis of the kinetic parameters of CYP11B1 for A4 and T. This study showed that CYP11B1 has a higher catalytic efficiency towards A4 than it does towards T. This is due to the lower apparent K_m ($\sim 0.21 \mu\text{M}$) and 2-fold higher V_{max} value ($\sim 315.77 \text{ pmol/min/mg protein}$) towards A4. This result provides insight into the manner in which the adrenal modulates steroid output, specifically the steroids produced to due conversion by CYP11B1 reflected in the significantly higher production of 11OHA4 and 11OHT.

While this study provides insight into the modulation of adrenal steroidogenesis by *S. tortuosum*, further insight can be gained by assessing the influence of the individual

alkaloids found in *S. tortuosum*. Alkaloids are known to have beneficial clinical implications while others possess undesirable effects. The influence of *S. tortuosum* should also be assessed on androgen metabolism in PCa cells as it is clear from this study that androgen metabolism is markedly influenced by the plant. 3β HSD2 is expressed in peripheral steroidogenic tissue, including the prostate, with the conversion of DHEA to A4 and subsequently leading to T and the production of DHT adding to the active androgen pool. Findings in the H295R cell model also suggests possible inhibition of 17β HSD5, currently a drug target in the treatment of PCa.

Taken together, this study shows that *S. tortuosum* influences the production of androgens and cortisol in the adrenal by specifically inhibiting CYP21A2, CYP11B1, and 3β HSD2. Assessing the influence of Abi provided further evidence for the inhibition of CYP21A2, however, further evaluation of effects on adrenal enzymes is required. Comparatively, Abi resulted in a greater inhibition of the steroid shunt in the androgen pathway than in the glucocorticoid pathway, whereas *S. tortuosum* resulted in a greater decrease in the steroid shunt in the glucocorticoid pathway than in the androgen pathway. Neither Abi nor *S. tortuosum* exhibited any effect on the production of aldosterone and its immediate precursors. Overall, based on the data presented in this thesis, together with existing literature surrounding *S. tortuosum*, it appears that *S. tortuosum* may offer potential as a therapeutic agent in aiding the treatment of hormone-dependent diseases characterised by hypercortisolism and excess androgen production.

References

1. Polat S, Kulle A, Karaca Z, et al (2014) Characterisation of three novel CYP11B1 mutations in classic and non-classic 11 β -hydroxylase deficiency. *Eur J Endocrinol* 170:697–706 . doi: 10.1530/EJE-13-0737
2. Harvey AL, Young LC, Viljoen AM, Gericke NP (2011) Pharmacological actions of the South African medicinal and functional food plant *Sceletium tortuosum* and its principal alkaloids. *J Ethnopharmacol* 137:1124–1129 . doi: 10.1016/j.jep.2011.07.035
3. Gericke N, Viljoen AM (2008) *Sceletium*-A review update. *J Ethnopharmacol* 119:653–663 . doi: 10.1016/j.jep.2008.07.043
4. Swart AC, Smith C (2016) Modulation of glucocorticoid, mineralocorticoid and androgen production in H295 cells by Trimesemine???, a mesembrine-rich *Sceletium* extract. *J Ethnopharmacol* 177:35–45 . doi: 10.1016/j.jep.2015.11.033
5. Jin Z (2009) Amaryllidaceae and *Sceletium* alkaloids. *Nat Prod Rep* 26:363–381 . doi: 10.1039/c3np70005d
6. Coetzee DD, Lopez V, Smith C (2016) High-mesembrine *Sceletium* extract (Trimesemine) is a monoamine releasing agent, rather than only a selective serotonin reuptake inhibitor. *J Ethnopharmacol* 177:111–116 . doi: 10.1016/j.jep.2015.11.034
7. Terburg D, Syal S, Rosenberger LA, et al (2013) Acute effects of *sceletium tortuosum* (Zembrin), a dual 5-HT reuptake and PDE4 inhibitor, in the human amygdala and its connection to the hypothalamus. *Neuropsychopharmacology* 38:2708–2716 . doi: 10.1038/npp.2013.183
8. Aunis D (1998) Exocytosis in chromaffin cells of the adrenal medulla. *Int Rev Cytol* 181:
9. Coupland RE (1953) On the morphology and adrenaline–noradrenaline content of chromaffin tissue. *J Endocrinol* 9:194–200
10. Bornstein SR, Ehrhard-Bornstein M, Usadel H, et al (1991) Morphological evidence for a close interaction of chromaffin cells with cortical cells within the adrenal gland. *Cell Tissue Res* 265:1–9
11. Palacios G, Lafarga M (1975) Chromaffin cells in the glomerular zone of adult rat adrenal cortex. *Cell Tissue Res* 164:275–8
12. Miller WL, Auchus RJ (2011) The molecular biology, biochemistry, and physiology of

- human steroidogenesis and its disorders. *Endocr Rev* 32:81–151 . doi: 10.1210/er.2010-0013
13. Rege J, Nakamura Y, Satoh F, et al (2013) Liquid Chromatography–Tandem Mass Spectrometry Analysis of Human Adrenal Vein 19-Carbon Steroids Before and After ACTH Stimulation. *J Clin Endocrinol Metab* 98:1182–1188
 14. Swart AC, Schloms L, Storbeck KH, et al (2013) 11beta-Hydroxyandrostenedione, the product of androstenedione metabolism in the adrenal, is metabolized in LNCaP cells by 5alpha-reductase yielding 11beta-hydroxy-5alpha-androstenedione. *J Steroid Biochem Mol Biol* 138:132–142 . doi: 10.1016/j.jsbmb.2013.04.010
 15. du Toit T, Bloem LM, Quanson JL, et al (2016) Profiling adrenal 11 β -hydroxyandrostenedione metabolites in prostate cancer cells, tissue and plasma: UPC2-MS/MS quantification of 11 β -hydroxytestosterone, 11keto-testosterone and 11keto-dihydrotestosterone. *J Steroid Biochem Mol Biol*. doi: <http://dx.doi.org/10.1016/j.jsbmb.2016.06.009>
 16. Pretorius E, Africander DJ, Vlok M, et al (2016) 11-Ketotestosterone and 11-ketodihydrotestosterone in castration resistant prostate cancer: Potent androgens which can no longer be ignored. *PLoS One* 11:1–17 . doi: 10.1371/journal.pone.0159867
 17. Patnala S, Kanfer I (2017) *Sceletium Plant Species: Alkaloidal Components, Chemistry and Ethnopharmacology*. In: *Alkaloids – Alternatives in Synthesis, Modification and Application*. pp 85–101
 18. Smith M, Crouch N, Gericke N, Hirst M (1996) Psychoactive constituents of the genus *Sceletium* N.E.Br and other Mesembryanthemaceae: a review. *J Ethnopharmacol* 50:119–130
 19. Dimpfel W, Schombert L, Gericke N (2016) Electropharmacogram of *Sceletium tortuosum* extract based on spectral local field power in conscious freely moving rats. *J Ethnopharmacol* 177:140–147 . doi: 10.1016/j.jep.2015.11.036
 20. Carey S (2011) A South African herb that may rival Prozac. *African Bus.* 52–54
 21. Krstenansky JL (2017) Mesembrine alkaloids: Review of their occurrence, chemistry, and pharmacology. *J Ethnopharmacol* 195:10–19 . doi: 10.1016/j.jep.2016.12.004
 22. Harvey AL, Young LC, Viljoen AM, Gericke NP (2011) Pharmacological actions of the South African medicinal and functional food plant *Sceletium tortuosum* and its principal alkaloids. *J Ethnopharmacol* 137:1124–1129 . doi: 10.1016/j.jep.2011.07.035
 23. Patnala S, Kanfer I (2009) Investigations of the phytochemical content of *Sceletium*

- tortuosum following the preparation of “Kougoed” by fermentation of plant material. *J Ethnopharmacol* 121:86–91 . doi: 10.1016/j.jep.2008.10.008
24. Jeffs PW, Archie WC, Hawks RL, Farrier DS (1971) Sceletium alkaloids. IV. Biosynthesis of mesembrine and related alkaloids. Amino acid precursors. *J Am Chem Soc* 93:3752–3758 . doi: 10.1021/ja00744a032
 25. Jeffs PW, Karle JM, Martin NH (1978) Cinnamic acid intermediates as precursors to mesembrine and some observations on the late stages in the biosynthesis of the mesembrine alkaloids*. *J Ethnopharmacol* 17:719–728
 26. Meyer GMJ, Wink CSD, Zapp J, Maurer HH (2015) GC-MS, LC-MSn, LC-high resolution-MSn, and NMR studies on the metabolism and toxicological detection of mesembrine and mesembrenone, the main alkaloids of the legal high “Kanna” isolated from *Sceletium tortuosum*. *Anal Bioanal Chem* 407:761–778 . doi: 10.1007/s00216-014-8109-9
 27. Waterhouse G, De Wet G., Pheiffer R. (1979) Simon van der Stel’s Journey to Namaqualand in 1685. Human & Rousseau, Cape Town
 28. Gericke NP, Van Wyk B (2011) Pharmaceutical compositions containing mesembrine and related compounds.
 29. Nell H, Siebert M, Chellan P, Gericke N (2013) A Randomized, Double-Blind, Parallel-Group, Placebo-Controlled Trial of Extract *Sceletium tortuosum* (Zembrin) in Healthy Adults. *J Altern Complement Med* 19:898–904 . doi: 10.1089/acm.2012.0185
 30. Chiu S, Gericke N, Farina-Woodbury M, et al (2014) Proof-of-concept randomized controlled study of cognition effects of the proprietary extract scelletium tortuosum (Zembrin) targeting phosphodiesterase-4 in cognitively healthy subjects: Implications for Alzheimer’s dementia. *Evidence-based Complement Altern Med* 2014: . doi: 10.1155/2014/682014
 31. Dimpfel W, Gericke N, Suliman S, Dipah GNC (2016) Psychophysiological Effects of Zembrin® Using Quantitative EEG Source Density in Combination with Eye-Tracking in 3-Armed Study with Parallel Design. *Neurosci Med* 7:114–132
 32. Mescher AL (2013) Junqueira’s Basic Histology Text & Atlas, 13th ed
 33. You L (2004) Steroid hormone biotransformation and xenobiotic induction of hepatic steroid metabolizing enzymes. *Chem Biol Interact* 147:233–246
 34. Mason JI, Rainey WE (1987) Steroidogenesis in the human fetal adrenal: a role for cholesterol synthesized de novo. *J Clin Endocrinol Metab* 64:
 35. Gwynne J., Strauss 3rd JF (1982) The role of lipoproteins in steroidogenesis and

- cholesterol metabolism in steroidogenic glands. *Endocr Rev* 3:299–329
36. Chang T., Chang C., Ohgami N, Yamauchi Y (2006) Cholesterol sensing, trafficking and esterification. *Annu Rev Cell Dev Biol* 22:129–157
 37. Miller W. (2007) StAR search - what we know about how the steroidogenic acute regulatory protein mediates mitochondrial cholesterol import. *Mol Endocrinol* 21:589–601
 38. Soccio R., Breslow J. (2003) StAR-related lipid transfer (START) proteins: mediators of intracellular lipid metabolism. *J Biol Chem* 278:22183–22186
 39. Omura T, Sato R (1962) A new cytochrome in liver microsomes. *J Biol Chem* 237:1375–1376
 40. Miller W. (2005) Regulation of steroidogenesis by electron transfer. *Endocrinology* 146:2544–2550
 41. Payne AH, Hales DB (2004) Overview of steroidogenic enzymes in the pathway from cholesterol to active steroid hormones. *Endocr Rev* 25:947–970 . doi: 10.1210/er.2003-0030
 42. Denisov IG, Makris TM, Sligar SG, Schlichting I (2005) Structure and chemistry of cytochrome P450. *Chem Rev* 105:2253–2277 . doi: 10.1021/cr0307143
 43. Agarwal A., Auchus RJ (2005) Minireview: Cellular redox state regulates hydroxysteroid dehydrogenase activity and intracellular hormone potency. *Endocrinology* 146:2531–2538
 44. Thomas J., Duax W., Addlagatta A, et al (2003) Structure/function relationships responsible for coenzyme specificity and the isomerase activity of human type 1 3beta-hydroxysteroid dehydrogenase/isomerase. *J Biol Chem* 278:35483–35490
 45. Lachance Y, Labrie C, Simard J, et al (1990) Characterization of Human S & Hydroxysteroid Dehydrogenase / delta 5- delta 4- Isomerase Gene and Its Expression in Mammalian Cells *. *J Biol Chem* 265:20469–20475
 46. Prevo D, Swart P, Swart AC (2008) The influence of *Sutherlandia frutescens* on adrenal steroidogenic cytochrome P450 enzymes. *J Ethnopharmacol* 118:118–126 . doi: 10.1016/j.jep.2008.03.019
 47. Schloms L, Storbeck KH, Swart P, et al (2012) The influence of *Aspalathus linearis* (Rooibos) and dihydrochalcones on adrenal steroidogenesis: Quantification of steroid intermediates and end products in H295R cells. *J Steroid Biochem Mol Biol* 128:128–138 . doi: 10.1016/j.jsbmb.2011.11.003
 48. Liu J, Heikkilä P, Meng QH, et al (2000) Expression of low and high density lipoprotein receptor genes in human adrenals. *Eur J Endocrinol* 142:677–82

49. Connelly M., Williams D. (2004) SR-BI and HDL cholesterol ester metabolism. *Endocr Res* 30:697–703
50. Rainey WE, Nakamura Y (2008) Regulation of the Adrenal Androgen Biosynthesis. *J Steroid Biochem Mol Biol* 108:281–286 . doi: 10.1002/nbm.3066.
51. Bloem LM, Storbeck KH, Swart P, et al (2015) Advances in the analytical methodologies: Profiling steroids in familiar pathways-challenging dogmas. *J Steroid Biochem Mol Biol* 153:80–92 . doi: 10.1016/j.jsbmb.2015.04.009
52. Connell JMC, Fraser R, Davies E (2001) Disorders of mineralocorticoid synthesis. *Best Pract Res Clin Endocrinol Metab* 15:43–60 . doi: 10.1053/beem.2000.0118
53. Liddle GW (1972) Pathogenesis of glucocorticoid disorders. *Am J Med* 53:638–648 . doi: 10.1016/0002-9343(72)90159-3
54. Gold R, Buttgereit F, Toyka K (2001) Mechanism of action of glucocorticosteroid hormones: possible implications for therapy of neuroimmunological disorders. *J Neuroimmunol* 117:1–8
55. Kannan CR (1988) DISEASES OF THE CORTEX ADRENAL.
56. Witchel SF (2017) Congenital Adrenal Hyperplasia. *J Pediatr Adolesc Gynecol* 30:520–534 . doi: 10.1016/j.jpag.2017.04.001
57. Smith C (2011) The effects of *Sceletium tortuosum* in an in vivo model of psychological stress. *J Ethnopharmacol* 133:31–36 . doi: 10.1016/j.jep.2010.08.058
58. Rijk JCW, Peijnenburg AACM, Blokland MH, et al (2012) Screening for Modulatory Effects on Steroidogenesis Using the Human H295R Adrenocortical Cell Line: A Metabolomics Approach. *Chem Res Toxicol* 25:1720–1731
59. Quanson JL, Stander MA, Pretorius E, et al (2016) High-throughput analysis of 19 endogenous androgenic steroids by ultra-performance convergence chromatography tandem mass spectrometry. *J Chromatogr B Anal Technol Biomed Life Sci* 1031:131–138 . doi: 10.1016/j.jchromb.2016.07.024
60. Taylor L. (2009) Supercritical fluid chromatography for the 21st century. *J Supercrit Fluids* 47:566–573
61. Stanczyk F., Clarke N. (2010) Advantages and challenges of mass spectrometry assays for steroid hormones. *J Steroid Biochem Mol Biol* 121:491–495
62. Taylor PJ (2005) Matrix effects : The Achilles heel of quantitative high-performance liquid chromatography – electrospray – tandem mass spectrometry. 38:328–334 . doi: 10.1016/j.clinbiochem.2004.11.007
63. Storbeck KH, Bloem LM, Africander D, et al (2013) 11b-Hydroxydihydrotestosterone and 11-ketodihydrotestosterone, novel C19 steroids with androgenic activity: A

- putative role in castration resistant prostate cancer? *Mol Cell Endocrinol* 377:135–146 . doi: 10.1371/journal.pone.0159867
64. Johnson KA, Goody RS (2011) The original Michaelis constant: Translation of the 1913 Michaelis-Menten Paper. *Biochemistry* 50:8264–8269 . doi: 10.1021/bi201284u
65. Van Wyk B, Van Oudtshoorn B, Gericke N (2010) Medicinal Plants of South Africa. *Chromatographia* 71:1151 . doi: 10.1365/s10337-010-1583-0
66. Li Z, Bishop AC, Alyamani M, et al (2015) Conversion of abiraterone to D4A drives anti-tumour activity in prostate cancer. *Nature* 523:347–51 . doi: 10.1038/nature14406
67. Li R, Evaul K, Sharma KK, et al Abiraterone Inhibits 3 β -Hydroxysteroid Dehydrogenase: A Rationale for Increasing Drug Exposure in Castration-Resistant Prostate Cancer. *Clin cancer Res* 18:3571–3579
68. Attard G, Reid AHM, A'Hern R, et al (2009) Selective inhibition of CYP17 with abiraterone acetate is highly active in the treatment of castration-resistant prostate cancer. *J Clin Oncol* 27:3742–3748 . doi: 10.1200/JCO.2008.20.0642
69. Kwak C, Wu TTL, Lee HM, et al (2014) Abiraterone acetate and prednisolone for metastatic castration-resistant prostate cancer failing androgen deprivation and docetaxel-based chemotherapy: A phase II bridging study in Korean and Taiwanese patients. *Int J Urol* 21:1239–1244 . doi: 10.1111/iju.12589
70. Lu JJ, Bao JL, Chen XP, et al (2012) Alkaloids isolated from natural herbs as the anticancer agents. *Evidence-based Complement Altern Med* 2012: . doi: 10.1155/2012/485042
71. Kumar V, Guru S., Jain S., et al (2016) A chromatography-free isolation of rohitukine from leaves of *Dysoxylum binectariferum*: Evaluation for in vitro cytotoxicity, Cdk inhibition and physicochemical properties. *Bioorg Med Chem Lett* 26:3457–3463
72. Keshri G, Oberoi R., Lakshmi V, et al (2007) Contraceptive and hormonal properties of the stem bark of *Dysoxylum binectariferum* in rat and docking analysis of rohitukine, the alkaloid isolated from active chloroform soluble fraction. *Contraception* 76:400–407
73. Isah T (2016) Anticancer Alkaloids from Trees: Development into Drugs. *Pharmacogn Rev* 10:90–99
74. Bruggisser R, von Daeniken K, Jundt G, et al (2002) Interference of plant extracts, phytoestrogens and antioxidants with the MTT tetrazolium assay. *Planta Med* 68:445–448

75. Malikova J, Brixius-Anderko S, Udhane SS, et al (2017) CYP17A1 inhibitor abiraterone, an anti-prostate cancer drug, also inhibits the 21-hydroxylase activity of CYP21A2. *J Steroid Biochem Mol Biol* 174:192–200 . doi: 10.1016/j.jsbmb.2017.09.007
76. Udhane S, Pandey A Effect of CYP17A1 inhibitors orteronel & galeterone on adrenal androgen biosynthesis. *Horm Res Paediatr*. doi: 10.3252/pso.eu.54espe.2015
77. Seamon KBKBB, Padgett W, Daly JWJWW (1981) Forskolin: unique diterpene activator of adenylate cyclase in membranes and in intact cells. *Proc Natl Acad Sci U S A* 78:3363–3367 . doi: 10.1073/pnas.78.6.3363
78. Schloms L, Storbeck KH, Swart P, et al (2012) The influence of *Aspalathus linearis* (Rooibos) and dihydrochalcones on adrenal steroidogenesis: Quantification of steroid intermediates and end products in H295R cells. *J Steroid Biochem Mol Biol* 128:128–138 . doi: 10.1016/j.jsbmb.2011.11.003
79. Schloms L, Swart AC (2014) Rooibos flavonoids inhibit the activity of key adrenal steroidogenic enzymes, modulating steroid hormone levels in H295R cells. *Molecules* 19:3681–3695 . doi: 10.3390/molecules19033681
80. Nielsen FK, Hansen CH, Fey JA, et al (2012) H295R cells as a model for steroidogenic disruption: A broader perspective using simultaneous chemical analysis of 7 key steroid hormones. *Toxicol Vitr* 26:343–350 . doi: 10.1016/j.tiv.2011.12.008